AN ARTIFICIAL NEURAL NETWORK APPROACH TO PREDICT THE PERFORMANCE AND EXHAUST EMISSIONS OF A COMPRESSION IGNITION (CI) ENGINE USING SPIRULINA BIODIESEL-NANOPARTICLES BLENDED FUEL

Thesis Submitted for the Award of the Degree of

DOCTOR OF PHILOSOPHY
in

Mechanical Engineering

By

Suravarapu Charan Kumar

Registration Number: 11919649

Supervised By

Dr. Amit Kumar Thakur (25010)

Professor

School of Mechanical Engineering

Lovely Professional University

Punjab, India

Co-Supervised by

Dr. J. Ronald Aseer

Assistant Professor

Department of Mechanical Engineering

National Institute of Technology Puducherry

Karaikal, Puducherry, India

LOVELY PROFESSIONAL UNIVERSITY, PUNJAB

2022

DECLARATION

I, hereby declared that the presented work in the thesis entitled "AN ARTIFICIAL NEURAL NETWORK APPROACH TO PREDICT THE PERFORMANCE AND EXHAUST EMISSIONS OF A COMPRESSION IGNITION (CI) ENGINE USING SPIRULINA BIODIESEL-NANOPARTICLES BLENDED FUEL" in fulfilment of degree of Doctor of Philosophy (Ph.D.) is outcome of research work carried out by me under the supervisionDr. Amit Kumar Thakur working as Professor, in the Aerospace Department (School of Mechanical Engineering) of Lovely Professional University, Punjab, India. In keeping with general practice of reporting scientific observations, due acknowledgements have been made whenever work described here has been based on findings of other investigator. This work has not been submitted in part or full to any other University or Institute for the award of any degree.

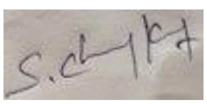

S. Charan Kumar

11919649

Mechanical Engineering (School of Mechanical Engineering)

Lovely Professional University,

Punjab, India

CERTIFICATE

This is to certify that the work reported in the Ph.D. thesis entitled "AN ARTIFICIAL NEURAL NETWORK APPROACH TO PREDICT THE PERFORMANCE AND EXHAUST EMISSIONS OF A COMPRESSION IGNITION (CI) ENGINE USING SPIRULINA BIODIESEL-NANOPARTICLES BLENDED FUEL" submitted in fulfillment of the requirement for the reward of degree of **Doctor of Philosophy (Ph.D.)** in the Mechanical Engineering (School of Mechanical Engineering), is a research work carried out S. Charan Kumar, 11919649, is bonafide record of his/her original work carried out under my supervision and that no part of thesis has been submitted for any other degree, diploma or equivalent course.

Dr. Amit Kumar Thakur
Professor,
School of Mechanical Engineering,
Lovely Professional University,
Punjab, India.

Dr. J. Ronald Aseer
Assistant Professor,
Department of Mechanical Engineering,
National Institute of Technology Puducherry,
Karaikal, Puducherry, India.

ABSTRACT

As a result of the expanding demographic and changing lifestyles, energy usage is continuously rising enormously across all sectors. An ever-increasing need for energy leads to a greater reliance on conventional fuels. Long term energy sustainability is seriously threatened by the finite character of these fuel assets. Fuels from renewable sources could serve as a perfect substitute in this scenario. Renewable fuels will satisfy energy requirements for upcoming decades, and their use will become more widespread globally to save the environment. Over the recent times, biofuels have gained prominence as an appealing solution to conventional fuels.

In this current analysis, biodiesel derived from third generation microalgae spirulina is assessed as a replacement for diesel. Also, the influence of nano additives Al_2O_3 and MgO in microalgae spirulina amalgams on compression ignition engine attributes are studied. Additionally, using an Artificial Neural Network (ANN), an optimization model was designed to characterize the test variables. Spirulina biodiesel amalgams of varied volumetric proportions ranging between 20 and 100% were analyzed. The $Al_2O_3$and MgO additives were disseminated at a concentration of 25 ppm with biodiesel mixtures. Using 19 distinct samples of the test fuels (SB0, SB20, SB35, SB50, SB65, SB80, SB100, SB20 Al_2O_3, SB35 Al_2O_3, SB50 Al_2O_3, SB65 Al_2O_3, SB80 Al_2O_3, SB100 Al_2O_3, SB20 MgO, SB35 MgO, SB50 MgO, SB65 MgO, SB80 MgO, and SB100 MgO), the emittants and the performance parameters nitrogen oxides (NO_X), carbon dioxide (CO_2), hydrocarbons (HC), brake thermal efficiency (BTE) and brake specific fuel consumption (BSFC) of a 5.2 kW, water-cooled, 4-stroke, 1-cylinder CI engine was explored.

Test investigation revealed that, compared to diesel (SB0), the heating value of the $Al_2O_3$and MgO doped fuel mixtures is 3.8091 and 3.448% (on median) less, signifying reduced performance. However, compared to spirulina blends, the heating value of the Al_2O_3 and MgO doped fuel mixtures improved by 1.45 and 1.82% (on median), respectively. At peak load, the overall drop in BTE was observed to be 3.55, 3.18, and 4.16 respectively, for Al_2O_3, MgO doped blends, and biodiesel mixture (without additive), than SB0. On the other hand, the BSFC of Al_2O_3, MgO doped blends, and biodiesel mixture enhanced by 5.77, 5.31, and 7.49%, respectively. Furthermore, it was observed that in contrast to SB0, NO_X and HC concentrations decreased, and CO_2 increased for test fuel mixtures without and with additives. At peak load,

CO_2 emittants of Al_2O_3, MgO doped blends, and spirulina biodiesel mixture were 9.35%, 10.11%, and 7.584% higher than SB0. NO_X of Al_2O_3, MgO doped blends, and spirulina biodiesel amalgams decreased by 7.79%, 8.3%, and 10.31%, respectively, at full load. On the other hand, a reduction of HC about 13.37%, 13.66%, and 12.91% for amalgams with Al_2O_3, MgO additives, and without additives is observed.

ANN model based on supervised learning was built to predict the CI engine attributes. Three sets of transfer functions namely softplus, softmax, and sigmoid along with optimizers adagrad, nadam, and adam were tried to develop the model. The model trained with adam optimizer with 16 neurons in the hidden layer stands out as the best among other algorithms with the least MSE and strong r. The r and MSE of engine characteristics NO_X, HC, CO_2, BTE, BSFC are 0.99992, 0.99888, 0.99959, 0.99989, 0.99969 and 0.00002, 0.00015, 0.00007, 0.00003, 0.00004 respectively. This research reveals that the ANN strategy can be employed effectively to predict the engine characteristics.

ACKNOWLEDGMENTS

Several people have contributed, either directly or indirectly, to the work presented in this thesis and for their contributions, I am extremely thankful.

Firstly, I would like to express my utmost gratitude to my supervisor and co-supervisor, Dr. Amit Kumar Thakur and Dr. J. Ronald Aseer for their advice, guidance, and support throughout my research. They taught me the skills required for independent research and allowed me the freedom to explore my ideas, whilst providing appropriate guidance and criticism to ensure that I carried out my research professionally and completed my work on time. A special thanks to Dr. Sendhil Kumar Natarajan and Dr. Rajasekhar Dondapati for his support during research work. I express my heartfelt thanks to Dr. Vijay Kumar Singh (HOS-Mechanical Engineering).

I attended several conferences and workshops during my Ph.D., and I am extremely grateful to those with whom I have collaborated or who have provided comments and constructive criticism of my work.

Finally, I must thank all of my friends and family for their love and support. My parents, Mr. S. Vaikuntha Rao and Mrs. S. Lakshmi have supported me in all of my pursuits and encouraged me to set my goals for achievement high. My brother, Mr. S. Sandeep Kumar, has supported me wholeheartedly. I must also thank my wife Mrs. S. Kanchana for supporting and encouraging me always. The emotional support required to complete a Ph.D. is often underestimated. I would like to thank God Almighty for giving me the opportunity and guidance to achieving my goal and to be successful in this part.

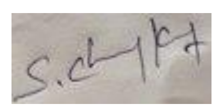

S. Charan Kumar

TABLE of CONTENTS

LIST of FIGURES

LIST of TABLES

NOMENCLATURE

%	Percentage
AI	Artificial Intelligence
Al_2O_3	nano Alumina
ANN	Artificial Neural Network
BNN	Biological Neural Network
BSFC	Brake Specific Fuel Consumption
BTE	Brake Thermal Efficiency
CI	Compression Ignition
CO_2	Carbon dioxide
CR	Compression Ratio
EDS	Energy Dispersive X-ray Spectroscopy
GDP	Gross Domestic Product
GOI	Government of India
HC	Hydro Carbons
HRR	Heat Realease Rate
ID	Ignition Delay
IP	Ignition Pressure
IT	Ignition Temperature
KB	Knowledge-based Systems
LCV	Lower Calorific Value
LHV	Lower Heating Value
MAE	Mean Absolute Error
MgO	Magnesium Oxide
ML	Machine Learning
MRE	Mean Relative Error
nm	Nano meter
NO_X	Nitrous Oxide
O_2	Oxygen
PM	Particulate Matter

ppm	Parts Per Million
r	Correlation Coefficient
RMSE	Root Mean Squared Error
SI	Spark Ignition
SL	Supervised Learning
SO_2	Sulphur dioxide
Train.	Training
USL	Unsupervised Learning
Val.	Validation

CHAPTER 1

INTRODUCTION

In 1800, Thomas Young introduced the term "energy", which originated from the Greek word “energeia”. The varied forms of energy are categorized into non-renewable and renewable resources [1-4]. Energy is among the vital valuable assets for the sustained growth of humanity. Approximately 75% to 85% of the world's energy requirements are met by fossil fuels. Energy consumption is continuously increasing on a daily basis throughout the world, due to advancements on a wide variety of fronts which includes people's basic needs in daily lives, substantial growth in the motor industry for commercial and personal transit, rapid modernization, etc. Oil reserves are only found in specified locations of the world, and their availability is gradually decreasing each day. Figure 1.1 shows the top 10 countries with total proved oil reserves at the end of 2020. A lack of energy supply to support industrial activity in any sector can have a negative impact on a nation's economic development.

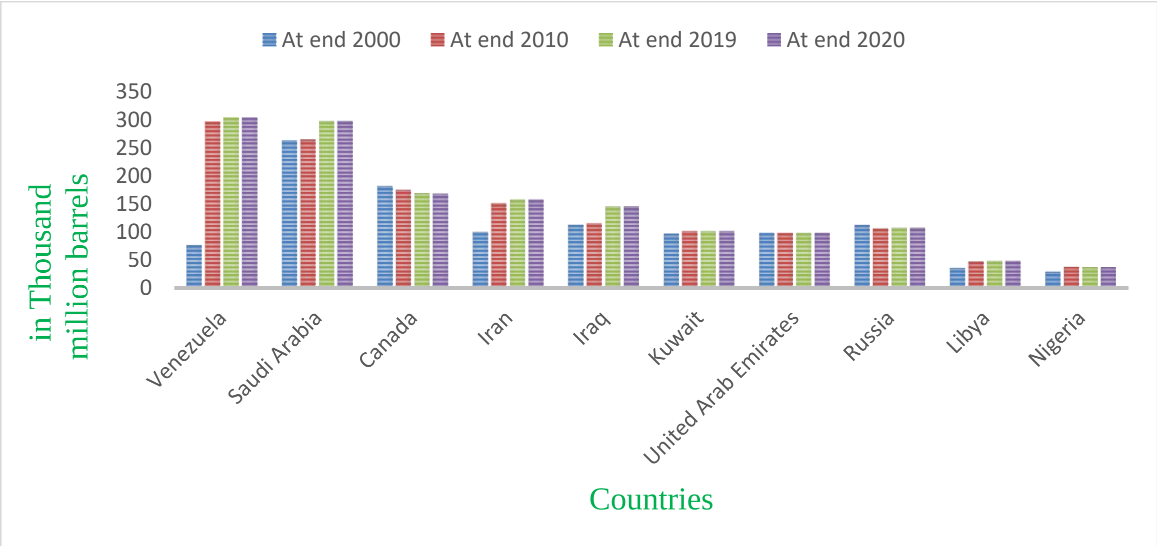

Figure 1.1 Top 10 oil reserve countries [5]

The use of automotive transportation is increasing at an alarming rate, which has a significant influence on oil reserves. The unsustainable condition of the world's energy oil deposits has an especially adverse effect on the transportation sector, which was completely reliant on crude oil. There will be a significant change in terms of end-user applications and energy transporters, caused by an imbalance between the demand and supply chain of fuel (petro-diesel).

Compression Ignition mixture is heterogeneous in nature, as compared to Spark Ignition where the ignitable mixture is often homogeneous. Unlike SI engines, CI engines are known for their superior fuel efficiency and compression ratio, low fuel cost, and hence they are widely used in the auto sector. Figure 1.2 shows the production rate of automobiles in India from 2016 to 2022.With the rise in the number of automobiles, fuel demand is also increasing exponentially. The major challenges that can arise as a result of increased fuel consumption are the non-availability of these reserves and environmental degradation. Diesel and gasoline consume the majority of the energy used for transit worldwide. The primary emission concentrations emitted by petro-diesel-powered vehicles include PM, NO_X, HC, CO, partial oxides of aldehydes, and SO_2 [6-8]. Furthermore, these emissions are hazardous to the environment and mankind. Pollutants from engine exhaust and their health impact on mankind are given in Table 1.1.

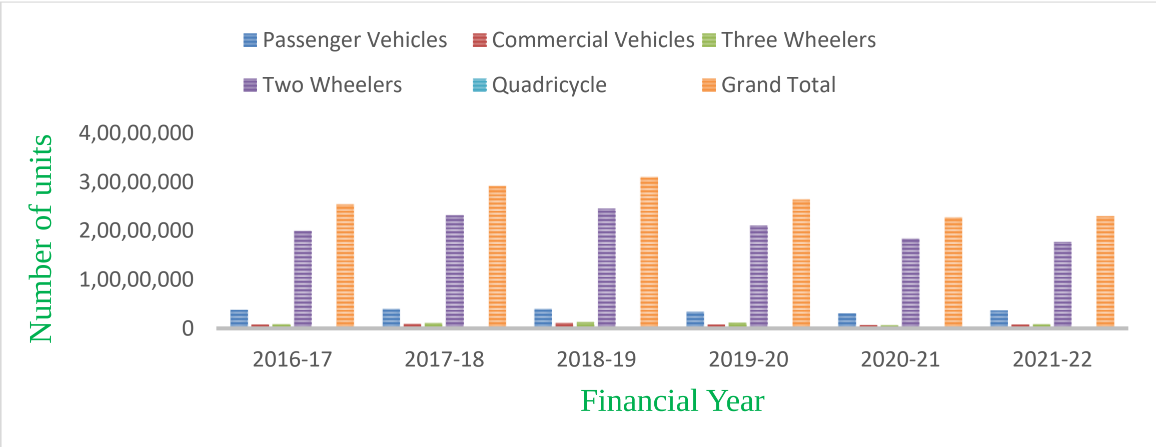

Figure 1.2 Automobiles production in India (2016-2022) [9]

Table 1.1 Effect of pollutants on human health [10]

Name of the Pollutant	Impact on human health
HC	Possibility of causing cancer.
Lead	Affects the kidney and liver. Lowers a child's I.Q by affecting their brain.
PM	Damages the immune system. Long term effect on lung tissue.
SO_2	Adverse effect on lungs.
NO_X	Causes throat and nose irritations. Also causes respiratory problems on pro-long exposure. Pulmonary diseases and increased infection rate.
CO	Affects the nervous and cardiovascular system.

Therefore, researchers are exploring fuel with superior characteristics to diesel to address the aforementioned constraints. Hence, alternative energy sources such as LPG-liquefied petroleum gas [11-14], CNG-compressed natural gas [15-18], alcohols [19-22], LNG-liquefied natural gas [23-25], and biofuels [26-28] were investigated. The majority of the research studies have demonstrated that alcohol fuels such as butanol, propanol, ethanol, and methanol [29] are feasible substitutes for gasoline engines. Alternative fuels such as CNG and LPG are used effectively in most parts of India. Research studies revealed that biofuels have the potential to become a viable alternative fuel for CI engines [30-32].

1.1 Biofuels

Biofuels are renewable fuels derived from biomass and are categorized into gaseous biofuels (such as syngas, biomethane, biogas, etc.), liquid biofuels (such as biodiesel, bioethanol), and solid biofuels (such as animal waste, wood pellets, wood residues, municipal waste, etc.). Biodiesel is a non-toxic biodegradable liquid fuel consisting of long chain fatty acids of mono alkyl esters with zero sulphur emissions. According to the International Renewable Energy Agency, by 2030, liquid biofuels contribute to 10% of the automotive industry’s energy consumption. Figures 1.3 and 1.4 portray the global liquid biofuel production and consumption of biodiesel in various sectors. Researchers [33, 34] have highlighted the following merits and demerits of using biodiesel in CI engines.

Merits

- Non-toxic in nature.
- Produced from renewable energy resources.
- Without any improvements in design changes, biodiesel can be utilized in CI engines.
- Low concentrations of CO and HC.
- Higher flash point, resulting in safe handling and storage.

Demerits

- Less volatile.
- Higher viscosity.

- Lower energy content (heating value).
- Increased NO_X concentrations.
- High SFC.

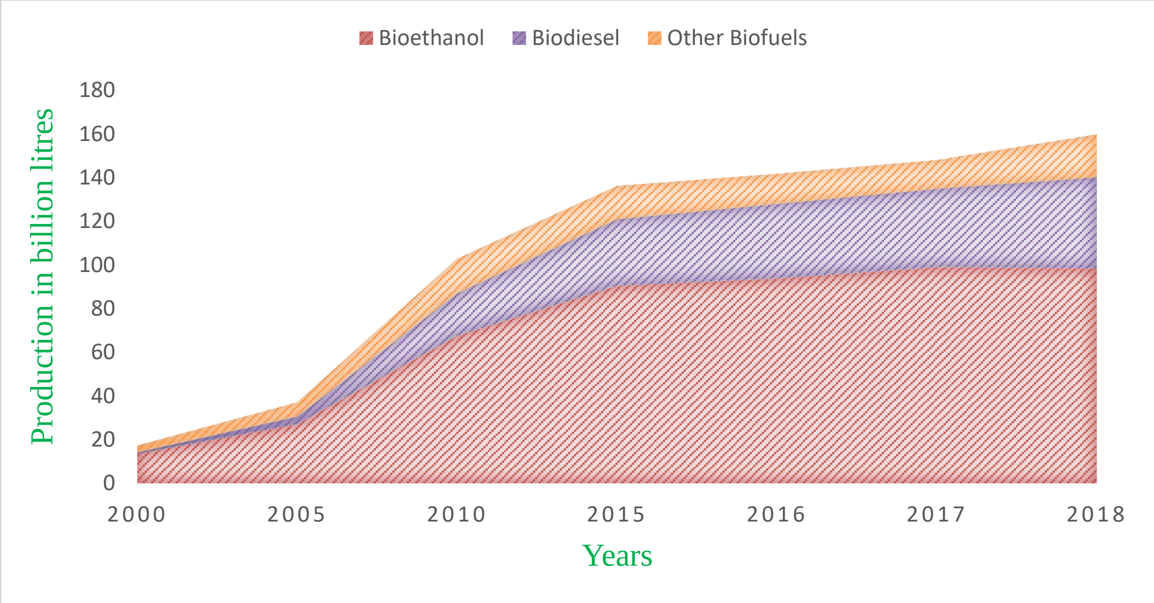

Figure 1.3 Production rate of liquid biofuels globally [35]

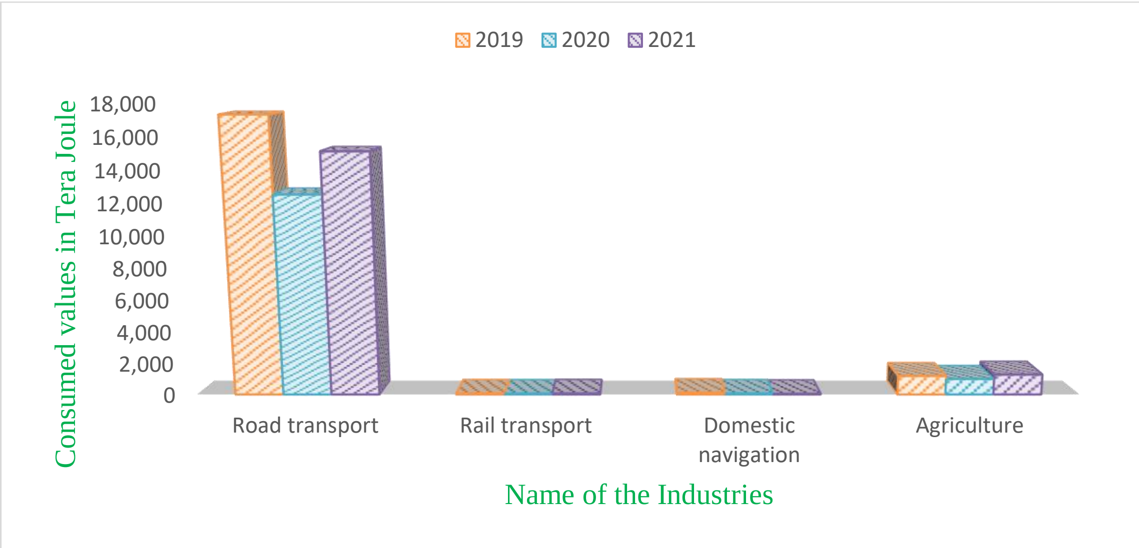

Figure 1.4 Biodiesel energy consumption in various sectors [36]

The various generations of biodiesel depending on their origin (biomass) and production (feedstock) are categorized as edible biomass also known as the first generation, non-edible biomass commonly referred to as the second generation, and algal biomass as the third generation [37-39]. Biomass derived from edible feedstock such as starch crops, grains, and vegetable oils are referred as the first generation. They include tamarind oil [40-42], sunflower oil [43-45], rapeseed oil [46-48], palm oil [49-51], sesame oil [52], coconut oil [53-55], ground nut oil [56-58], corn oil [59-61], etc (in Figure 5). They clash with food requirements, resulting in an increase in food prices. Biomass derived from non-edible feedstock such as abundant plant waste, agricultural bio waste, aquatic biomass, and forest residue are referred as the second generation. They include waste cooking oil [62-64], neem oil [65-67], castor oil [68-70], pongamia oil [71-73], jatropha oil [74-76], etc (in Figure 1.5). Owing to their non-corrosiveness, they are preferred over the first generation. Biodiesel from this generation eradicate food scarcities. Biomass derived from microalgae and macroalgae feedstock such as blue-green algae, golden-brown algae, yellow-green algae are referred as the third generation. They include chlorella protothecoides [77-79], botryococcus baraunii [80-82], neochloris oleoabundans [83-84], chlorella vulgaris [85-87], chlorella variabillis [88], etc. Consumes less water, can be harvested in a short period and can grow in saline, marine, and wastewater. Algae biodiesel extraction consists of four stages cultivation of algae, algae harvesting, algal oil extraction and algal oil conversion to biodiesel. Madras University, The Energy Research Institute, University of Pune are some of the institutes that are working on algae biodiesel in India.

Figure 1.5 Feedstocks of various I and II generation biodiesel [89]

1.2 National Policy on Biofuels – 2018: Government of India (GOI)

The advancement of human’s livelihoods depends heavily on energy. The development goals of GOI emphasize a common perspective for human well-being and equity, economic progress, capacity building and technology up-gradation, and national development. By 2030, the country's energy policy intends to meet the Govt's current ambitious disclosures in the energy sector, such as the contribution of non-fossil fuel-based electrical power generation is intended to be greater than 40%, and decrease in energy emissions concentrations by 33%-35%. Renewable energy sources are almost inexhaustible, non-polluting, and indigenous. On the other hand, fossil fuel resources must be utilized judiciously since they are non-renewable and limited. Only 17.9% of the demand is met by domestic crude oil, and the remaining portion is fulfilled by importing it. Currently, petrol and diesel alone account for 23% and 72% of transit fuel consumption, and the remaining portion is met by LPG and CNG. The road transport sector contributes 6.7% of India's GDP. 3.6% of the world's transit energy requirements in 2021, especially for road transport, were met by biofuels. Biofuels are also used in aviation sector for the past few years. Airliners that have used biofuels for their commercial flights include Azul Airlines, British Airways, Jet Blue, KLM, Lufthansa, Scandinavian Airlines, United Airlines, Virgin Australia, and Virgin Atlantic.

Biofuels are strategically significant in India because they align with the GOI ongoing projects like Waste to Wealth Creation, Employment Generation, Doubling Farmers' Income, Swachh Bharat Abhiyan, and Make in India. The GOI has made numerous efforts over the last decade to boost biofuels with initiatives like Biodiesel Blending Program, National Biodiesel Mission, and the Ethanol Blended Petrol Program. The policy has outlined to promote and develop indigenous feedstock for producing biofuels to gradually replace conventional fuels, and this policy also contributes to tackling climate change. By 2030, GOI set a target of achieving 5% blending of biodiesel in diesel and 20% blending of ethanol in petrol. Currently, 0.1% of biodiesel and 2% of ethanol is blended in diesel and petrol, respectively. India has an abundance of resources for renewable energy. Table 1.2 shows the indigenous raw materials [26,27] for biofuel production in India. The GOI has planned to achieve the goal by

- Establishing a conducive atmosphere for biofuels and integrating them with base fuels.
- Development of novel technology for biofuel conversion.

- Developing new resources of biofuel feedstock.
- Constructing bio refineries.
- Enhancing domestic production to support ongoing ethanol and biodiesel supplies.

Table 1.2Raw materials for biofuel production

Biofuel	Raw materials
Biodiesel	Algal feedstock, Acid oil, Animal tallow,
	Used cooking oil, Non-edible oil seeds, etc.
Ethanol	Food grains during the surplus phase, Food grains that
	have been damaged and inappropriate for human consumption,
	Substances that include starch such as rotten potatoes, corn, etc.
	Substances that include sugar such as sweet sorghum, sweet sorghum, etc.
	Agriculture residues, sugar cane juice.

1.3 Fuel additives

Numerous researchers have explored the diesel engine attributes utilizing varied mixtures of biodiesel feedstock and observed that, compared to diesel, the thermal efficiency of biodiesel-fueled CI engine decreases, and fuel consumption and NO_X concentrations are enhanced [90-92]. The drawbacks associated with using biodiesel as fuel in CI engines can be overcome by adding hybrid fuel and fuel additives in biodiesel. Fuel additives are the chemical substances blended with base fuel to modify the fuel attributes. They are categorized into various groups namely polymer-based additives, tocopherol additives, water additives, nanoparticles-based additives, and oxygen-rich additives. The primary characteristics of fuel additives are summarized below [93].

- To enhance O_2 concentration during combustion.
- Enhanced calorific value.
- Shorter ignition delay.
- Enhance the fuel stability.
- Reduced flash point.
- Decreased concentrations of exhaust emissions.

1.4 Nanoparticles

A particle diameter of 1-100 nm in size is known as nano particles and is manufactured in varied shapes, including non-spherical (rod, cube, prism, etc.) and spherical, and possesses a high surface-to-volume ratio. They are further sub-divided based on their diameters: coarse particles (2500-10000 nm) and fine particles (100-2500 nm). The nano additives utilized in the CI engines include magnetic nano particles (such as ferro fluids), carbon nanotube nano particles, metal oxide nano particles (such as zinc oxide, titanium oxide, aluminum oxide, etc.) [94-102], and metal nano particles (such as titanium, zinc, silver, boron, iron, aluminum, etc.) [103-111]. Applications of nano additives in CI engines include enhancing thermal efficiency, decreasing fuel consumption, reducing friction and wear, etc.

1.5 Organization of Thesis

The thesis is organized in the following order:

Chapter 1: The thesis begins with an overview that briefly discusses the significance of energy derived using renewable resources and their need as a substitute fuel in CI engines. Also explains the significance of fuel additives.

Chapter 2: Provides a literature review on the utilization of biodiesel as a substitute fuel for diesel engines and the effect of nano additives blended fuel on CI engine characteristics. The studies related to ANN are also discussed. Finally, research objectives were defined.

Chapter 3: The research methodology and the experimental test rig used for the present investigation are discussed in this chapter.

Chapter 4: Discusses the optimization techniques and the concept of ANN. An ANN model developed for the present investigation is also explained. In addition, the analysis of ANN on performance and emissions attributes is discussed.

Chapter 5: Explains the impact of spirulina biodiesel and its blends with aluminum oxide and magnesium oxide nano additives on CI engine attributes.

Chapter 6: Concludes the major findings of the current research investigation.

CHAPTER 2

LITERATURE REVIEW

Compression Ignition engines are presently among the most effective energy systems available worldwide. With or without improvements, a diverse array of renewable fuels can be combusted in CI engines. One of such fuels is biofuels. Biofuels as substitutes for conventional fuel have piqued the attention of investigators. Tests using biodiesel derived from tamarind seed were carried out [41]. In their investigation, B100 and B20 compositions were used. They reported a significant reduction in HC and CO emittants. The effect of varied injection timing (27° bTDC, 23° bTDC and 19° bTDC) utilizing tamarind seed biodiesel was investigated [42]. With 23° bTDC injection timing BTE deteriorated by 5.14%. The researchers also reported that for all IT BSFC remained lower in contrast to diesel. Sunflower Oil Methyl Ester as a viable alternative in CI engine was investigated [43]. Under the varied ID Period, emissions and performance analysis of DICI engine was analyzed. The investigation revealed that with 250 bar IP at IT of 23° bTDC lower emissions concentrations and better efficiency were obtained.

Experimental investigations employing rapeseed oil was executed [47].The study analyzed the impact of 20, 10, and 0% of volumetric concentrations of rapeseed oil in the base fuel of air-cooled CI engine. Measurements of engine attributes at varied rpm were studied. Results revealed, at 3000 rpm, NO_x and CO deteriorated. Furthermore, the lowest SFC and higher torque were reported for B10D90. The potential of rapeseed biodiesel was reviewed as a fuel substitute [48]. Review findings revealed that higher BSFC, lower BTE and HRR, and reduced ID can be achieved with either blended or pure rapeseed biodiesel. Additionally, the engine components are not adversely impacted by its use. The combination of amalgams of higher alcohol and palm oil biodiesel were tested [50]. The fuel used was POBD70O30, POBD80O20, POBD90O10, and POBD100. Trials were conducted on a 4.2 kW, multi cylinder CI engine. The addition of octanol enhances the fuels oxidation stability, thereby reducing the emissions concentrations. For POBD80O20 higher BTE was observed.

The biofuel production using sesame Oil was experimented [52]. Investigators obtained sesame oil from M/S Gattumal Aausdhalya, Bareilly. Using the transesterification technique oil was converted into biodiesel. They observed that with2.3% w/voil sodium hydroxide and 10:1 ethanol to oil ratio, using the esterification process, maximum biodiesel yield was attained. Synthesis of biodiesel from coconut oil was carried out with 0.5% NaOH at 60◦C [55]. The biodiesel's density, heating value, and viscosity were evaluated. The mean deviations were noticed to be 2.44, 2.62, and 1.12% respectively, for heating value, density, and viscosity.

Ethyl esters of groundnut oil and their blends were analyzed as a replacement fuel in DI diesel engine [57]. In the entire experimentation, test engine observations were recorded at 1500 rpm. B80EEGAO, B60EEGAO, B40 EEGAO, and B20EEGAO are the test fuel compositions. At maximum load, compared to diesel, lower smoke density for B20EEGAO was reported by investigators. Amalgam B20EEGAO has the higher BTE of 28.80%. They concluded that without necessitating any engine improvements, the B20EEGAO can be employed as an alternate solution for diesel. Trails in naturally aspirated water-cooled CI engine were performed using blends of waste cooking oil [63]. CI engine attributes were correlated with diesel. For waste cooking oil blends NO_X, CO_2 enhanced and CO, HC declined. A feasibility study was carried out on neem oil biodiesel [66, 67]. Substantial reductions in CO and unburned hydrocarbons were noticed, while running the engine with neem oil blends.

The influence of the use of jatropha biodiesel amalgams was analyzed [75]. J50, J40, J30, J20, J10, and J5 were the fuel compositions explored. With higher compositions, BTE reduced considerably from 4.4% to 7.7%. The blends exhibited lower concentrations of nitrous oxide and hydrocarbon emissions. Chlorella emersonii as an alternate fuel was explored [79]. The engine was fueled with 100, 40, 30, 20, and 10% of volumetric ratios of chlorella emersonii biodiesel. The biodiesel amalgams exhibited a shorter ID. In terms of performance, the B20 amalgam was on par with diesel. The CP and HRR were also comparatively lower, at peak load. Emissions namely acetaldehyde and toluene showed a downturn. With chlorella emersonii amalgams lower concentrations of HC and oxides of nitrogen were reported.

In a DI diesel engine, experiments were carried out utilizing amalgams of botryococcus braunii and oxy-acetylation [82]. Mass flow rates of acetylene employed are 300, 200, 150, and 100 g/hr. As per ASTM standards, fuel characteristics are determined. They reported; oxy-acetylation and botryococcus braunii possess enhanced calorific value. The use of oxy-acetylation showed improved performance, compared to diesel. Due to acetylation addition BTE increased by 5, 4.2, 3.8, and 3.7% respectively.

Reduction in emissions HC, CO, NO_X, and CO_2 was found for oxy-acetylation and botryococcus braunii blends. Influence of biodiesel blends on CI engine attributes is given in Table 2.1. The role of additives in biodiesel was reviewed [90 91]. A comprehensive review on characterization, preparation, and usage of nano additives CI engine was reported by ref [92, 93]. They concluded that metal based additives can be used to enhance performance attributes and reduced emittants. An attempt to enhance the CI engine characteristics by adding nano additives was analyzed [94]. By doping 30ppm cerium oxide and alumina nano particles, an investigation was carried out on a single cylinder diesel engine. As compared to B100, cerium oxide and alumina blended fuel resulted in a 44% downturn in HC, 60% downturn in carbon monoxide, 30% reduction in NO emiitants, respectively. Also, they reported that BTE improved by 12%, with the addition of additives.

An investigation on graphene oxide was carried out as a performance enhancer in biodiesel mixtures [96]. The mass fractions of 100, 75, 50, and 25 ppm graphene oxide were doped in biodiesel. The efficient reduction in BSFC was reported by the investigators. Additionally, BTE improved further, due to the enhanced heating value of the nano additives mixtures. Effect of metal oxide was analyzed as a fuel catalyst [100]. Metal oxide of doping concentrations 150 and 100 ppm were investigated. For mixture preparation magnetic stirrer was employed. They revealed a 15.91 and 5.21% increment in BTE for nano doped fuel mixtures. Furthermore investigators found that with 150 and 100 ppm nano doped fuel, BSFC decreased by 14.06 and 7.14% respectively. The addition of metal oxide nano additive led to significant downturn in CO, HC, and NO_X emissions.

Emissions and performance analysis was executed using nano particle cerium oxide in mahua oil blends [102]. Ultrasonication method was used to prepare the homogenous mixture. The cerium oxide 150, 100, and 50 100 were dispersed in the mahua biodiesel mixture (B20). The obtained outcomes were compared with B20. Their results disclose a decreasing trend in BSFC and improved BTE for nano doped blends. Also, a drop in CO, HC, and NO_X was reported. The research work on silicon oxide, carbon nano tube, and ferrous oxide nano additives were carried out [103, 104]. They concluded that nano additives play a pivotal role in reducing the harmful emissions and achieving better performance. Table 2.2 represents the influence of nano additives in biodiesel mixtures on CI engine attributes.

For evaluating both multi and single characteristics of test parameters that influence target variables, optimization techniques are regarded as efficient and cost-effective [112], and these models are rapidly emerging and extensively employed tools for a diverse array of industrial complexities. System design, product and process optimization, energy applications, and analytical chemistry are some of the scientific areas where ANN has been vastly implemented [113]. A comparative review was carried out on ANN for the prediction of waste cooking oil fuelled CI engine characteristics [119]. They stated that in comparison to mathematical models, ANN is the most productive tool for forecasting engine attributes. The application of ANN in mechanical engineering was reviewed by ref [120].

ANN model utilizing a quasi-newton learning algorithm was proposed [122] for forecasting engine attributes fuelled with orange-peel oil. The algorithm outcomes resulted in least mean relative error. An ANN model was constructed [124] using trainlm algorithm with target variables smoke concentrations, nitrogen oxide, hydrocarbons, thermal efficiency, carbon monoxide, and specific fuel consumption. They built a multi-input multi-output intelligent ANN model. The performance accuracy of their model was revealed to be 88.61%. In a different study [126], ANN projected the engine characteristics with a root mean square of 0.0359%. They concluded that ANN can indeed be a reliable tool for forecasting emission attributes. Optimization models based on nelder-meads simplex and ANN (MIMO) were investigated [128]. For non-linear mapping between target and input parameters, Multi layer perception (MLP) was employed. The logsig and tansig were chosen as activation functions for output and hidden layers. The optimum ANN architecture is found to be 3-7-5. They concluded that both the models exhibited a strong correlation, found in the range of 0.94 to 0.99, respectively.

Performance parameter using varied injection timings of diesel engine was assessed [132]. Furthermore, an ANN model was also constructed for projecting the performance parameters. For varied training algorithms ANN model was tested. This analysis was performed by varying the neurons in hidden layer from 4 to 20. The predicted MRE is in the range 0.62–4.82% and R values were in between 0.97 to 0.99. ANN model based on the back propagation algorithm was established [137] to forecast the target variables based on input parameters (fuel blending ratio, engine speed, and engine load). Mean relative error and R of the ANN model was explored. The

MRE was well within the acceptable range, and hence they concluded that for projecting engine attributes ANN optimization is highly recommended. Using MATLAB modeling tool ANN has been effectively employed for predicting attributes of CI engine [155, 156]. Based on the design of laboratory test results modeling computational techniques namely ANN and RSM were generated to establish a forecasting model [157]. Their investigation concluded that an optimal response for the ANN model was more reliable and accurate than RSM model. Using an ANN a micro-tri-generation [158] model was developed for assessing experimental data (emittants and performance attributes) obtained from varied fuel amalgams namely karanja biodiesel, karanja oil, and diesel. Their results indicated that the micro-tri-generation ANN model was capable of precisely forecasting the engine attributes with R values of 0.9948, 0.9944, 0.9945, and 0.9950 for R_{all}, R_{test}, R_{val} and R_{train}, respectively. Table 2.3 gives the interpretations of varied ANN models.

2.1 Research gap

Following an investigation of the literature, it was revealed that biofuels can be utilized as a diesel substitute. The resources of biofuels include algae (micro and macro), non-edible, and edible feedstock. There is an abundance of literature exists on the parameters of DICI engines, fuelled with non-edible and edible biofuels. To date, very limited investigation has been carried out on algal biodiesel as a replacement for conventional fuel. Furthermore, from the literature survey, it is evident that nano metal oxides additives enhances efficiency and reduce emittants.

2.2 Research objectives

The following objectives have been framed for the current investigation based on the research gap.

- To investigate the physicochemical properties of spirulina biodiesel blends.
- To investigate the effect of spirulina biodiesel blends on engine performance and emissions.
- Investigating the effect of nanoparticles magnesium oxide and nano alumina as an additive in spirulina biodiesel blends on engine performance and emissions.
- Prediction of performance and emissions characteristics using Artificial Neutral Network.

Table 2.1 Interpretation of CI engine attributes of various generations of biodiesel and their blends

Engine operating condition	Biodiesel derived from	Blend	UHC	CO_2	NOX	BTE	BSFC	Ref
			Compared with base fuel at full load					
Constant IT, IP 17.5 CR	Tamarind seed	B100 B20 B10	Reduced	Enhanced	Enhanced	Reduced	Enhanced	[41]
Varied IT (19°bTDC)	Tamarind	B20	Reduced	NA	Reduced	Reduced	Enhanced	[42]
23°bTDC	seed		Enhanced	NA	Identical	Reduced by 5.14 %		
27°bTDC			Enhanced	NA	Enhanced	Reduced		
Constant IT, IP, CR 22.6 CR	Sunflower oil	B100 B20 B5	Reduced	Enhanced by 14%	Enhanced by 5%	Reduced	Enhanced by 11%	[44]
Constant IT, IP, CR	Sunflower oil	B75 B50 B25	Reduced	Enhanced	Enhanced	Reduced	Enhanced	[45]
Constant IT, IP, CR 17.5 CR	Rapeseed oil	B100 B75 B50 B25	Reduced by 42.1 % Reduced by 32.2 % Reduced by 26.7 % Reduced by 15.4 %	NA	Enhanced by 32.9% Enhanced by 28.5% Enhanced by 21.6% Enhanced by 14.4%	Reduced	Enhanced by 29.6% Enhanced by 24.1% Enhanced by 19.2% Enhanced by 8.5%	[46]
Constant IT, IP 17.5 CR	Palm oil	B100 B20	Reduced	NA	Enhanced	Reduced	Enhanced	[49]
Constant IT, IP 16.5 CR	Palm oil	B100 B50 B10	Reduced	Enhanced	Enhanced	Reduced	Enhanced	[51]
Constant IT, IP 16.7 CR	Coconut oil	B100 B20	Reduced	NA	Reduced by 14.63% Reduced by 8.14%	Reduced by 13.65% Reduced by 9.08%	Enhanced by 6.59% Enhanced by 5.40%	[53]
Constant IT, IP 17 CR	Butanol Coconut oil	C20B20 C20B10	Reduced Reduced	Reduced by 8.8% Reduced by 6.2%	Reduced by 7.4% Reduced by 5.9%	NA NA	Enhanced by 7.97% Enhanced by 5.54%	[54]

Constant IT, IP 17.5 CR	Groundnut oil	B50 B30 B10	Reduced	Enhanced	Reduced	Reduced	Enhanced	[56]
Constant IT, IP 16 CR	Corn oil	B30 B20 B10	Enhanced	NA	Reduced	Reduced	Enhanced	[59]
Constant IT, IP 17.1 CR	Corn oil	B100 B80 B60 B40 B20	Reduced	Reduced	NA	Enhanced by 8.56%	Reduced by 4.43%	[61]
Constant IT, IP	Waste cooking oil	B100 B70 B50 B30 B20 B10 B5	Reduced by 5%	NA	Reduced by 10%	Reduced by 6%	Enhanced by 10-30%	[62]
Constant IT, IP 17.5 CR	Waste cooking oil	B20 B10	Reduced	Enhanced	Enhanced	Identical	Identical	[64]
Constant IT, IP 17.5 CR	Neem oil	B20	Reduced by 18.75%	Enhanced	Enhanced	Reduced by 4.4%	Enhanced by 6%	[65]
Constant IT, IP 17 CR, 1500, and 2000 rpm	Castor oil	B20 B5	Reduced	Enhanced	Reduced	Reduced	Enhanced	[68]
Constant IT, IP 17.5 CR	Castor oil	B20 B10 B5	Reduced	Enhanced	Reduced	Reduced	Enhanced	[69]

Constant IT, IP 16.7 CR	Pongamia oil	B30 B20 B10	Reduced by 13.8%	NA	Enhanced by 36.71%	Reduced by 28.68%	Enhanced by 17.36%	[71]
Constant IT, IP 16 CR	Pongamia oil	B100	Reduced by 36%	NA	Reduced by 12.7%	NA	Enhanced by 9.4%	[73]
Constant IT, IP 17 CR	Jatropha	B100 B80 B60 B40 B20	NA	NA	Enhanced by 47%	Reduced by 33%	NA	[74]
Varied engine speeds 1770-3800 rpm	Chlorella protothecoides	B100 B50 B20	NA	Reduced by 4.2% at 2900 rpm	Reduced by 7.4% at 2900 rpm	NA	Enhanced by 10.2% at 2900 rpm	[77]
Constant IT, IP 17.5 CR	Chlorella protothecoides	B100 B20 B15 B10 B5	NA	Enhanced by 4.67%	Reduced by 13.54%	Reduced by 3.15%	Enhanced by 15.96%	[78]
Constant IT, IP 17.5 CR	Botryococcus braunii	B30 B20	NA	Reduced by 12% Reduced by 8%	Reduced by 11% Reduced by 4%	Reduced by 10.41% Reduced by 7.5%	Enhanced by 17.3% Enhanced by 11.92%	[80]
Constant IT, IP 17.5 CR	Botryococcus braunii	B20	Reduced	Reduced	Reduced	NA	NA	[81]
Constant IT, IP 16.5 CR	Neochloris oleoabundans	B20	Reduced	NA	Reduced	Reduced	Enhanced	[83]
Constant IT, IP 17.5 CR	Chlorella vulgaris	B60 B50 B40 B30	Reduced 13-13.8%	Reduced by 1-1.5%	Reduced by 4-6%	Reduced by 12.7% Reduced by 6.66% Reduced by 3.31% Reduced by 1.67%	Enhanced	[85]
Constant IT, IP 17.5 CR	Chlorella vulgaris	B20	Reduced	Reduced	Reduced	Reduced	Enhanced	[87]

Constant IT, IP 17.5 CR	Dunaliella tertiolecta	B20	Reduced	Reduced	Reduced by 12.11%	Reduced by 2.8%	Enhanced	[153]
	Scenedesmus obliquus	B20	Reduced	Reduced	Reduced	Reduced by 3.85%	Enhanced	
	Scenedesmus dimorphu	B20	Reduced	Reduced	Reduced by 14.16%	Reduced by 3.91%	Enhanced by 3.22%	
Constant IT, IP 17.5 CR	Raw Algal oil	B30	Reduced	Reduced by 4.26%	Reduced	Reduced	Enhanced	[154]
		B20	Reduced by 1.08%	Reduced by 4.22%	Reduced	Reduced by 1.53 %	Enhanced by 3.38 %	
		B10	Reduced	Reduced by 3.99%	Reduced	Reduced	Enhanced	

Table 2.2 Interpretation of CI engine attributes on the influence of nano additives in biodiesel mixtures

Engine operating condition	Nano additive	Biodiesel derived from	Test fuels	UHC	CO_2	NOX	BTE	BSFC	Ref
				Compared with base fuel at full load					
Constant IT, IP 16.5 CR	Ruthenium oxide	Neochloris oleoabu- ndans	B20+100RO B20+75RO B20+50RO B20+25RO	Reduced by 32.5%	NA	Enhanced by 11.3%	Enhanced by 3.5%	Reduced by 29.4%	[83]
Constant IT, IP 17.5 CR	Ruthenium oxide	Chlorella vulgaris	B20+100RO B20+50RO	Reduced by 7.02%	NA	Enhanced by 1.29%	Enhanced by 1.56 % Enhanced by 0.82 %	Reduced by 6.34 % Reduced by 3.51 %	[87]
Constant IT, IP 17.5 CR	Alumina Cerium oxide	Jatropha	B100A30C30 B20A30C30	Reduced by 0.6% Reduced by 0.52%	NA	Enhanced	Reduced by 4.03% Reduced by 3.91%	Enhanced	[94]
Constant IT, IP varied CR	Alumina	Neem oil	B10A50 B10A25	Reduced	Enhanced	NA	Reduced	Enhanced	[95]
Constant IT, IP 17.5 CR	Cerium oxide	Mahua oil	BC25	Reduced by 43.67%	NA	Reduced by 26.80%	Reduced	Enhanced	[97]
Constant IT, IP 17.5 CR	Alumina	Palm oil	B20A75 B20A50 B20A25	Reduced by 13.08%	Enhanced by 8.3%	Reduced by 7.1%	Enhanced by 11.8%	Reduced by 12.5%	[98]
Constant IT, IP 17.5 CR	Alumina	Rubber seed	B25A50 B25A25	Reduced by 24 ppm Reduced by 20 ppm	Enhanced by 14% Enhanced by 9%	Enhanced	Enhanced	Reduced	[99]
Constant IT, IP 17.5 CR	Iron	Palm oil	B30I75 B30I50	Reduced	Enhanced	Reduced	Enhanced by 2.3% Enhanced by 2.2%	Reduced	[101]
Constant IT, IP 17.7 CR	Silicon oxide carbon nano	Diesel	DC100 DC50 DC25	Reduced by 16.6 ppm	Enhanced by 2.73%	Enhanced	Enhanced by 17.1%	Enhanced by 1.94%	[103]
	Alumina		DA100	Reduced by 17.8 ppm	Enhanced by 1.52%		Enhanced by 14.3%	Enhanced by 0.54%	

			DA50 DA25 DS100 DS50	Reduced by 16 ppm	Reduced by 1.55%		Enhanced by 11.9%	Enhanced by 0.24%	
Constant IT, IP 19.5 CR	Zinc oxide Cerium oxide	Soybean oil	B25ZC75 B25ZC50 B25ZC25	Reduced by 21.5% Reduced by 19.1 ppm Reduced by 15%	NA	Reduced by 11.46%	Enhanced	Reduced	[105]
Constant IT, IP 17.5 CR	Cerium oxide	Waste cooking oil	B20W80 B20W30 B20W10	Reduced by 7%	NA	Reduced	NA	Reduced by 4.5%	[106]
Constant IT, IP 17.5 CR	Titanium dioxide	Diesel	DT25	Reduced by 18%	Enhanced by 25%	Enhanced by 32.2%	Enhanced by 1.4%	Reduced by 3.8%	[109]

Table 2.3 Interpretation of CI engine attributes of varied ANN models

Evaluation metrics	UHC	BTE	CO_2	BSFC	NO_X	Training algorithm	Optimum topology	Ref
MRE (%)	3.42	0.864	NA	0.568	4.01	Quasi	NA	[122]
R^2	0.994	0.994		0.986	0.997	newton		
R^2	0.9264	0.9784	NA	0.985	0.9979	Levenberg marquardt	NA	[123]
RMSE	1.9667	0.344	NA	1.8537	1.9493	Levenberg	2-13-6	[124]
R^2	0.9997	0.9991		0.9885	0.9991	marquardt		
R^2	0.97	0.99894	NA	0.9971	0.99015	Levenberg marquardt	4-8-7	[125]
RMSE (%)	0.54	0.54	NA	NA	4.89	Levenberg	2-17-5	[126]
R	0.99579	0.9985			0.9956	marquardt		
MAE (%)	1.07	1.07			0.36			
R^2	0.9883	0.9994	NA	0.999	0.999	Levenberg marquardt	2-25-5	[127]
RMSE (%)	1.79	2.03	NA	0.00045	14.71	Levenberg	3-7-5	[128]
R^2	0.842	0.998		0.811	0.601	marquardt		
RMSE (%)	0.0195	0.0152	0.01584	0.0264	0.0103	Levenberg	4-16-3	[129]
R	0.9937	0.99976	0.99974	0.998	0.9998	marquardt	4-14-14-6	

MRE (%) R^2	NA NA	4.2 0.982	NA NA	4.15 0.9851	2.99 0.9781	Levenberg marquardt	2-10-5	[130]
MAPE (%)	8.21	1.89	4.05	2.27	6.43	Levenberg marquardt	5-28-8	[131]
MRE (%) R	2.495 0.992	3.078 0.996	2.495 0.989	NA	0.621 0.99	Levenberg marquardt	3-14-11	[132]
R^2	0.997	NA	0.998	0.99788	NA	Levenberg marquardt	2-5-7	[133]
R	0.99899,	NA	NA	NA	0.9998	Levenberg marquardt	3-12-4	[134]
MSE R	0.015 0.985	0.001 0.999	0.001 0.999	0.98 0.02	0.001 0.999	Levenberg marquardt	2-17-9	[135]
RMSE (%) R^2	3.935 0.8847	0.421 0.9073	NA	NA	0.596 0.9082	Levenberg marquardt	NA	[136]
MRE (%) R^2	3.33 0.983	0.51 0.9829	NA	0.662 0.985	4.06 0.9831	Levenberg marquardt	3-11-8	[137]
R	NA	NA	0.951	NA	0.946	Levenberg marquardt	1-15-7	[138]
MSE R	0.0213 0.98506	NA	0.0088 0.99977	0.00086 0.99912	0.00025 0.9998	NA	2-X-5	[139]

CHAPTER 3

MATERIALS and METHODS

This chapter explains in detail regarding the experimental investigation and numerical optimization of the present research work. The CI engine attributes (NO_X, CO_2, HC, BTE, and BSFC) are assessed using biodiesel derived from spirulina and their blends without and with nano additives. Numerical optimization is performed, using ANN to predict the output parameters. The methodology employed for the current investigation is represented in Figure 3.1.

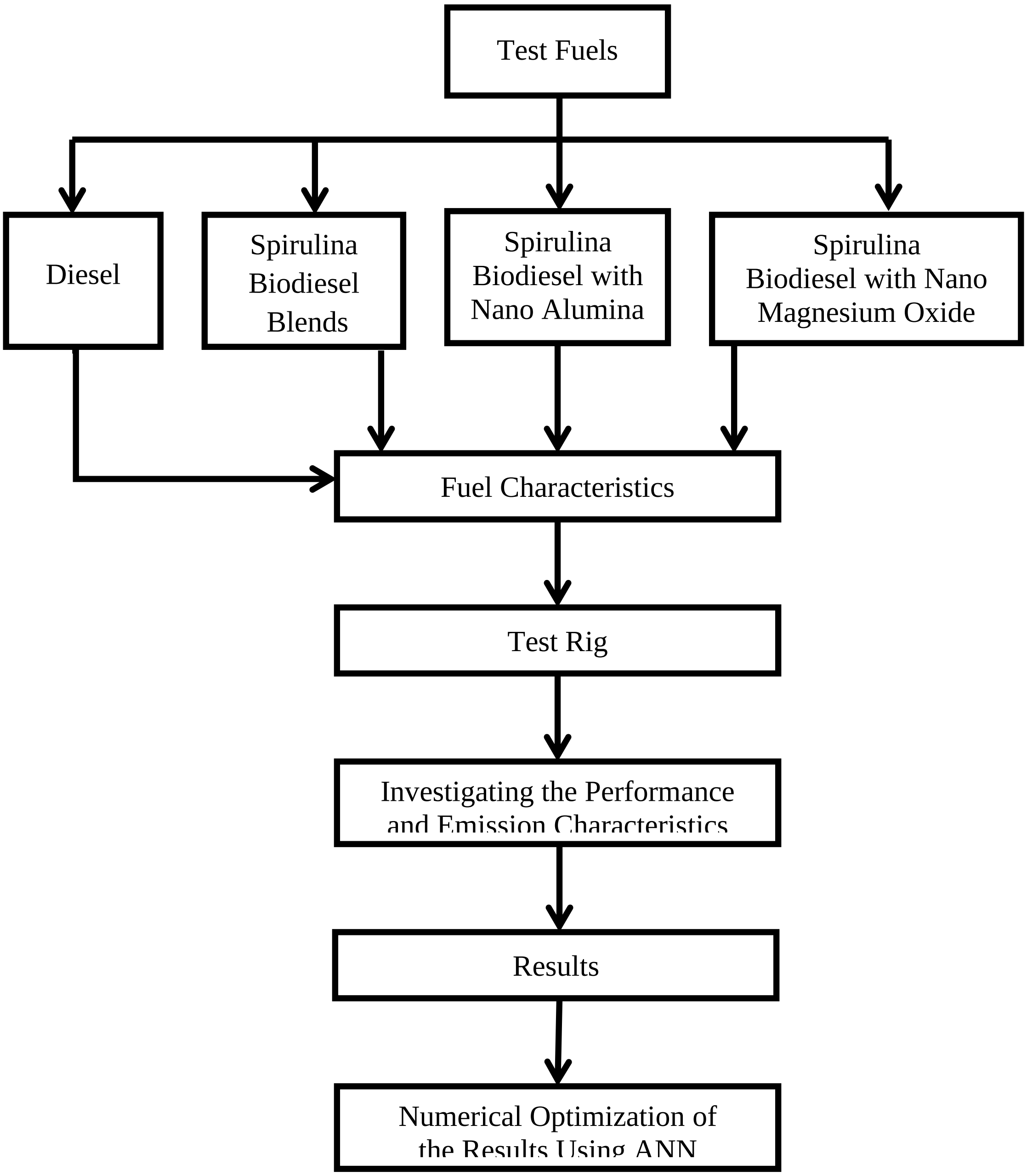

Figure 3.1 Flow chart of research methodology

3.1 Preparation of Test Fuels

Biodiesel obtained from third generation feedstock namely microalgae spirulina, and their blends were evaluated as test fuels in the first phase of this research work. Microalgae spirulina biodiesel is procured from Planet Industries Pvt Ltd, New Delhi. Diesel fuel was purchased from a local fuel pump vendor. Based on the volume concentrations, test fuels were termed as:

- SB0: 100% diesel.
- SB20: 80% diesel + 20% microalgae spirulina biodiesel.
- SB35: 65% diesel + 35% microalgae spirulina biodiesel.
- SB50: 50% diesel + 50% microalgae spirulina biodiesel.
- SB65: 35% diesel + 65% microalgae spirulina biodiesel.
- SB80: 20% diesel + 80% microalgae spirulina biodiesel.
- SB100: 100% microalgae spirulina biodiesel.

In the second phase, nano additive aluminum oxide (Al_2O_3) is dispersed into the microalgae spirulina biodiesel. Nano Wings Pvt Ltd, Khammam, India, supplied the nano additives. Table 3.1 and Figure 3.2 give the specifications and EDS analysis of the Al_2O_3nano additive. The Al_2O_3nano additive (in Figure 3.3) with a volumetric composition of 25 ppm is weighed using a digital electronic weighing instrument and dispersed using an ultrasonicator [93] device into the microalgae spirulina biodiesel amalgams and the resultant test fuel was named as:

- SB0: 100% diesel.
- SB20Al_2O_3: 80% diesel + 20% microalgae spirulina biodiesel + 25ppm Al_2O_3.
- SB35Al_2O_3: 65% diesel + 35% microalgae spirulina biodiesel + 25ppm Al_2O_3.
- SB50Al_2O_3: 50% diesel + 50% microalgae spirulina biodiesel + 25ppm Al_2O_3.
- SB65Al_2O_3: 35% diesel + 65% microalgae spirulina biodiesel + 25ppmAl_2O_3.
- SB80Al_2O_3: 20% diesel + 80% microalgae spirulina biodiesel + 25ppm Al_2O_3.
- SB100Al_2O_3: 100% microalgae spirulina biodiesel + 25ppm Al_2O_3.

Ultrasonication technique was carried out for 35 minutes duration at a frequency and power of 50 kHz and 120W. Ultrasonication is the effective strategy for dispersing nano particles in a fuel because it enables nano particles that may have agglomerated to rebound to the nanometer scale. Sonication is a technique that utilizes sound waves to agitate particulates in a fluid. Figure 3.4 displays the ultrasonicator device utilised in the dispersing of nanopartciles.

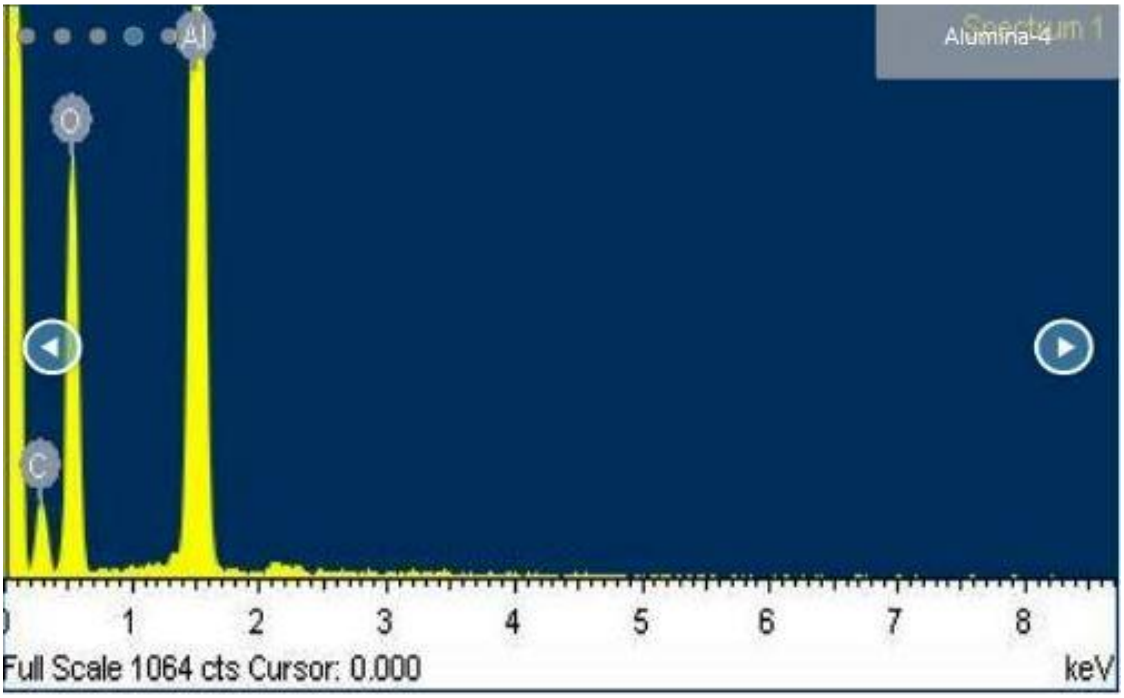

Figure 3.2 EDS analysis of nano alumina (Datasheet)

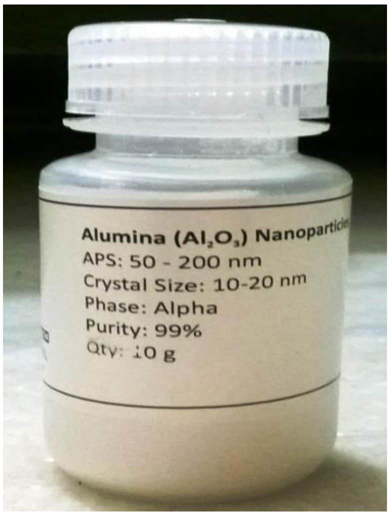

Figure 3.3 Nano alumina

Figure 3.4 Ultrasonicator

In the third phase, nano additive magnesium oxide (MgO) is dispersed into the microalgae spirulina biodiesel. Table 3.1 gives the specifications of MgO nanopartciles. Figure 3.5 gives EDS analysis of the MgO nano additive. The above methodology is applied for dispersing MgO nano additive with a volumetric composition of 25 ppm in the biodiesel blends. The resultant test fuel was termed as:

- SB0: 100% diesel.
- SB20MgO: 80% diesel + 20% microalgae spirulina biodiesel + 25ppm MgO.
- SB35MgO: 65% diesel + 35% microalgae spirulina biodiesel + 25ppm MgO.
- SB50MgO: 50% diesel + 50% microalgae spirulina biodiesel + 25ppm MgO.
- SB65MgO: 35% diesel + 65% microalgae spirulina biodiesel + 25ppm MgO.
- SB80MgO: 20% diesel + 80% microalgae spirulina biodiesel + 25ppm MgO.
- SB100MgO: 100% microalgae spirulina biodiesel + 25ppm MgO.

Table 3.1 Specifications of alumina and magnesium oxide nano additive

Parameters	Alumina NP	Magnesia NP	Units
HSN Code	28182090	25199040	
Form	white powder	White powder	appearance
Thermal conductivity	30	48	W/mK
Purity	99	99	%
Molar mass	101.96	40.304	g/mol
Crystal Size	10-20	10-20	nm
Density	3.987	3.6	g/cm^3

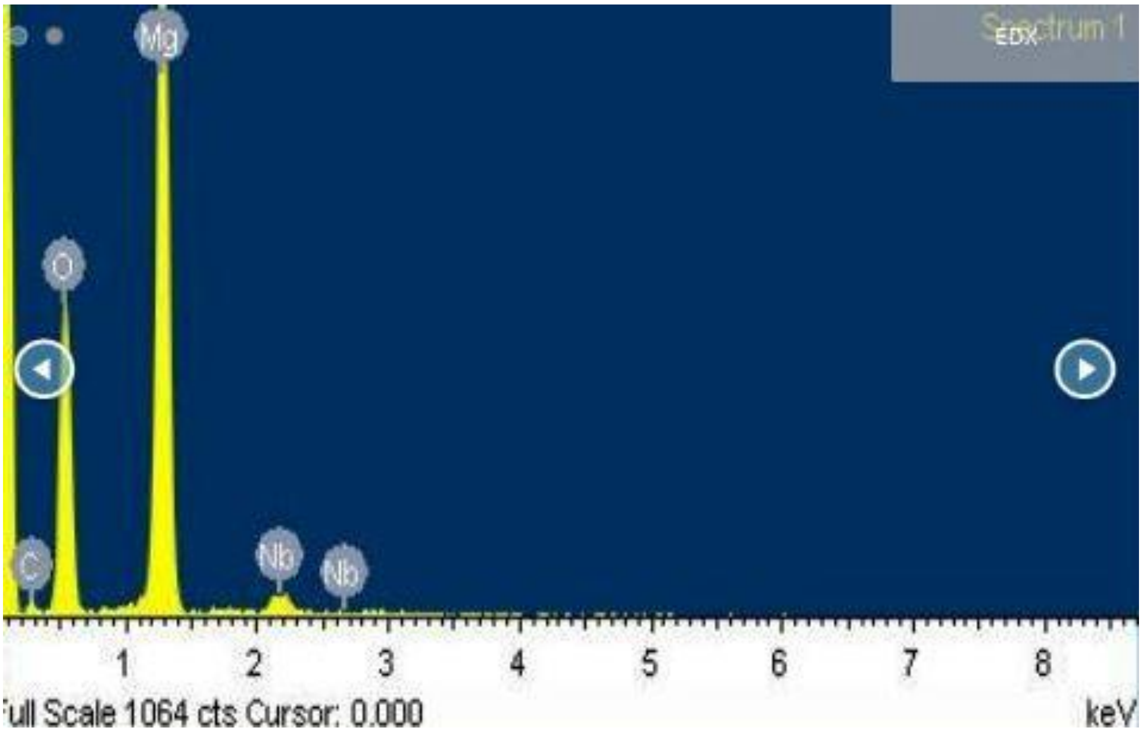

Figure 3.5 EDS analysis of magnesium oxide nano particle (Data sheet)

3.2 Fuel Characteristics

The fuel attributes have a significant effect on the performance and emission characteristics [91]. They are categorized based on their thermal, chemical, and physical properties [90]. Thermal properties include thermal conductivity, specific heat value, etc. Sulphur and ash concentrations, heating value, chemical structure, etc, come under chemical properties. The physical properties comprise freezing point, flash and fie point, cloud point, density, viscosity, etc. The physcio-chemical tests were undertaken in accordance with the ASTM standards. Diesel fuel was considered as the base line fuel for assessing the properties of test fuel samples. The analyzed results of the test fuel properties are given in Table 3.2.

3.2.1 Viscosity

It is a metric for a fluid's flow resistance. Viscosity represents the thickness of the liquid and is calculated by assessing the time required for a particular liquid to pass via a specified aperture. The viscosity of the test fuels were measured using redwood viscometer (ASTM D445) (in Figure 3.6). Lower viscosity leads to lack of lubrication (to fuel injector and pump). Higher viscosity results in carbon and soot formation due to the incomplete combustion caused by the poor atomization of the fuel.

3.2.2 Calorific value

Calorific value is a crucial parameter while considering a fuel. It gives the fuel energy content. It is the total heat released or generated on the complete combustion of fuel. By using a bomb calorimeter the calorific value (ASTM D2015) of all test fuels was measured (in Figure 3.7). It was revealed that the calorific values of all test fuel samples were lower than diesel, which leads to higher fuel consumption and lower power output.

3.2.3 Flash point

The lowest temperature at which fuel ignites without continuous burning when an ignition source is provided is known as a flash point. High flash point results in safe storage and handling of fuels. Flash point (ASTM D93) was measured using a closed pensky martens apparatus (in Figure 3.8). It was observed that diesel fuel has the least flash point temperature as compared to all other test fuels.

3.2.4 Density

It is a physical characteristic that is used to determine the appropriate amount of fuel required to provide adequate combustion. The ratio of mass per unit volume is referred to as density. Hydrometer (ASTM D1298) (in Figure 3.9) was used to measure the density of the test fuels. The lower density of the fuel results in a reduced mass of fuel consumption for the same volume. Higher the density, the higher the fuel consumption.

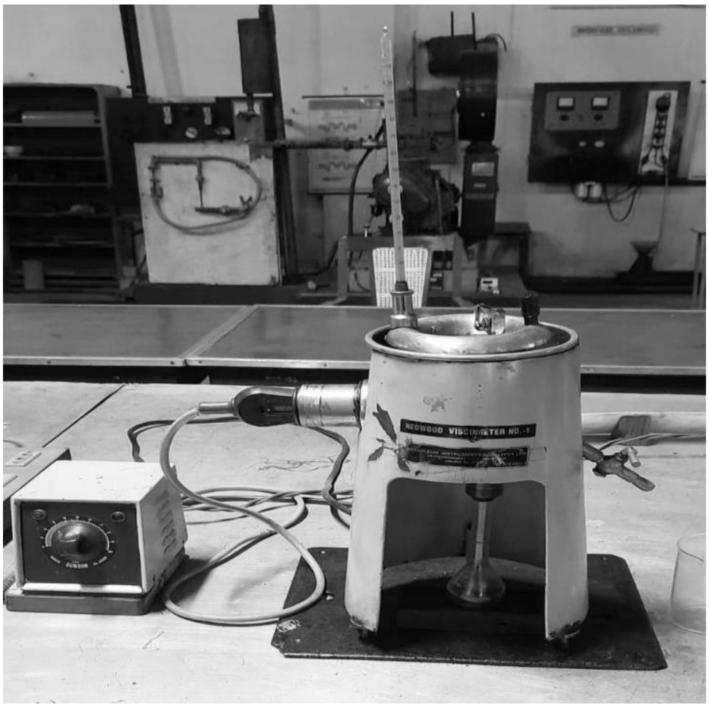

Figure 3.6 Redwood viscometer

Figure 3.7 Bomb calorimeter

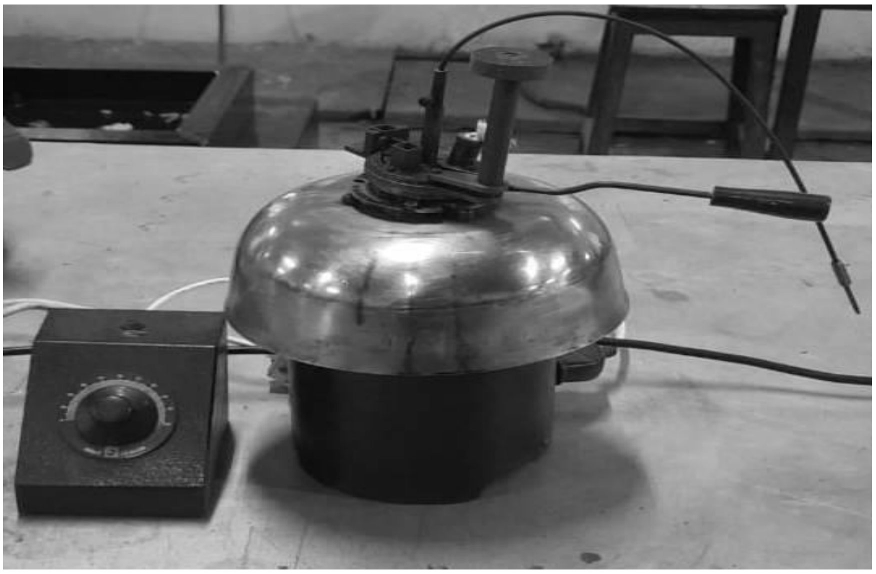

Figure 3.8 Pensky martens flash point apparatus

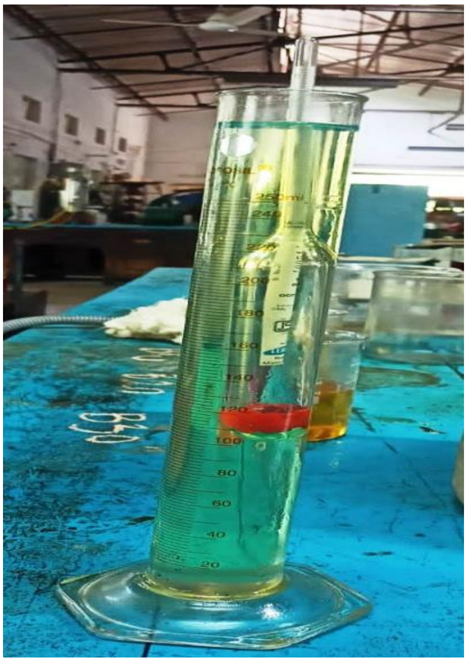

Figure 3.9 Hydrometer

Table 3.2 Test fuels properties

Test fuel samples	Viscosity (mm^2/sec)	Calorific Value (MJ/kg)	Flash Point (°C)	Density (kg/m^3) at 15°C
SB0	3	43.5	70	830
SB20	3.19	42.6	86.5	835.7
SB35	3.56	41.97	95.3	840.9
SB50	3.92	41.63	100.7	843.4
SB65	4.37	41.46	108.5	849.1
SB80	4.63	41.29	118.3	854.8
SB100	5.22	41	130	860
SB20 Al_2O_3	3.42	42.77	87	837.8
SB35 Al_2O_3	3.75	42.3	96.9	842
SB50 Al_2O_3	4.2	41.81	102.4	845.1
SB65 Al_2O_3	4.51	41.59	109.8	850.7
SB80 Al_2O_3	4.86	41.4	119	855.9
SB100 Al_2O_3	5.43	41.22	136	861.9
SB20 MgO	3.31	42.98	88	837
SB35 MgO	3.69	42.53	97.4	841.6
SB50 MgO	4.16	41.9	103.8	844.8
SB65 MgO	4.45	41.71	111.2	850.1
SB80 MgO	4.77	41.52	120	855.6
SB100 MgO	5.39	41.36	139	861.4

3.3 Experimental test rig

One of the most widely utilized engines for large, medium and small-scale commercial applications is a Kirloskar diesel engine. Its high CR enables it to sustain the peak pressure. The investigations have been carried out on the fixed CR, singe cylinder, DI-CI engine with 19 distinct fuel samples (SB0, SB20, SB35, SB50, SB65, SB80, SB100, SB20 Al_2O_3, SB35 Al_2O_3, SB50 Al_2O_3, SB65 Al_2O_3, SB80 Al_2O_3, SB100 Al_2O_3, SB20 MgO, SB35 MgO, SB50 MgO, SB65 MgO, SB80 MgO, and SB100 MgO) to examine emissions and performance attributes under varied loads. Table 3.3 gives the test rig parameters. The engine is installed on a mild steel channel base structure that is centrally balanced and is connected to the eddy current dynamometer using a flexible rubber coupling. The test rig incorporates a panel box that houses an engine and process indicator, fuel and airflow measuring unit, manometer, fuel tank, and air box. The line diagram and schematic diagram of the experimental test rig are depicted in Figures 3.10 and 3.11.

Table 3.3 Parameters of the test rig

Parameters	Units	Value
Dynamometer type		Eddy current
Combustion chamber		Hemispherical
Fuel injection timing		23^o CA bTDC
Rated speed	rpm	1500
Rated output	kW	5.2
Compression ratio		17.5:1
Orientation		Vertical
Swept volume	cc	661
Exhaust valve closing		4.5^oaTDC
Exhaust valve opening		35.5^obBDC
Intake valve closing		35.5^oaBDC
Intake valve opening		4.5^obTDC
Bore	mm	87.5
General details		Direct injection water cooled Four stroke Single cylinder
Stroke	mm	110
Test rig model and make		TV1, Kirloskar
Connecting rod length	mm	234

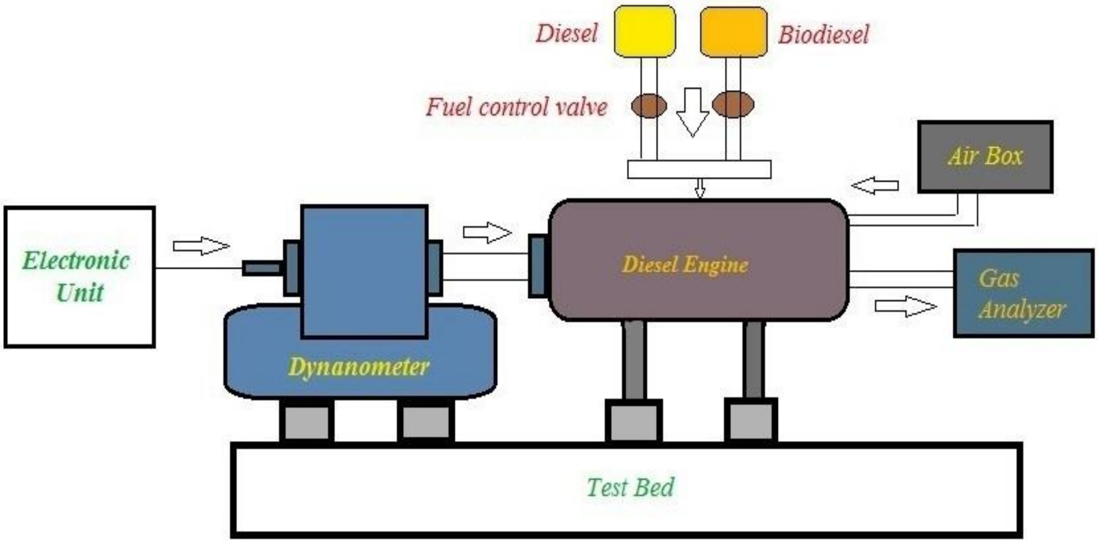

Figure 3.10 Line diagram of the test rig

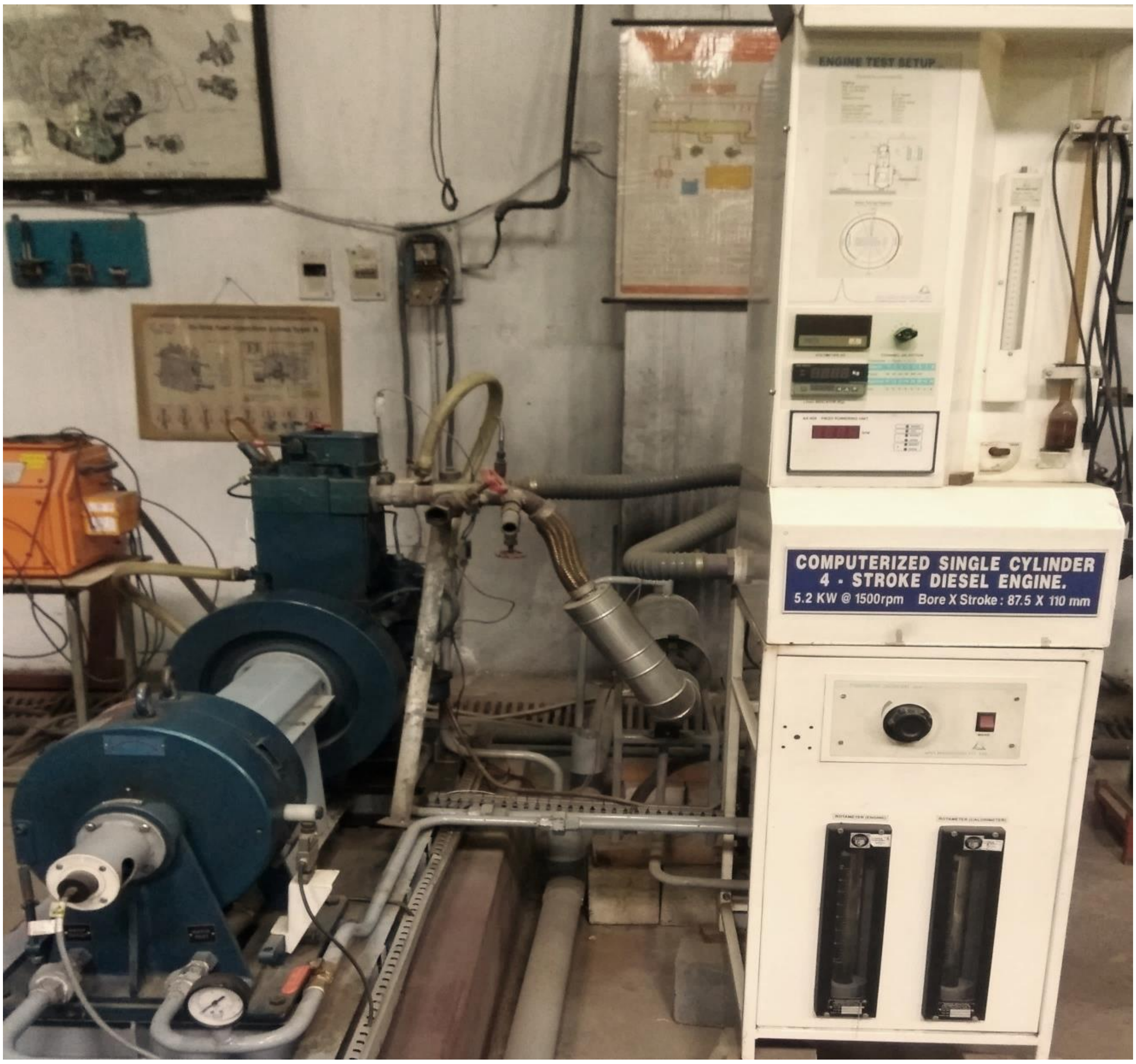

Figure 3.11Test rig set up

The engine received fuel from two separate fuel tanks, one for diesel and another for biodiesel amalgams without and with nano additives. Performance parameters brake thermal efficiency (BTE) and brake specific fuel consumption (BSFC) were evaluated. The frictional power of the engine is determined using Willian's line approach. Exhaust emissions were analyzed using the MN-05 multi gas (Mars Technologies) analyzer. Emissions namely nitrogen oxides (NO_X), carbon dioxide (CO_2), and hydrocarbons (HC) were measured. Table 3.4 and 3.5 shows the specifications of the gas analyzer and the uncertainty analysis.

Table 3.4 Exhaust gas analyzer specifications

Parameter	Resolution	Range
NO_X	1 ppm vol	0-5000 ppm
O_2	0.1 % vol	0-25 % vol
CO_2	0.01 % vol	0-20 % vol
HC	1 ppm	0-15000 ppm
CO	0.001 % vol	0-9.99 % vol

Table 3.5 Uncertainty analysis.

Parameter	Device	Uncertainty %
NO_x	MN-05 Multi gas analyzer	±0.5
CO_2	MN-05 Multi gas analyzer	±1.0
UHC	MN-05 Multi gas analyzer	±0.3
BTE		±1.05
Fuel consumption	Liquid column heights	±0.5
BSFC		±1.02
rpm	Speed indicator	±0.1
Load	Dynamometer	±0.2

3.4 Experimental methodology

The approach used in the experiment is detailed below.

- Before the start of the experiment engine, cooling and fuel system have been checked for proper functioning.
- Using diesel fuel, the engine was started and operated at the rated speed in no-load condition for 20 minutes, in order to attain steady operating conditions.

- After achieving a steady state, time taken (in sec) for 10 cc or 10 ml of fuel consumption was recorded using a stopwatch, and a manometer reading (in mm) was taken down. The corresponding rpm was measured using the tachometer device.
- Emittants CO_2 (in %), NO_X (in ppm), and HC (in ppm) were recorded using a gas analyzer.
- Gradually engine load varied from no load to full load (i.e. 0 to 10 kg) and their corresponding parameters reading were recorded.
- The above methodologies were employed in the varied fuel blends (SB20, SB35, SB50, SB65, SB80, SB100, SB20 Al_2O_3, SB35 Al_2O_3, SB50 Al_2O_3, SB65 AL2O3, SB80 Al_2O_3, SB100 Al_2O_3, SB20 MgO, SB35 MgO, SB50 MgO, SB65 MgO, SB80 MgO, and SB100 MgO) trials as well.

3.5 Formulas for determining performance parameters (BTE and BSFC)

$$m_f = \frac{X \times specific gravity of fuel}{1000 \times t} \times 3600 \qquad (1)$$

$$BP = \frac{2\pi NT}{60{,}000} \qquad (2)$$

$$T = F \times r \times 9.81 \qquad (3)$$

$$\eta_{BTE} = \frac{BP \times 3600}{m_f \times CV} \qquad (4)$$

$$BSFC = \frac{m_f}{BP} \qquad (5)$$

Where

t = Time taken for 10 ml of fuel consumption (in seconds); and x = 10 ml

m_f= mass of the fuel consumed (kg / hr); BP = brake power (kW); T = Torque (N-m)

N = engine speed (in rpm); F = applied load; r = radius of the dynamometer (in m)

CV = calorific value (kJ / kg); BSFC = brake specific fuel consumption (kg / kWhr)

CHAPTER 4

ARTIFICIAL NEURAL NETWORK (ANN)

4.1 Artificial intelligence (AI) and Machine learning (ML)

In the analysis of CI engine characteristics, exploratory techniques are generally employed, that generate a strong and excellent level of precision findings. It is essential to execute this exploratory investigation of the CI engine characteristics in compliance with the appropriate testing procedures that are outlined in various international guidelines. These investigations are time-consuming, expensive, and technically complex in nature, and the availability of a good research facility to execute these investigations is limited. As a result, Artificial Intelligence (AI), statistical and mathematical models have been explored by the researchers [112, 113] to predict the CI engine characteristics.

Artificial intelligence (AI) is a rapidly evolving tool for obtaining an optimal solution to engineering challenges. The theory and development of computer system able to perform tasks normally requiring human intelligence is termed as artificial intelligence [114]. Knowledge-based (KB) systems or expert systems were utilized in the early scientific areas of AI. It is a computer program built to tackle complicated problems and offer decision-making abilities similar to those of a human expert. An expert system strategy is only suitable for specific areas such as problems with a well-documented history of prior issues and responses, etc. The then-available (1960-1970) computers lacked the necessary processing capacity to execute more advanced AI techniques like Machine Learning (genetic algorithms, artificial neural networks, etc.), while expert systems would perform effectively. The benefits and drawbacks of using expert systems are given below.

Benefits

- Offer an extremely quick response time to a specific query.
- These are not influenced by fatigue, tension, and emotions; hence their performance remains consistent.
- If the knowledge base has accurate knowledge, the possibility of error is reduced.
- They can be highly reproducible.

Drawbacks

- Incapable of self-learning and thus necessitates manual updates.
- One of the key constraints is the need for a specific expert system for each domain.
- Development and maintenance costs are high.
- If the KB contains inaccurate data, the expert system's response could be incorrect.

Each AI technique has a distinct set of applications, and the algorithm is correlated with the nature of the problem. To achieve AI, Machine Learning (ML) is one of the ways. ML is an application of artificial intelligence that provides the system (computer) the ability to learn and automatically improve through experience [115]. Figure 4.1 depicts the types of ML and their subtypes.

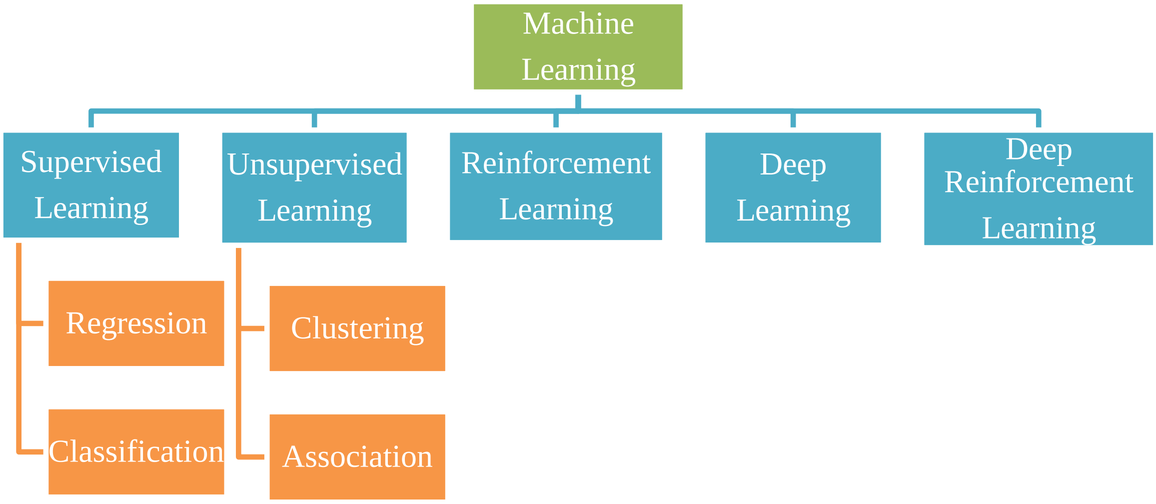

Figure 4.1 ML types and their subtypes

In this section supervised learning (SL) and unsupervised learning (USL) is discussed. In SL the output is predicted by the model using well-labeled training data that has been used to train the model. The term "labeled data" refers to input variables that have already been assigned the appropriate output. Supervised learning is a process of providing input data as well as correct output data to the machine learning model [116]. They are further categorized as classification and regression. Classification is used when there are two classes (i.e. output variables are categorical) such as true-false, male-female, yes-no, etc. To predict the continuous-valued dependent variable based on a set of independent variables, regression is used. Unlike SL, unsupervised learning (USL) has no associated output data corresponding to its input. Unsupervised learning is a type of machine learning in which models are trained using an unlabeled dataset and are allowed to act on that data without any supervision[117]. The difference between unsupervised learning and supervised learning is given in Table 4.1.

Table 4.1 Comparison of Unsupervised learning and Supervised learning

Unsupervised learning	Supervised learning
Finds the hidden patterns in data.	Predicts the model output.
Supervision is not required to train the model.	To train the model supervision is required.
Trained using unlabeled data.	Trained using labeled data.
Only input data is provided.	Output data is given to the model along with its input.
As compared to SL gives less accurate result.	Model gives an accurate result.
Require a large amount of data sets.	Require a small amount of data sets as compared to USL.

4.2 Artificial neural network (ANN)

Computers are incredibly fast in executing tasks such as algebraic and numerical computations. However, they fall well short of the capabilities of human brains when it comes to operations like image and speech recognition. The development of an ANN originates from designing AI based on biological neural networks of human brain. The correlation between Biological Neural Network **(**BNN) and ANN is depicted in Figure 4.2. The human brain is made up of a massive network of linked neurons. A network of interlinked neurons is capable of completing complicated tasks efficiently and precisely with incredible speed, compared to millions of steps required by a computer to complete the same operation. Neural networks (NN) are often referred to as connectionism because data is encrypted in the complex connections of the neuron network. The ANN is the interconnectivity of nodes, similar to neurons in a BNN. Each neural network is comprised of three important elements: learning processes, network structure, and node characteristics.

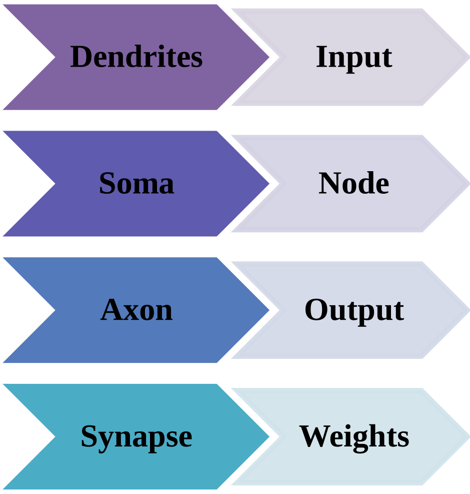

Figure 4.2 Relationship between BNN and ANN [118]

4.2.1 Node character

Figure 4.3 represents the primary model of an ANN node. How signals are processed by the node is determined by the node character. It includes the activation function and the number of inputs-outputs with their corresponding weights. Each node receives varied inputs from nearest neighbors through connections with corresponding weights. The node activates and transfers the information via the transfer function to its adjacent nodes when the weighted sum of inputs exceeds its threshold value. This procedure can be represented mathematically [113].

$$y = f\left(\sum_{i=1}^{n} w_i x_i - T\right) \qquad (6)$$

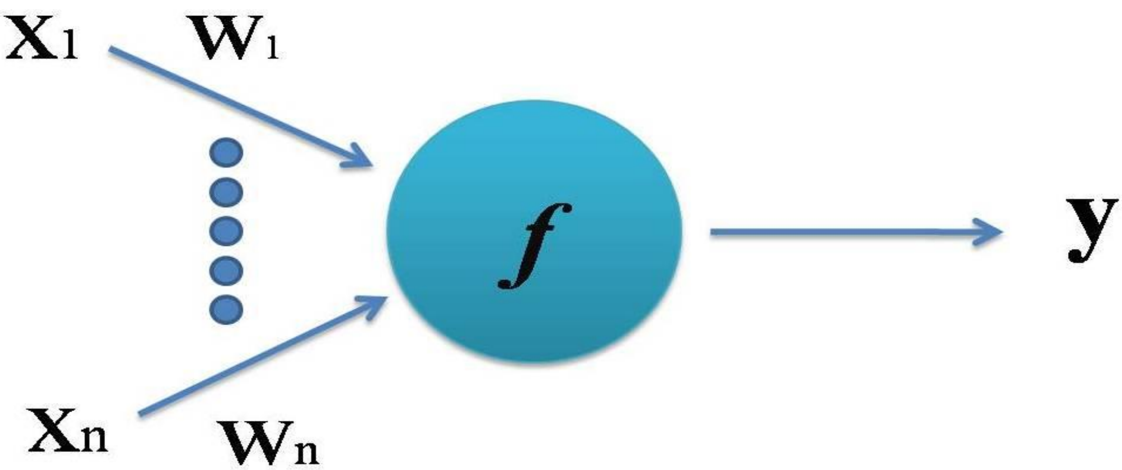

Figure 4.3 Single node ANN

4.2.2 Network topology

The connectivity and organization of nodes are governed by the network topology or network structure. These nodes are arranged into three layers namely input layers, hidden layers, and output layers (in Figure 4.4). It involves the building of a network by considering the number of layers, and their corresponding nodes at each layer by specifying the direction of the linkages between the nodes. Depending on the task, there may be one or more hidden layers. The network structure is categorized as feedback (loopback connection) and feed-forward (no loopback connection) network. The feedback network is dynamic, and the feed-forward network is static.

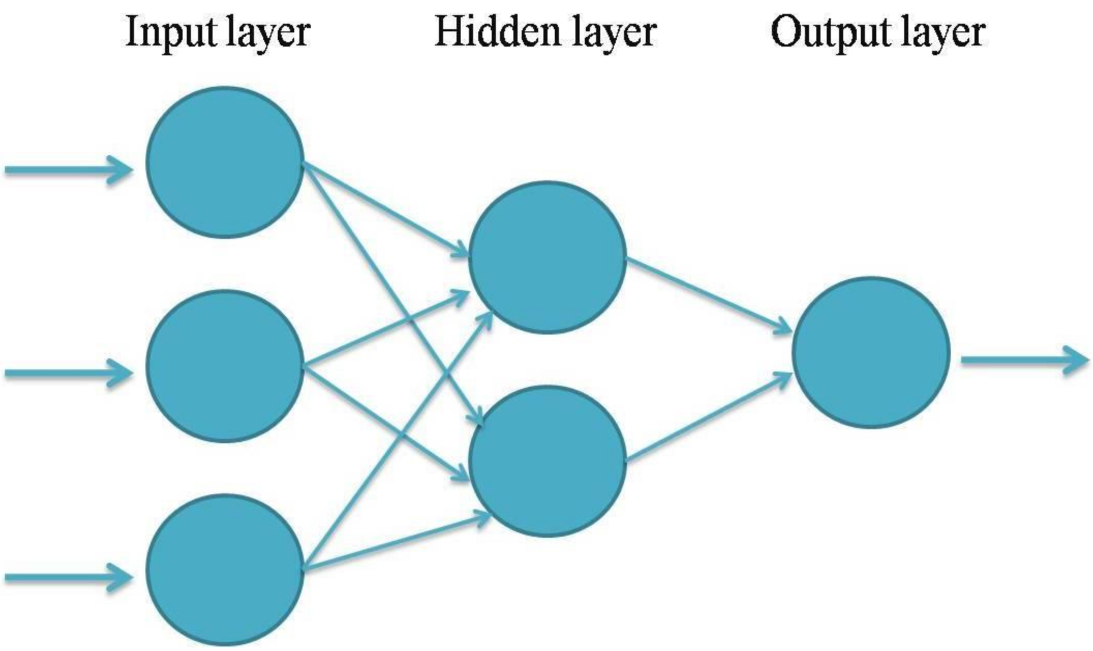

Figure 4.4 ANN topology

4.2.3 Learning process

The initialization and adjustment of the weights are determined by learning rules. They are used to train the network. ANN has three modes: training mode, testing mode, and validating mode. Firstly, the network is trained using 70% of the data set, and the remaining proportion of the data set is used for testing and validating the network. The learning process is categorized into two broad classifications namely unsupervised learning and supervised learning. An appropriate learning algorithm is used to train the NN to initiate the learning process. Learning algorithms of supervised learning are displayed in Figure 4.5

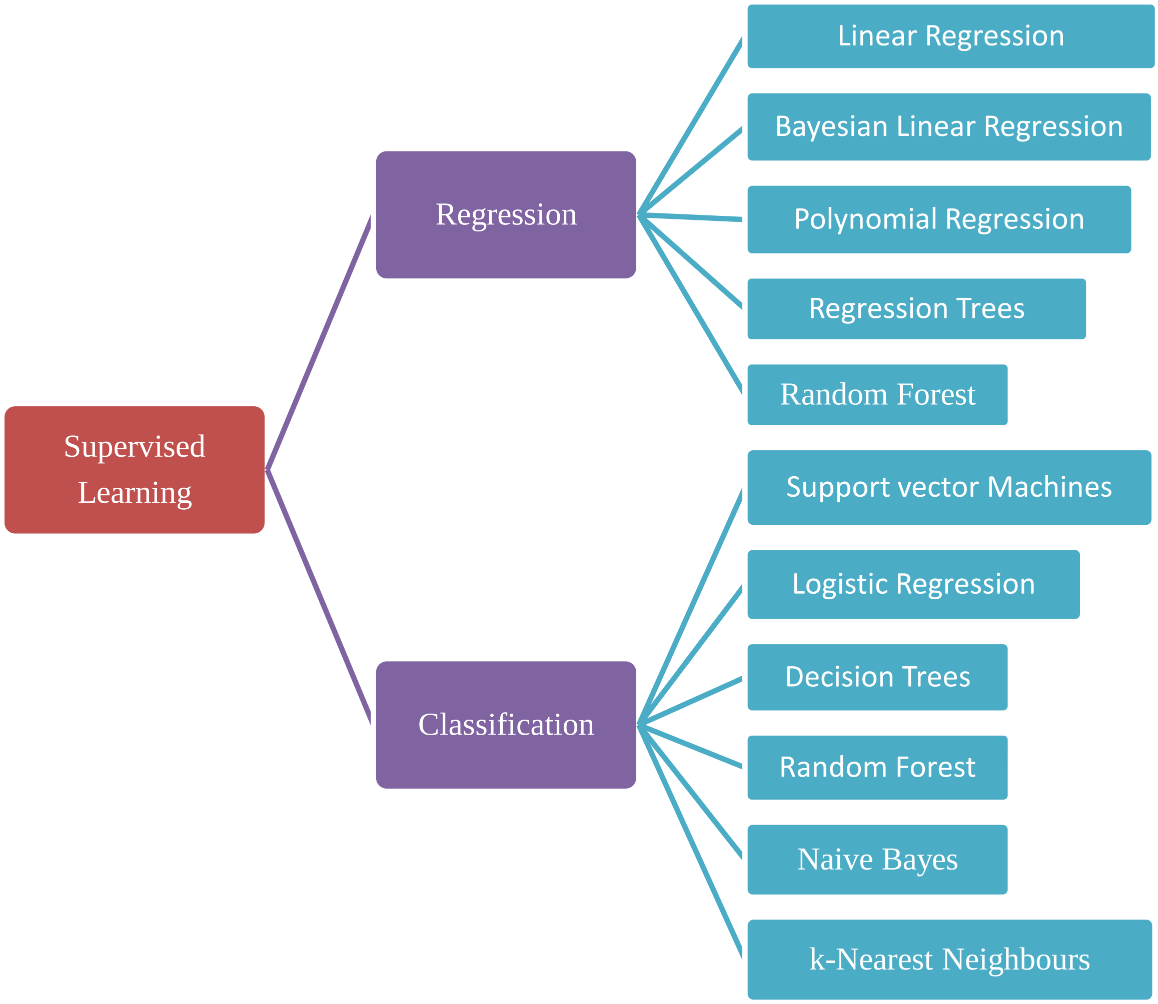

Figure 4.5 Supervised learning algorithms

4.3 ANN optimization

ANNs are machine learning systems based on BNN. They are utilized to tackle a wide array of issues in science and technology, especially in those situations when traditional modelling techniques fall short [119]. It can forecast multiple output variables based on multiple input variables. An ANN that has been properly trained can be utilized as a prediction model for a particular task. They can perform tasks such as inferring, learning, determining, and memorizing [120]. ANNs can recognize and learn correlation relationships between input and output variables. They are effective modelling techniques, particularly when the underlying data relationship is unavailable. Its learning ability i.e. "learn by example" makes ANN a powerful tool for modelling.

Applications of ANN in mechanical engineering are given below:

- Geometrical modeling, design and optimization**.**
- Forecast of thermal properties.
- Structural analysis.
- Validation of data.
- Fault diagnosis of equipment.

4.4 Terminologies used in ANN

4.4.1 Loss or Cost function

It is one of the key parameters in ANN. A prediction error of NN is known as loss. The methodology for determining this loss is known as the cost function. “Loss function evaluates how well the algorithm models the given data, used to predict error between obtained and desired output.” The model which gives the least loss is recommended. For a given task, the cost function is chosen based on the prediction of output variables (i.e. binary, real value, etc.). Examples are root mean squared error (RMSE), mean relative error (MAE), categorical cross entropy, binary cross entropy, etc.

4.4.2 Activation or Transfer function

They are mathematical equations that determine a NN model's output (in Figure 4.6). “Transfer function defines the output of a node that has to go as input to neurons in the next layer.” The output values can range between -∞ to +∞. In order to obtain the appropriate predictions or generalised findings, it is therefore essential to confine the output. The transfer function decides at what values a neuron should be activated or not. Mathematically [121] it is expressed as:

$$Z = Activation\ function\ (weight\ \times input\ + bias) \qquad (7)$$

Transfer function types include exponential linear units (ELU), rectified linear units (Relu), Softplus, Softmax, Tanh or Hyberbolic, Binary, Linear, and Logistic or Sigmoid. Table 4.2 gives the range of various transfer functions.

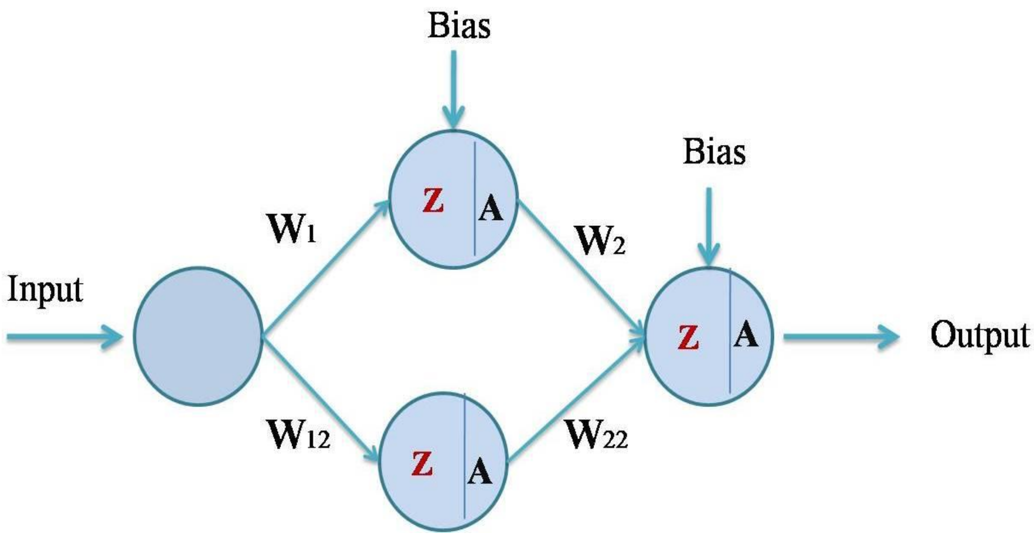

Figure 4.6Network with Activation function

Table 4.2Range of transfer functions

Activation Function	Range
Relu	[0 , +∞)
Soft plus	(0, +∞)
Soft max	(0 , 1)
Tanh	(-1 , 1)
Binary	{0, 1}
Sigmoid	(0 , 1)
Linear	(-∞ , +∞)

4.5 ANN methodology

Steps involved in the ANN network analysis is given below:

- Development of proposed ANN strategy (in Figure 4.7).
- Steps for executing the proposed task (in Figure 4.8).
- Collection of experimental data set.
- Defining input variables (3 parameters) and output variables (5 parameters):

  Input variables: BP, Load, and test fuels (SB20, SB35, SB50, SB65, SB80, SB100, SB20 Al_2O_3, SB35 Al_2O_3, SB50 Al_2O_3, SB65 Al_2O_3, SB80 Al_2O_3, SB100

Al_2O_3, SB20 MgO, SB35 MgO, SB50 MgO, SB65 MgO, SB80 MgO, and SB100 MgO).

Output variables: BSFC, HC, NO_X, BTE, andCO_2.

- Tabulation of input and output parameters in .csv (comma-separated values) format.
- Normalization of input and output data:

  The data given to an ANN determines its effectiveness, hence scaling output and input variables is essential. The provided data must fit inside a predetermined range in order to improve network training. Using preprocessing technique [121] namely MinMaxScaler (eq 8) data is normalized in the range0 to +1.

$$X_{Pre-processing} = \frac{X - X_{min}}{X_{max} - X_{min}} \qquad (8)$$

- Building of network:
  - The ANN network is evaluated for following conditions.
  - By varying the hidden layer neurons.
  - Varying the transfer functions.
  - Number of epochs.
  - Determining the optimizers ("Optimizers are algorithms or methods used to change the attributes of your neural network such as weights and learning rate in order to reduce the losses").
- Evaluated ANN model is depicted in Figure 4.9.
- ANN model is executed using Python with Tensor Flow as backend, using the Keras framework.
- Learning and testing of build ANN network:
  - The current model is a regression based supervised learning.
  - Selection of Regression algorithms (in Figure 4.10).
  - A feed forward network with a linear regression algorithm is employed for the present study.
  - Learning of the network was executed using 70% of the data. The remaining 30% of data was equally distributed for testing and validation of the network.

- Transfer functions namely softplus, softmax, and sigmoid along with optimizers adagrad, nadam, and adam were evaluated for a varied epochs (200, 400, 600, 800, and 1000) and neurons in the hidden layer (8, 16, 24, and 32).

- Network evaluation metrics is measured in terms of regression coefficient (r) and MSE (Mean Squared Error) [121] in equations 9 and 10. Where O_i: Output for ith trail case, T_i: Target for ith trial case.

$$r = \sqrt{1 - \left(\frac{\sum_{i=1}^{n}(T_i - O_i)^2}{\sum_{i=1}^{n} O_i{}^2}\right)} \qquad (9)$$

$$MSE = \frac{1}{n}\sum_{i=1}^{n}(T_i - O_i) \qquad (10)$$

- Plotting and tabulation of associated data.
- A value close to zero indicates the best line fit, hence the network with the least validation MSE loss is considered.
- The r was considered to assess the strength and direction between the parameters. Direction of the relationship is indicated by the negative and positive signs. A value near 1 indicates a strong correlation.

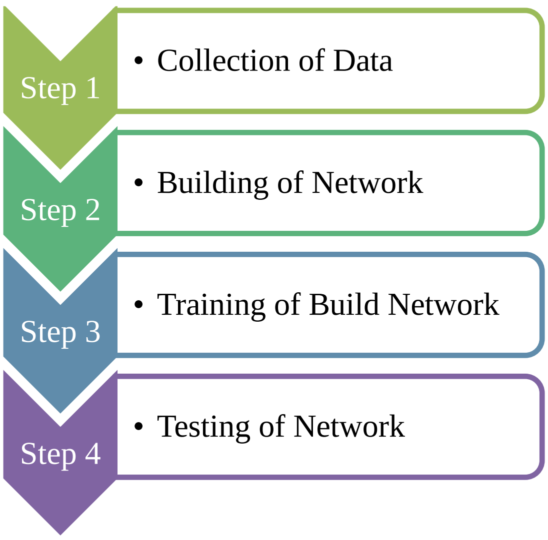

Figure 4.8 Steps for executing ANN

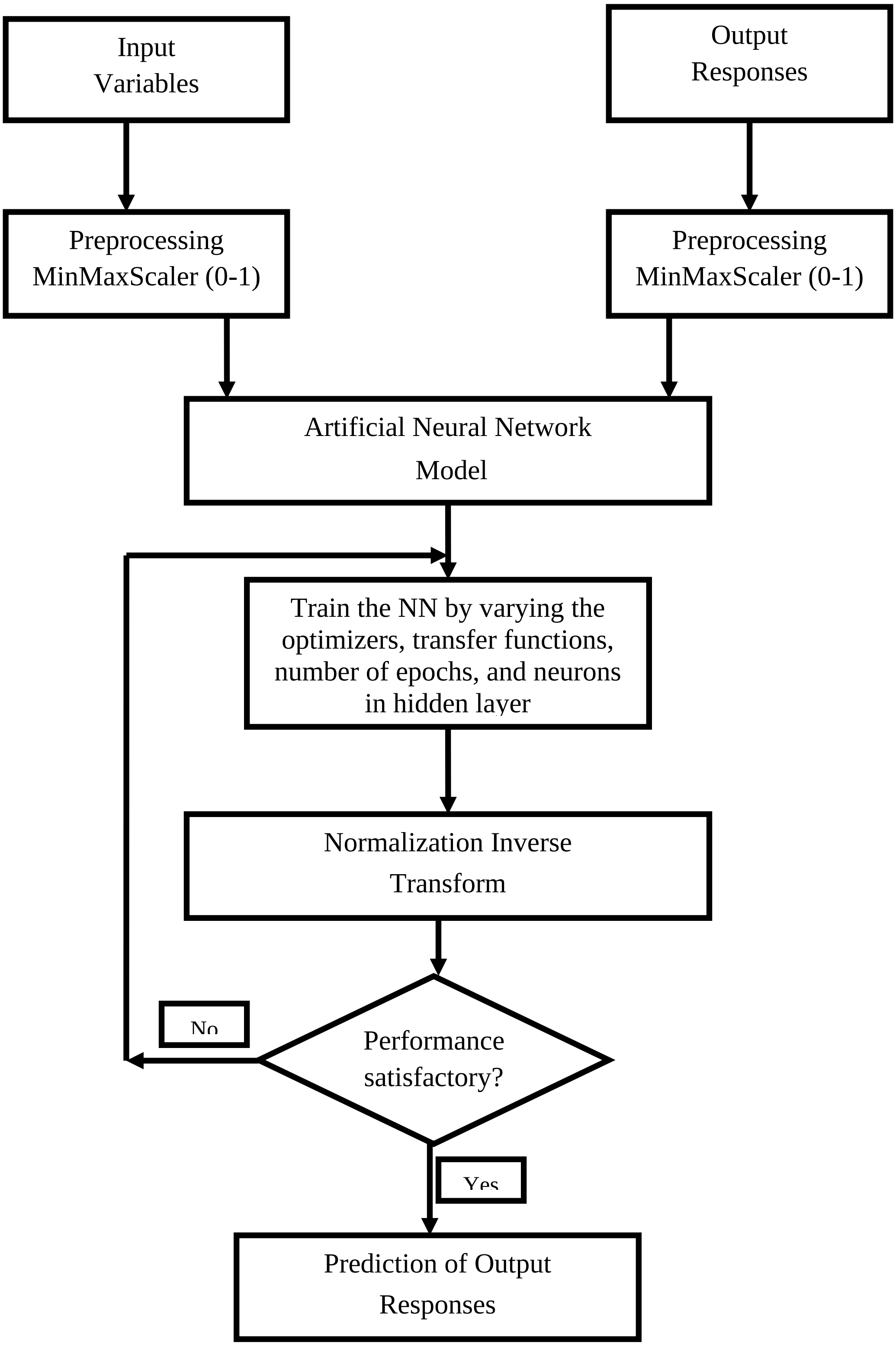

Figure 4.7 Proposed ANN strategy

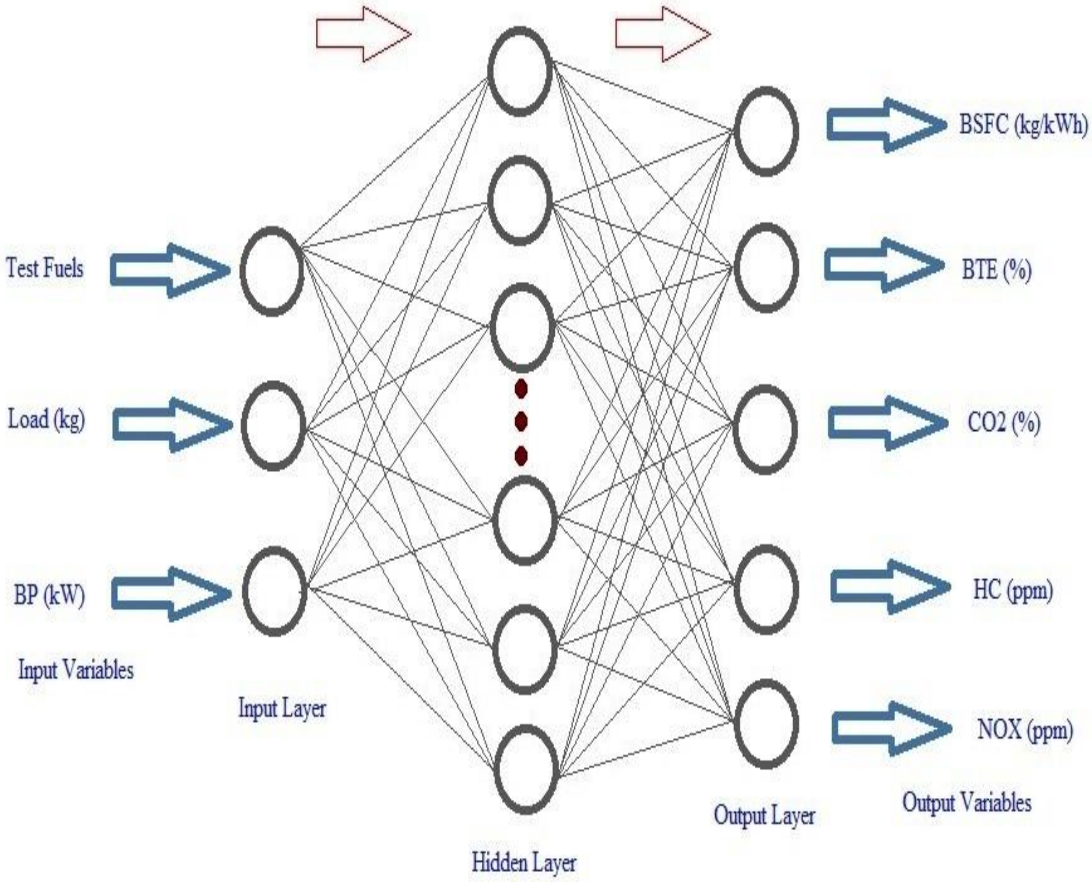

Figure 4.9 Evaluated ANN model of CI engine attributes

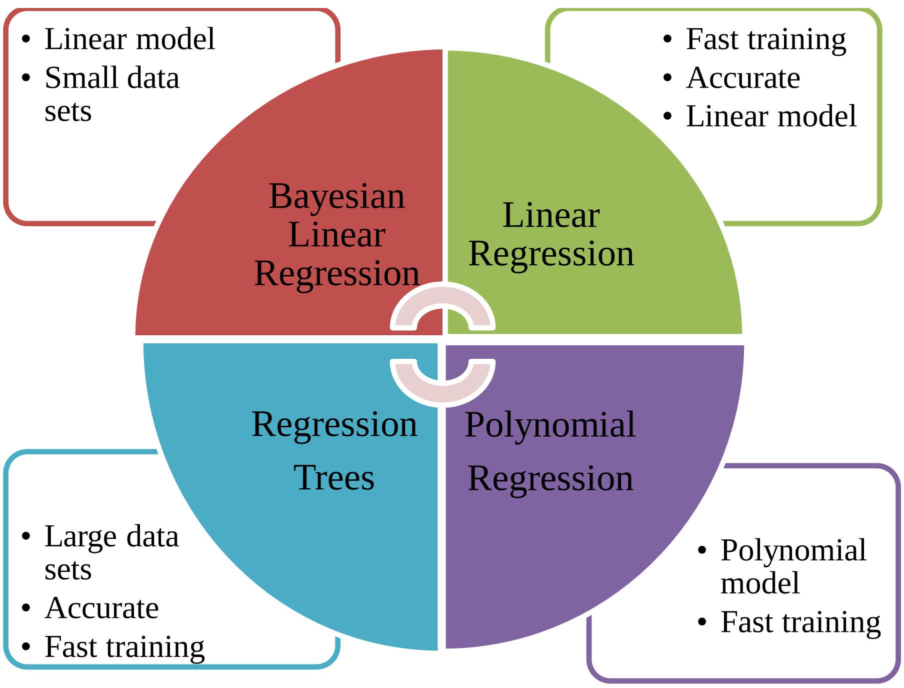

Figure 4.10 Regression algorithms

4.6 ANN analysis

For ANN training, the essential data is acquired from the experimentations, partitioned into target and input variables, and fed in array format. The experimental values are regarded as the network structure's data points, and these points are normalized in the range zero and one. The ANN model prediction is executed with five target variables (BSFC, HC, NO_X, BTE, and CO_2) and three input variables (BP, Load, and test fuels). With a single hidden layer, the ANN model was constructed, and the model topology is 3-X-5, where X is the number of hidden layer neurons. By varying the hidden layer neurons (8-32), each optimizer (adagrad, nadam, and adam) with three varied activation functions (softplus, softmax, and sigmoid) was explored. Training of the model was executed using five varied iterations (200, 400, 600, 800, and 1000). To weigh the performance of the model, obtained predictions were de-normalized. MSE and r are considered to be indicators for assessing network performance. Table 4.3 provides a brief summary of the findings of r and MSE values of the evaluated network. From Table 4.3, it is evident that sigmoid activation function with adam optimizer and 16 hidden layer neurons exhibited the least MSE (validation). The optimum network topology was found to be 3-16-5. Table 4.4 shows the network's optimal configuration. The deviation of MSE loss and r score as a function of epochs is portrayed in Figures 4.11 and 4.12. From Figure 4.11, it is observed that the MSE decreases with the increased epochs and validation-training MSE of target parameters are almost similar [125,127]. The r value of the target parameters (validation-training) tends to be 1 as per Figure 4.12, asserting a strong correlation. Figure 4.13 represents the r and MSE values of target parameters (predicted and experimental). The coincidence of predicted and experimental values, as shown in Figure 4.13, indicates that the model performance is satisfactory and the data points are well mapped to the fitting line [132, 133]. The MSE and r values of the target parameters NO_X, HC, CO_2, BTE, BSFC are 0.00002, 0.00015, 0.00007, 0.00003, 0.00004 and 0.99992, 0.99888, 0.99959, 0.99989, 0.99969 respectively. Hence, the ANN is revealed to be an effective modeling technique for assessing engine attributes.

Table 4.3MSE and r values of target parameters

Attributes	Val. Reg: Coeff:	Train. Reg: Coeff:	Val. MSE Loss	Train. MSE Loss	Over all MSE Loss Train.	Over all MSE Loss Val.	Hidden layer neurons	Number of epochs	Transfer Function	Optimizer
NOX	0.89429	0.95499	0.02447	0.01112						
HC	0.97887	0.98315	0.00356	0.0023						
CO2	0.98346	0.99115	0.00234	0.00146	0.01688	0.01607	8	200	Softplus	Adagrad
BTE	0.99485	0.93282	0.0096	0.01527						
BSFC	-0.96204	0.34309	0.0404	0.05426						
NOX	0.98949	0.98028	0.00731	0.00489						
HC	0.96856	0.97656	0.00303	0.003						
CO2	0.98647	0.98923	0.00088	0.0017	0.01671	0.0113	8	400	Softplus	Adagrad
BTE	0.99501	0.91905	0.01038	0.01825						
BSFC	-0.8726	0.29948	0.03492	0.05569						
NOX	0.99007	0.9667	0.00796	0.0082						
HC	0.98548	0.97669	0.00147	0.00299						
CO2	0.95806	0.99065	0.0027	0.00149	0.01748	0.01332	8	600	Softplus	Adagrad
BTE	0.99123	0.92626	0.01188	0.01668						
BSFC	-0.90102	0.23686	0.04257	0.05806						
NOX	0.97511	0.95683	0.01383	0.01057						
HC	0.98907	0.98811	0.00097	0.00153						
CO2	0.99115	0.99424	0.00066	0.00092	0.01429	0.01393	8	800	Softplus	Adagrad
BTE	0.99924	0.95637	0.00886	0.01002						
BSFC	-0.93337	0.46367	0.04531	0.0484						
NOX	0.98634	0.9734	0.00696	0.00657						
HC	0.99764	0.98715	0.00047	0.00165						
CO2	0.99109	0.99589	0.00062	0.00065	0.01413	0.01201	8	1000	Softplus	Adagrad
BTE	0.99877	0.94445	0.00819	0.01268						
BSFC	-0.92702	0.456	0.04379	0.04908						

NOX	0.95706	0.96785	0.01492	0.00795	0.01705	0.01446	16	200	Softplus	Adagrad
HC	0.99357	0.97182	0.00106	0.00363						
CO2	0.96236	0.98805	0.00244	0.00189						
BTE	0.99009	0.9145	0.00601	0.01922						
BSFC	-0.98405	0.37901	0.04785	0.05254						
NOX	0.98371	0.97089	0.00715	0.00718	0.01573	0.0125	16	400	Softplus	Adagrad
HC	0.99735	0.98981	0.00026	0.00131						
CO2	0.98855	0.99325	0.00074	0.00107						
BTE	0.99287	0.93472	0.00997	0.01484						
BSFC	-0.9004	0.33647	0.0444	0.05425						
NOX	0.9823	0.97261	0.00717	0.00676	0.01563	0.0131	16	600	Softplus	Adagrad
HC	0.99507	0.99169	0.0004	0.00107						
CO2	0.99646	0.99517	0.00024	0.00076						
BTE	0.99238	0.93962	0.00908	0.01375						
BSFC	-0.98126	0.29905	0.04859	0.05579						
NOX	0.98944	0.97799	0.00634	0.00545	0.01493	0.01309	16	800	Softplus	Adagrad
HC	0.99087	0.9891	0.00063	0.0014						
CO2	0.9842	0.99503	0.00136	0.00079						
BTE	0.99152	0.92476	0.0117	0.01703						
BSFC	-0.95882	0.44119	0.04543	0.04996						
NOX	0.98206	0.96948	0.00879	0.00752	0.01475	0.01331	16	1000	Softplus	Adagrad
HC	0.99355	0.9926	0.00062	0.00096						
CO2	0.98839	0.99504	0.00091	0.00079						
BTE	0.99775	0.94571	0.00966	0.0124						
BSFC	-0.97709	0.38787	0.04656	0.05208						
NOX	0.99665	0.96328	0.00509	0.00902	0.01611	0.01081	24	200	Softplus	Adagrad
HC	0.99126	0.98955	0.00099	0.00135						
CO2	0.98208	0.99321	0.0012	0.00109						
BTE	0.99796	0.93826	0.0081	0.01405						
BSFC	-0.98385	0.31598	0.03866	0.05505						

NOX	0.97945	0.95988	0.01033	0.00984					
HC	0.99291	0.99191	0.00065	0.00104					
CO2	0.99519	0.99515	0.00034	0.00077	0.01442	0.01351	24	400	Softplus	Adagrad
BTE	0.99092	0.9559	0.00585	0.01013					
BSFC	-0.94242	0.4236	0.05041	0.05033					
NOX	0.9768	0.96297	0.00884	0.00909					
HC	0.99491	0.99115	0.00052	0.00114					
CO2	0.99588	0.99429	0.00038	0.0009	0.01575	0.01283	24	600	Softplus	Adagrad
BTE	0.99646	0.942	0.00881	0.01323					
BSFC	-0.97704	0.333	0.04558	0.05438					
NOX	0.98171	0.96544	0.00892	0.0085					
HC	0.9941	0.99127	0.00045	0.00113					
CO2	0.98842	0.99581	0.00096	0.00067	0.01547	0.01286	24	800	Softplus	Adagrad
BTE	0.99399	0.94171	0.00891	0.01329					
BSFC	-0.97975	0.34785	0.04505	0.05376					
NOX	0.98778	0.96845	0.00869	0.00777					
HC	0.9963	0.99345	0.00027	0.00085					
CO2	0.9902	0.99638	0.00074	0.00057	0.01502	0.01377	24	1000	Softplus	Adagrad
BTE	0.99275	0.93953	0.00932	0.01377					
BSFC	-0.95933	0.38514	0.04982	0.05215					
NOX	0.97469	0.96301	0.01117	0.00909					
HC	0.98258	0.98743	0.00151	0.00162					
CO2	0.99709	0.99593	0.00031	0.00065	0.0154	0.01314	32	200	Softplus	Adagrad
BTE	0.99363	0.94216	0.0081	0.0132					
BSFC	-0.96692	0.38119	0.04462	0.05244					
NOX	0.98488	0.97	0.00859	0.0074					
HC	0.99259	0.98603	0.00051	0.0018					
CO2	0.99237	0.99589	0.00061	0.00065	0.01559	0.01256	32	400	Softplus	Adagrad
BTE	0.99565	0.93721	0.00974	0.01428					
BSFC	-0.96181	0.34692	0.04334	0.05382					

NOX	0.97954	0.96626	0.00864	0.0083						
HC	0.9935	0.98691	0.00051	0.00168						
CO2	0.98523	0.99585	0.00101	0.00066	0.01499	0.0141	32	600	Softplus	Adagrad
BTE	0.99828	0.94077	0.01135	0.0135						
BSFC	-0.95945	0.4167	0.04901	0.05083						
NOX	0.98174	0.96633	0.00866	0.00828						
HC	0.99714	0.99265	0.00021	0.00095						
CO2	0.99044	0.99637	0.00066	0.00058	0.01459	0.01292	32	800	Softplus	Adagrad
BTE	0.99452	0.93981	0.00937	0.01371						
BSFC	-0.96861	0.44808	0.04571	0.04945						
NOX	0.98295	0.96712	0.00878	0.00809						
HC	0.99809	0.99395	0.00017	0.00078						
CO2	0.98959	0.99561	0.00076	0.0007	0.01351	0.01344	32	1000	Softplus	Adagrad
BTE	0.9973	0.94265	0.01054	0.01309						
BSFC	-0.93162	0.54329	0.04698	0.04488						
NOX	0.59457	0.18522	0.08968	0.12217						
HC	-0.82272	0.26987	0.04267	0.06262						
CO2	-0.59402	-0.36668	0.03878	0.08187	0.08235	0.04789	8	200	Softmax	Adagrad
BTE	0.95114	0.77347	0.04062	0.08437						
BSFC	-0.5659	0.08505	0.0277	0.06074						
NOX	0.99366	0.96129	0.0306	0.02338						
HC	0.9333	0.93836	0.00521	0.00781						
CO2	0.92388	0.96975	0.00649	0.00741	0.02199	0.01657	8	400	Softmax	Adagrad
BTE	0.99837	0.93557	0.00406	0.01711						
BSFC	-0.93226	0.35243	0.03647	0.05425						
NOX	0.98768	0.96358	0.00738	0.00956						
HC	0.94811	0.9513	0.00355	0.00623						
CO2	0.96729	0.9885	0.00277	0.00184	0.01693	0.01058	8	600	Softmax	Adagrad
BTE	0.99727	0.93698	0.00809	0.01434						
BSFC	-0.96414	0.38561	0.03112	0.0527						

NOX	0.96717	0.94067	0.01244	0.01442						
HC	0.93552	0.95801	0.00453	0.00533						
CO2	0.99264	0.98346	0.00217	0.00264	0.01631	0.01137	8	800	Softmax	Adagrad
BTE	0.99978	0.9602	0.0046	0.00935						
BSFC	-0.89939	0.44618	0.03313	0.04982						
NOX	0.96628	0.9551	0.00882	0.01098						
HC	0.95612	0.96811	0.00321	0.00407						
CO2	0.98196	0.98485	0.00378	0.00239	0.01637	0.01016	8	1000	Softmax	Adagrad
BTE	0.99971	0.94851	0.00462	0.01179						
BSFC	-0.94176	0.37808	0.03039	0.05262						
NOX	0.68976	0.44861	0.08108	0.11731						
HC	0.33723	0.8007	0.03652	0.05233						
CO2	0.19583	0.75144	0.03383	0.0675	0.07834	0.04312	16	200	Softmax	Adagrad
BTE	0.98226	0.89342	0.03606	0.0953						
BSFC	-0.95551	0.30659	0.02811	0.05926						
NOX	0.98769	0.96039	0.05102	0.05002						
HC	0.96856	0.93826	0.01076	0.01515						
CO2	0.9673	0.97928	0.01049	0.01995	0.03642	0.02193	16	400	Softmax	Adagrad
BTE	0.9929	0.89206	0.0123	0.03804						
BSFC	-0.53201	0.27572	0.02509	0.05893						
NOX	0.99575	0.9602	0.02484	0.03708						
HC	0.95704	0.92346	0.00544	0.01735						
CO2	0.95473	0.97478	0.00705	0.02413	0.0349	0.01451	16	600	Softmax	Adagrad
BTE	0.98517	0.9058	0.00716	0.03788						
BSFC	-0.96635	0.32564	0.02804	0.05808						
NOX	0.97034	0.9662	0.00904	0.00833						
HC	0.94319	0.94873	0.00434	0.00685						
CO2	0.97792	0.98878	0.00171	0.00178	0.01803	0.01198	16	800	Softmax	Adagrad
BTE	0.99681	0.9282	0.00663	0.01636						
BSFC	-0.98272	0.26704	0.03816	0.05681						

NOX	0.98248	0.96454	0.00736	0.00872						
HC	0.9713	0.96366	0.00196	0.00462						
CO2	0.95175	0.98367	0.00335	0.00261	0.01745	0.01048	16	1000	Softmax	Adagrad
BTE	0.99522	0.9328	0.00602	0.0153						
BSFC	-0.97353	0.29229	0.03372	0.056						
NOX	0.88016	0.81291	0.08386	0.11529						
HC	0.85593	0.74581	0.03628	0.0613						
CO2	0.88487	0.88728	0.03417	0.07463	0.08504	0.04534	24	200	Softmax	Adagrad
BTE	0.54667	0.57068	0.04753	0.11121						
BSFC	0.89213	-0.22507	0.02486	0.06275						
NOX	0.97161	0.83861	0.08562	0.11358						
HC	0.48025	0.80434	0.03616	0.05346						
CO2	0.93005	0.54205	0.03133	0.07511	0.08226	0.0454	24	400	Softmax	Adagrad
BTE	0.91573	0.84434	0.04984	0.10768						
BSFC	0.11287	-0.14364	0.02404	0.06149						
NOX	0.97629	0.93595	0.06197	0.07332						
HC	0.88519	0.83492	0.02287	0.03922						
CO2	0.99527	0.96728	0.01502	0.03458	0.0563	0.03228	24	600	Softmax	Adagrad
BTE	0.97629	0.85686	0.03192	0.07583						
BSFC	-0.96487	0.21505	0.02961	0.05857						
NOX	0.94684	0.9785	0.01567	0.00863						
HC	0.92253	0.92497	0.00597	0.01023						
CO2	0.97634	0.97926	0.00173	0.00548	0.02253	0.01238	24	800	Softmax	Adagrad
BTE	0.99314	0.90532	0.00574	0.03009						
BSFC	-0.9708	0.22976	0.03277	0.05823						
NOX	0.9585	0.97247	0.01339	0.00693						
HC	0.96592	0.93572	0.00425	0.00815						
CO2	0.94036	0.98472	0.00459	0.00386	0.01969	0.01273	24	1000	Softmax	Adagrad
BTE	0.99126	0.91187	0.01033	0.02322						
BSFC	-0.91282	0.28194	0.03108	0.05631						

NOX	0.11467	0.72332	0.09457	0.12129	0.08763	0.04983	32	200	Softmax	Adagrad
HC	-0.11001	-0.26413	0.03985	0.06543						
CO2	-0.48777	0.47245	0.03711	0.07662						
BTE	0.01781	0.70617	0.05301	0.11308						
BSFC	0.316	-0.2218	0.02459	0.06171						
NOX	0.77119	0.75133	0.08901	0.12003	0.08432	0.04533	32	400	Softmax	Adagrad
HC	0.92202	0.91375	0.0349	0.05827						
CO2	0.84715	0.72071	0.03224	0.07523						
BTE	0.93686	0.89816	0.04631	0.10662						
BSFC	0.01785	-0.08271	0.02418	0.06147						
NOX	0.95216	0.9085	0.0872	0.10905	0.07915	0.04548	32	600	Softmax	Adagrad
HC	0.91987	0.75436	0.03822	0.05815						
CO2	0.4581	0.8293	0.03401	0.06811						
BTE	0.99667	0.94224	0.04232	0.09895						
BSFC	-0.27486	-0.04528	0.02563	0.06147						
NOX	0.96696	0.96255	0.0711	0.08743	0.06779	0.0367	32	800	Softmax	Adagrad
HC	0.97442	0.95204	0.02467	0.04204						
CO2	0.83057	0.88907	0.02994	0.06727						
BTE	0.85975	0.87111	0.03377	0.08112						
BSFC	-0.16492	0.04125	0.02403	0.06107						
NOX	0.98101	0.97864	0.00765	0.00535	0.01935	0.01215	32	1000	Softmax	Adagrad
HC	0.97794	0.94712	0.00307	0.00687						
CO2	0.89921	0.97389	0.00693	0.00449						
BTE	0.97114	0.90481	0.01349	0.02183						
BSFC	-0.92958	0.22793	0.02961	0.05822						
NOX	0.91207	0.91714	0.05058	0.0358	0.02719	0.0254	8	200	Sigmoid	Adagrad
HC	0.96092	0.94944	0.00629	0.00879						
CO2	0.98026	0.9502	0.0087	0.0086						
BTE	0.98258	0.92332	0.01149	0.02856						
BSFC	-0.96496	0.33815	0.04994	0.02719						

NOX	0.9783	0.94932	0.01304	0.01236						
HC	0.98891	0.98121	0.00364	0.00302						
CO2	0.98129	0.97801	0.00225	0.00446	0.01714	0.01661	8	400	Sigmoid	Adagrad
BTE	0.97769	0.94763	0.00518	0.01304						
BSFC	-0.99292	0.3801	0.05894	0.05281						
NOX	0.95862	0.95024	0.01448	0.01215						
HC	0.97823	0.98871	0.00295	0.00156						
CO2	0.99911	0.99485	0.00077	0.00083	0.0158	0.01342	8	600	Sigmoid	Adagrad
BTE	0.99676	0.95067	0.00605	0.01153						
BSFC	-0.98929	0.36676	0.04286	0.05294						
NOX	0.96718	0.95027	0.01228	0.01213						
HC	0.9896	0.98926	0.00176	0.0014						
CO2	0.98463	0.99418	0.00114	0.00092	0.01531	0.01292	8	800	Sigmoid	Adagrad
BTE	0.99384	0.95588	0.00679	0.01013						
BSFC	-0.96009	0.38811	0.04263	0.05197						
NOX	0.96639	0.94431	0.01263	0.01355						
HC	0.96429	0.98352	0.00256	0.00214						
CO2	0.975	0.99134	0.00172	0.00137	0.01508	0.01335	8	1000	Sigmoid	Adagrad
BTE	0.99949	0.96588	0.00592	0.00788						
BSFC	-0.92603	0.42017	0.04393	0.05048						
NOX	0.97205	0.95334	0.0168	0.01577						
HC	0.9074	0.96002	0.01082	0.01265						
CO2	0.96966	0.98795	0.00227	0.00722	0.02265	0.01768	16	200	Sigmoid	Adagrad
BTE	0.98085	0.94372	0.00683	0.0238						
BSFC	-0.97885	0.34858	0.05168	0.05382						
NOX	0.96916	0.94859	0.01475	0.01264						
HC	0.99066	0.98563	0.00373	0.0027						
CO2	0.99621	0.99446	0.00111	0.00088	0.01618	0.01304	16	400	Sigmoid	Adagrad
BTE	0.99305	0.95115	0.00564	0.0112						
BSFC	-0.86272	0.35896	0.03996	0.05347						

NOX	0.97353	0.95454	0.01246	0.01111						
HC	0.9951	0.99258	0.00061	0.00096						
CO2	0.97753	0.99359	0.0014	0.00102	0.01556	0.01304	16	600	Sigmoid	Adagrad
BTE	0.99741	0.94991	0.00656	0.01147						
BSFC	-0.8964	0.36011	0.04415	0.05323						
NOX	0.97461	0.95228	0.01055	0.01165						
HC	0.99745	0.99605	0.00042	0.00051						
CO2	0.98484	0.99609	0.00097	0.00062	0.01528	0.01349	16	800	Sigmoid	Adagrad
BTE	0.99778	0.95172	0.00733	0.01106						
BSFC	-0.96061	0.37496	0.04818	0.05256						
NOX	0.97709	0.95379	0.01132	0.01129						
HC	0.99858	0.99498	0.00027	0.00065						
CO2	0.99221	0.99663	0.00074	0.00053	0.01495	0.01301	16	1000	Sigmoid	Adagrad
BTE	0.99799	0.9547	0.00682	0.0104						
BSFC	-0.97545	0.38939	0.04592	0.0519						
NOX	0.98013	0.91896	0.0291	0.0255						
HC	0.98772	0.96111	0.00325	0.00751						
CO2	0.95039	0.96446	0.00596	0.01769	0.02505	0.01656	24	200	Sigmoid	Adagrad
BTE	0.9706	0.93402	0.00587	0.01927						
BSFC	-0.91729	0.31106	0.03859	0.05526						
NOX	0.96988	0.95486	0.01249	0.01116						
HC	0.99272	0.98419	0.00208	0.00273						
CO2	0.98898	0.9915	0.00106	0.00137	0.01606	0.0133	24	400	Sigmoid	Adagrad
BTE	0.99596	0.94644	0.00487	0.01225						
BSFC	-0.97412	0.37007	0.04598	0.05279						
NOX	0.97239	0.95723	0.01022	0.01047						
HC	0.98489	0.98815	0.0012	0.00154						
CO2	0.97847	0.98952	0.00155	0.00167	0.01555	0.01376	24	600	Sigmoid	Adagrad
BTE	0.99845	0.95093	0.0075	0.01124						
BSFC	-0.95068	0.36882	0.04834	0.05285						

NOX	0.96695	0.95621	0.01266	0.01072						
HC	0.99361	0.99293	0.00053	0.00092						
CO2	0.98779	0.99654	0.00077	0.00055	0.01538	0.01379	24	800	Sigmoid	Adagrad
BTE	0.99722	0.95029	0.00739	0.01138						
BSFC	-0.96722	0.35709	0.04762	0.05336						
NOX	0.97809	0.95569	0.01054	0.01084						
HC	0.99725	0.9952	0.0003	0.00062						
CO2	0.98848	0.99683	0.00074	0.0005	0.01499	0.01345	24	1000	Sigmoid	Adagrad
BTE	0.99831	0.95338	0.00796	0.01069						
BSFC	-0.97272	0.38075	0.0477	0.0523						
NOX	0.96335	0.94839	0.02572	0.01497						
HC	0.98934	0.98851	0.00111	0.0017						
CO2	0.97757	0.98203	0.00197	0.00528	0.01782	0.01555	32	200	Sigmoid	Adagrad
BTE	0.99239	0.94173	0.00694	0.01394						
BSFC	-0.93427	0.36751	0.04202	0.05319						
NOX	0.99177	0.95575	0.00981	0.01083						
HC	0.99469	0.99022	0.00044	0.00126						
CO2	0.99272	0.99374	0.00056	0.00101	0.0157	0.0129	32	400	Sigmoid	Adagrad
BTE	0.99884	0.94727	0.00654	0.01208						
BSFC	-0.95492	0.35811	0.04716	0.05332						
NOX	0.97394	0.95525	0.01326	0.01094						
HC	0.99767	0.99429	0.00019	0.00074						
CO2	0.98717	0.9967	0.00084	0.00052	0.01526	0.01441	32	600	Sigmoid	Adagrad
BTE	0.99491	0.94996	0.00749	0.01145						
BSFC	-0.98303	0.37281	0.05027	0.05267						
NOX	0.97727	0.95895	0.01026	0.01006						
HC	0.99786	0.99451	0.0002	0.00071						
CO2	0.99429	0.99667	0.00046	0.00053	0.0153	0.01402	32	800	Sigmoid	Adagrad
BTE	0.9969	0.94838	0.00803	0.01181						
BSFC	-0.97244	0.35635	0.05115	0.0534						

NOX	0.97905	0.95684	0.0105	0.01056						
HC	0.99705	0.9948	0.00029	0.00067						
CO2	0.98807	0.99654	0.00078	0.00055	0.01511	0.01301	32	1000	Sigmoid	Adagrad
BTE	0.99656	0.95119	0.00746	0.01118						
BSFC	-0.97342	0.37434	0.04601	0.0526						
NOX	0.99494	0.98922	0.01007	0.01192						
HC	0.99734	0.9936	0.0015	0.00143						
CO2	0.97714	0.99221	0.00478	0.00299	0.00972	0.012	8	200	Softplus	Nadam
BTE	0.98964	0.99367	0.00165	0.00151						
BSFC	-0.54926	0.79573	0.04201	0.03075						
NOX	0.99482	0.99749	0.00214	0.00198						
HC	0.99248	0.9893	0.00213	0.00195						
CO2	0.98273	0.99416	0.00199	0.00172	0.00282	0.00402	8	400	Softplus	Nadam
BTE	0.9973	0.99882	0.00067	0.00069						
BSFC	0.35824	0.93785	0.01318	0.00776						
NOX	0.99678	0.99743	0.00942	0.00262						
HC	0.99242	0.99068	0.00426	0.00316						
CO2	0.98249	0.99374	0.00588	0.00294	0.00358	0.00778	8	600	Softplus	Nadam
BTE	0.99792	0.99897	0.00341	0.00147						
BSFC	0.30687	0.94403	0.01596	0.0077						
NOX	0.99133	0.99636	0.0131	0.00406						
HC	0.99868	0.99389	0.00183	0.003						
CO2	0.98993	0.99287	0.0036	0.00323	0.00328	0.00512	8	800	Softplus	Nadam
BTE	0.99915	0.99885	0.00348	0.00166						
BSFC	0.94562	0.98993	0.0036	0.00446						
NOX	0.99203	0.99618	0.00347	0.00399						
HC	0.99544	0.99484	0.0036	0.00278						
CO2	0.98974	0.99483	0.00201	0.00264	0.00307	0.00268	8	1000	Softplus	Nadam
BTE	0.99847	0.99852	0.00135	0.00155						
BSFC	0.97604	0.99612	0.00297	0.00439						

NOX	0.9937	0.99754	0.01428	0.01745						
HC	0.99569	0.994	0.00816	0.00603						
CO2	0.9866	0.99493	0.00891	0.01016	0.00984	0.01034	16	200	Softplus	Nadam
BTE	0.99728	0.99881	0.0024	0.00327						
BSFC	0.33384	0.94633	0.01795	0.01229						
NOX	0.9925	0.99705	0.00324	0.00368						
HC	0.99278	0.99076	0.00259	0.00241						
CO2	0.98697	0.99587	0.00229	0.00237	0.0026	0.00299	16	400	Softplus	Nadam
BTE	0.99866	0.99871	0.00105	0.00157						
BSFC	0.74484	0.97816	0.00578	0.00295						
NOX	0.99134	0.99669	0.01033	0.00394						
HC	0.99819	0.99639	0.00071	0.00183						
CO2	0.98033	0.99558	0.00469	0.00301	0.0026	0.00399	16	600	Softplus	Nadam
BTE	0.99969	0.99909	0.00276	0.00106						
BSFC	0.97375	0.9941	0.00149	0.00316						
NOX	0.99283	0.99711	0.0087	0.00325						
HC	0.99746	0.99515	0.00223	0.00242						
CO2	0.98457	0.99566	0.00395	0.00255	0.0027	0.00418	16	800	Softplus	Nadam
BTE	0.99838	0.99927	0.00261	0.00097						
BSFC	0.88756	0.98982	0.00339	0.00431						
NOX	0.99438	0.99705	0.00253	0.00314						
HC	0.99432	0.99595	0.00373	0.00239						
CO2	0.9893	0.99541	0.00188	0.00238	0.00259	0.00263	16	1000	Softplus	Nadam
BTE	0.99787	0.99891	0.00069	0.00099						
BSFC	0.91708	0.99443	0.00432	0.00403						
NOX	0.99541	0.99696	0.00276	0.00135						
HC	0.99387	0.99299	0.00148	0.00098						
CO2	0.98326	0.99418	0.00183	0.00108	0.00379	0.00701	24	200	Softplus	Nadam
BTE	0.99261	0.99728	0.0011	0.00064						
BSFC	-0.29334	0.87425	0.02786	0.0149						

NOX	0.99483	0.99763	0.00468	0.00707						
HC	0.99553	0.99399	0.00659	0.00588						
CO2	0.9829	0.99464	0.00475	0.00583	0.00518	0.00514	24	400	Softplus	Nadam
BTE	0.99836	0.99937	0.00124	0.00247						
BSFC	0.63138	0.97166	0.00845	0.00465						
NOX	0.99373	0.99711	0.00579	0.008						
HC	0.99602	0.9958	0.00649	0.00584						
CO2	0.98267	0.99621	0.00443	0.0048	0.00501	0.00458	24	600	Softplus	Nadam
BTE	0.99982	0.99917	0.00255	0.00481						
BSFC	0.84451	0.98737	0.00364	0.00161						
NOX	0.99402	0.99676	0.00959	0.00357						
HC	0.99678	0.99606	0.00148	0.00175						
CO2	0.98321	0.99613	0.003	0.00219	0.00238	0.00371	24	800	Softplus	Nadam
BTE	0.99836	0.99961	0.00173	0.00053						
BSFC	0.90155	0.9913	0.00277	0.00384						
NOX	0.99162	0.99669	0.00328	0.00349						
HC	0.99632	0.99642	0.00219	0.0016						
CO2	0.98266	0.99612	0.00232	0.00227	0.00216	0.00206	24	1000	Softplus	Nadam
BTE	0.9997	0.99964	0.0004	0.00083						
BSFC	0.99046	0.9982	0.00211	0.00262						
NOX	0.99119	0.99029	0.00468	0.00247						
HC	0.99845	0.99595	0.00059	0.00052						
CO2	0.99134	0.99406	0.00096	0.00095	0.00428	0.00698	32	200	Softplus	Nadam
BTE	0.99708	0.99598	0.00129	0.00094						
BSFC	-0.45507	0.86568	0.02739	0.01652						
NOX	0.9894	0.99635	0.00307	0.00244						
HC	0.99767	0.99576	0.00176	0.00143						
CO2	0.98567	0.99664	0.00193	0.0017	0.00176	0.00244	32	400	Softplus	Nadam
BTE	0.9991	0.99962	0.00041	0.00058						
BSFC	0.78979	0.98163	0.00506	0.00267						

NOX	0.9956	0.99722	0.00249	0.00319						
HC	0.99624	0.99515	0.00373	0.00321						
CO2	0.98732	0.99619	0.00255	0.00289	0.00263	0.00296	32	600	Softplus	Nadam
BTE	0.99759	0.99905	0.00084	0.00185						
BSFC	0.77276	0.98475	0.00518	0.002						
NOX	0.99089	0.99699	0.00975	0.00402						
HC	0.99702	0.99709	0.00125	0.00232						
CO2	0.98191	0.99623	0.00351	0.00205	0.00249	0.00342	32	800	Softplus	Nadam
BTE	0.99918	0.99969	0.00159	0.00092						
BSFC	0.98368	0.99584	0.001	0.00315						
NOX	0.99129	0.99668	0.00334	0.0034						
HC	0.99794	0.99714	0.00292	0.00194						
CO2	0.98627	0.99638	0.00171	0.00171	0.00185	0.00201	32	1000	Softplus	Nadam
BTE	0.99976	0.99956	0.00091	0.00166						
BSFC	0.96818	0.99767	0.00117	0.00054						
NOX	0.99374	0.99639	0.00259	0.00271						
HC	0.99097	0.99461	0.00107	0.00146						
CO2	0.986	0.99507	0.00364	0.00604	0.00389	0.00371	8	200	Softmax	Nadam
BTE	0.99748	0.9994	0.00334	0.00282						
BSFC	0.70891	0.96453	0.00793	0.0064						
NOX	0.99854	0.99898	0.00302	0.00347						
HC	0.99484	0.99657	0.00308	0.00488						
CO2	0.98764	0.99796	0.0017	0.00277	0.00307	0.00262	8	400	Softmax	Nadam
BTE	0.99617	0.99928	0.00267	0.00228						
BSFC	0.93676	0.99359	0.00264	0.00197						
NOX	0.99791	0.99929	0.00302	0.00117						
HC	0.9862	0.99412	0.00696	0.00273						
CO2	0.98751	0.9989	0.00682	0.00249	0.00308	0.00548	8	600	Softmax	Nadam
BTE	0.99193	0.9991	0.00516	0.00417						
BSFC	0.97227	0.99656	0.00545	0.00484						

NOX	0.99958	0.99924	0.00751	0.00473						
HC	0.9861	0.99383	0.00381	0.00159						
CO2	0.98534	0.99812	0.01163	0.00498	0.00298	0.00558	8	800	Softmax	Nadam
BTE	0.99728	0.99919	0.00183	0.00166						
BSFC	0.94325	0.99727	0.00311	0.00196						
NOX	0.99954	0.99938	0.01006	0.00517						
HC	0.98654	0.99543	0.00807	0.00348						
CO2	0.9848	0.99888	0.01379	0.00579	0.00319	0.00679	8	1000	Softmax	Nadam
BTE	0.99438	0.99958	0.00073	0.00026						
BSFC	0.97351	0.99744	0.00131	0.00125						
NOX	0.99728	0.99947	0.00559	0.00454						
HC	0.98685	0.99574	0.00818	0.00352						
CO2	0.98454	0.99802	0.00771	0.00394	0.00468	0.00743	16	200	Softmax	Nadam
BTE	0.99849	0.99972	0.00298	0.00238						
BSFC	0.672	0.98197	0.0127	0.00901						
NOX	0.99906	0.9997	0.01083	0.0062						
HC	0.98467	0.99526	0.00317	0.00143						
CO2	0.9896	0.99874	0.00801	0.00416	0.00394	0.00632	16	400	Softmax	Nadam
BTE	0.99497	0.99914	0.00462	0.00452						
BSFC	0.91015	0.99495	0.00498	0.00337						
NOX	0.99937	0.99957	0.0073	0.00303						
HC	0.99193	0.99869	0.01371	0.00529						
CO2	0.99021	0.9993	0.00439	0.00174	0.0024	0.00588	16	600	Softmax	Nadam
BTE	0.99266	0.99938	0.00206	0.0012						
BSFC	0.97141	0.99822	0.00194	0.00075						
NOX	0.99965	0.99949	0.00552	0.00195						
HC	0.99148	0.99843	0.0007	0.00203						
CO2	0.98968	0.99922	0.0063	0.00215	0.00139	0.00297	16	800	Softmax	Nadam
BTE	0.99185	0.99941	0.00135	0.00036						
BSFC	0.97286	0.99811	0.001	0.00045						

NOX	0.99944	0.99973	0.0016	0.00034						
HC	0.99228	0.99859	0.0047	0.0008						
CO2	0.99366	0.99938	0.00187	0.00052	0.00288	0.00462	16	1000	Softmax	Nadam
BTE	0.99308	0.99956	0.01328	0.01239						
BSFC	0.9731	0.99815	0.00163	0.00035						
NOX	0.99528	0.99873	0.00333	0.00163						
HC	0.99534	0.99863	0.00314	0.00146						
CO2	0.9891	0.99893	0.00355	0.0023	0.00354	0.00418	24	200	Softmax	Nadam
BTE	0.99862	0.9992	0.00296	0.00567						
BSFC	0.72687	0.98656	0.00792	0.00662						
NOX	0.99914	0.99949	0.0135	0.00692						
HC	0.99532	0.99828	0.00545	0.00196						
CO2	0.98792	0.99898	0.00828	0.00343	0.00321	0.00666	24	400	Softmax	Nadam
BTE	0.99731	0.99932	0.00133	0.00072						
BSFC	0.89353	0.99585	0.00475	0.003						
NOX	0.9992	0.99952	0.00082	0.0024						
HC	0.99389	0.99882	0.00044	0.00175						
CO2	0.9929	0.99932	0.00161	0.00324	0.00185	0.00109	24	600	Softmax	Nadam
BTE	0.98891	0.99921	0.00149	0.00161						
BSFC	0.97097	0.99807	0.0011	0.00025						
NOX	0.99891	0.99951	0.00056	0.00184						
HC	0.99184	0.99783	0.00126	0.00417						
CO2	0.99377	0.99941	0.00073	0.00021	0.00222	0.00119	24	800	Softmax	Nadam
BTE	0.98781	0.99916	0.00089	0.00032						
BSFC	0.96194	0.99675	0.0025	0.00458						
NOX	0.99881	0.99914	0.00185	0.00357						
HC	0.99609	0.99895	0.00028	0.00168						
CO2	0.98986	0.99913	0.00102	0.00183	0.00224	0.00112	24	1000	Softmax	Nadam
BTE	0.98664	0.99945	0.00078	0.0003						
BSFC	0.98586	0.99804	0.00166	0.0038						

NOX	0.99755	0.99742	0.00488	0.00685						
HC	0.99542	0.99773	0.00236	0.00526						
CO2	0.99283	0.9981	0.00471	0.0062	0.00527	0.00475	32	200	Softmax	Nadam
BTE	0.99803	0.999	0.00631	0.00431						
BSFC	0.83489	0.99216	0.00547	0.00372						
NOX	0.99717	0.99954	0.00802	0.00508						
HC	0.99225	0.99847	0.01178	0.00452						
CO2	0.99275	0.99922	0.00741	0.00239	0.00362	0.0074	32	400	Softmax	Nadam
BTE	0.99553	0.99872	0.00088	0.00085						
BSFC	0.92847	0.99495	0.00892	0.00527						
NOX	0.9991	0.99938	0.00075	0.00237						
HC	0.99237	0.99864	0.00059	0.00111						
CO2	0.99138	0.99947	0.00078	0.00141	0.00124	0.00082	32	600	Softmax	Nadam
BTE	0.991	0.99916	0.00096	0.00086						
BSFC	0.96263	0.99749	0.00103	0.00047						
NOX	0.99882	0.9997	0.01019	0.00463						
HC	0.99629	0.99861	0.0116	0.00541						
CO2	0.99666	0.99957	0.00563	0.00133	0.00321	0.00712	32	800	Softmax	Nadam
BTE	0.99068	0.99969	0.00253	0.00115						
BSFC	0.93366	0.99737	0.00567	0.00352						
NOX	0.99924	0.99966	0.00376	0.00101						
HC	0.99123	0.99878	0.01614	0.00751						
CO2	0.99287	0.99943	0.00275	0.00031	0.00355	0.00724	32	1000	Softmax	Nadam
BTE	0.98953	0.99956	0.00539	0.00285						
BSFC	0.96263	0.99815	0.00816	0.00607						
NOX	0.99665	0.99664	0.00134	0.00085						
HC	0.99146	0.99502	0.00062	0.00071						
CO2	0.9816	0.99445	0.00161	0.00093	0.00322	0.00522	8	200	Sigmoid	Nadam
BTE	0.98572	0.99568	0.00207	0.0011						
BSFC	0.0798	0.89313	0.02045	0.01251						

NOX	0.99687	0.9983	0.00635	0.00589						
HC	0.99623	0.99653	0.00149	0.00156						
CO2	0.9896	0.99751	0.00471	0.00493	0.0039	0.0048	8	400	Sigmoid	Nadam
BTE	0.99768	0.99851	0.00555	0.00291						
BSFC	0.83721	0.98283	0.00592	0.0042						
NOX	0.99568	0.9986	0.00393	0.00218						
HC	0.9918	0.99653	0.00068	0.00096						
CO2	0.98671	0.99664	0.00485	0.00256	0.00219	0.00346	8	600	Sigmoid	Nadam
BTE	0.9963	0.99811	0.00364	0.00121						
BSFC	0.9382	0.98933	0.00419	0.00402						
NOX	0.99594	0.99887	0.00475	0.00427						
HC	0.99293	0.99731	0.00978	0.0045						
CO2	0.99131	0.99597	0.00563	0.00438	0.00462	0.00678	8	800	Sigmoid	Nadam
BTE	0.99858	0.99923	0.00408	0.00407						
BSFC	0.9444	0.98409	0.00966	0.00588						
NOX	0.99726	0.99877	0.00509	0.00286						
HC	0.99377	0.99721	0.00098	0.00275						
CO2	0.99128	0.99755	0.00244	0.00305	0.00293	0.00308	8	1000	Sigmoid	Nadam
BTE	0.9991	0.99872	0.00366	0.00285						
BSFC	0.92079	0.99165	0.00325	0.00314						
NOX	0.99428	0.99602	0.00232	0.00103						
HC	0.99845	0.99769	0.00139	0.00045						
CO2	0.98981	0.99595	0.00097	0.00072	0.00432	0.00782	16	200	Sigmoid	Nadam
BTE	0.98967	0.99264	0.00307	0.00237						
BSFC	-0.39034	0.85564	0.03137	0.01705						
NOX	0.99541	0.99747	0.00967	0.00493						
HC	0.99748	0.99681	0.01018	0.00594						
CO2	0.99396	0.99758	0.01066	0.00502	0.00548	0.00916	16	400	Sigmoid	Nadam
BTE	0.9939	0.99831	0.00373	0.0035						
BSFC	0.65064	0.93605	0.01158	0.008						

NOX	0.99649	0.99888	0.00139	0.00161						
HC	0.99859	0.99811	0.00084	0.00025						
CO2	0.99263	0.99853	0.00221	0.00099	0.00225	0.00217	16	600	Sigmoid	Nadam
BTE	0.99947	0.99923	0.00143	0.00169						
BSFC	0.90732	0.99139	0.00496	0.00672						
NOX	0.99626	0.99896	0.00414	0.00451						
HC	0.99754	0.99811	0.00115	0.00029						
CO2	0.98437	0.99681	0.00356	0.00337	0.00193	0.0022	16	800	Sigmoid	Nadam
BTE	0.99976	0.99913	0.00031	0.00083						
BSFC	0.93132	0.99498	0.00185	0.00065						
NOX	0.99597	0.99931	0.00659	0.00453						
HC	0.99435	0.99849	0.00091	0.00027						
CO2	0.99461	0.99863	0.00211	0.00302	0.00395	0.0066	16	1000	Sigmoid	Nadam
BTE	0.99984	0.99899	0.00228	0.00256						
BSFC	0.85387	0.98659	0.02108	0.00936						
NOX	0.98931	0.99196	0.0038	0.00223						
HC	0.99845	0.99681	0.00027	0.00046						
CO2	0.9877	0.99604	0.00079	0.00066	0.00309	0.00535	24	200	Sigmoid	Nadam
BTE	0.99577	0.99905	0.00043	0.0003						
BSFC	-0.22736	0.91035	0.02149	0.01183						
NOX	0.9962	0.99768	0.00109	0.00058						
HC	0.99669	0.99711	0.00059	0.00037						
CO2	0.9857	0.99772	0.00109	0.00036	0.00121	0.00259	24	400	Sigmoid	Nadam
BTE	0.99723	0.99957	0.00022	0.0001						
BSFC	0.57807	0.96156	0.01001	0.00462						
NOX	0.99442	0.99761	0.00106	0.0006						
HC	0.99645	0.9974	0.00059	0.00034						
CO2	0.99212	0.99762	0.00051	0.00038	0.00046	0.00106	24	600	Sigmoid	Nadam
BTE	0.99981	0.99947	0.0001	0.00012						
BSFC	0.87547	0.99301	0.00305	0.00086						

NOX	0.99456	0.9989	0.00216	0.00067						
HC	0.99749	0.99839	0.00036	0.00036						
CO2	0.99077	0.99907	0.00063	0.00039	0.00043	0.00093	24	800	Sigmoid	Nadam
BTE	0.99917	0.99946	0.00025	0.00037						
BSFC	0.96896	0.99776	0.00124	0.00038						
NOX	0.9975	0.99938	0.00157	0.00055						
HC	0.99623	0.99819	0.00048	0.00052						
CO2	0.9975	0.99871	0.00053	0.00054	0.00063	0.00134	24	1000	Sigmoid	Nadam
BTE	0.99963	0.99934	0.00042	0.00062						
BSFC	0.92088	0.99526	0.00369	0.0009						
NOX	0.99036	0.99656	0.00183	0.00087						
HC	0.99829	0.99683	0.0006	0.00041						
CO2	0.98695	0.9963	0.00083	0.00059	0.00196	0.00332	32	200	Sigmoid	Nadam
BTE	0.99556	0.99934	0.00031	0.00016						
BSFC	0.34772	0.93556	0.01303	0.00779						
NOX	0.98857	0.99654	0.00207	0.00086						
HC	0.99538	0.99588	0.00064	0.00053						
CO2	0.98546	0.99751	0.00091	0.00039	0.00067	0.0013	32	400	Sigmoid	Nadam
BTE	0.99991	0.99937	0.0002	0.00015						
BSFC	0.89006	0.98854	0.00269	0.00141						
NOX	0.99556	0.99823	0.00129	0.00052						
HC	0.99791	0.99723	0.00086	0.00043						
CO2	0.99168	0.99812	0.00127	0.00036	0.00077	0.00175	32	600	Sigmoid	Nadam
BTE	0.99973	0.99941	0.00002	0.00022						
BSFC	0.78111	0.9808	0.00532	0.00233						
NOX	0.99684	0.99918	0.00066	0.00022						
HC	0.99728	0.99811	0.00087	0.00031						
CO2	0.98885	0.99846	0.0007	0.00025	0.00043	0.00082	32	800	Sigmoid	Nadam
BTE	0.9997	0.99958	0.00016	0.00013						
BSFC	0.9717	0.99835	0.00172	0.00125						

NOX	0.9972	0.99928	0.00316	0.00344						
HC	0.99794	0.99741	0.00584	0.00396						
CO2	0.9889	0.99792	0.00495	0.00427	0.0033	0.00371	32	1000	Sigmoid	Nadam
BTE	0.99895	0.99935	0.00334	0.00358						
BSFC	0.99292	0.99919	0.00128	0.00126						
NOX	0.98825	0.99098	0.00699	0.00226						
HC	0.99379	0.98829	0.00133	0.00151						
CO2	0.98643	0.99397	0.00095	0.00096	0.00413	0.00712	8	200	Softplus	Adam
BTE	0.99091	0.99717	0.00105	0.00066						
BSFC	-0.2725	0.86662	0.02527	0.01525						
NOX	0.99417	0.99801	0.00196	0.0005						
HC	0.99646	0.9948	0.00089	0.00067						
CO2	0.98734	0.99649	0.00105	0.00056	0.00168	0.00311	8	400	Softplus	Adam
BTE	0.9966	0.99948	0.00064	0.00012						
BSFC	0.48551	0.94503	0.01101	0.00645						
NOX	0.99465	0.99791	0.00175	0.00052						
HC	0.99504	0.99439	0.00098	0.00072						
CO2	0.98689	0.9968	0.00087	0.00051	0.00126	0.00209	8	600	Softplus	Adam
BTE	0.99583	0.99875	0.00075	0.00029						
BSFC	0.73125	0.9647	0.00609	0.00426						
NOX	0.99379	0.99803	0.00175	0.00049						
HC	0.99789	0.99712	0.00048	0.00037						
CO2	0.98944	0.99667	0.00075	0.00053	0.00034	0.00076	8	800	Softplus	Adam
BTE	0.99999	0.99945	0.00038	0.00013						
BSFC	0.99714	0.99854	0.00046	0.00018						
NOX	0.99156	0.997	0.00187	0.00075						
HC	0.99568	0.99539	0.00061	0.0006						
CO2	0.98833	0.99669	0.0009	0.00052	0.0008	0.00171	8	1000	Softplus	Adam
BTE	0.99982	0.99857	0.00066	0.00034						
BSFC	0.80244	0.98537	0.00454	0.00178						

NOX	0.99639	0.99729	0.00352	0.00068						
HC	0.99585	0.99247	0.00158	0.00097						
CO2	0.9749	0.99537	0.00177	0.00073	0.00309	0.00597	16	200	Softplus	Adam
BTE	0.99375	0.99889	0.00037	0.00026						
BSFC	-0.01931	0.88926	0.02259	0.0128						
NOX	0.99606	0.99816	0.0022	0.00046						
HC	0.9966	0.99389	0.00111	0.00079						
CO2	0.98129	0.99611	0.00145	0.00062	0.00247	0.00485	16	400	Softplus	Adam
BTE	0.99328	0.99881	0.0004	0.00028						
BSFC	0.1273	0.91305	0.01908	0.01018						
NOX	0.99018	0.99757	0.00223	0.00061						
HC	0.9976	0.99638	0.00053	0.00047						
CO2	0.98911	0.9968	0.00073	0.00051	0.00069	0.00149	16	600	Softplus	Adam
BTE	0.99978	0.99945	0.00039	0.00013						
BSFC	0.84746	0.98566	0.00358	0.00175						
NOX	0.99433	0.99804	0.00192	0.00049						
HC	0.99891	0.99748	0.00034	0.00033						
CO2	0.98767	0.99693	0.00098	0.00049	0.00062	0.00153	16	800	Softplus	Adam
BTE	0.99705	0.99966	0.00022	0.00008						
BSFC	0.82077	0.98577	0.00421	0.00174						
NOX	0.99328	0.99812	0.00266	0.00047						
HC	0.99745	0.99802	0.00048	0.00026						
CO2	0.98751	0.99703	0.00086	0.00047	0.0003	0.00098	16	1000	Softplus	Adam
BTE	0.99911	0.99973	0.00012	0.00006						
BSFC	0.98349	0.99815	0.00079	0.00023						
NOX	0.99013	0.9746	0.00828	0.0064						
HC	0.99441	0.98537	0.00051	0.00198						
CO2	0.98957	0.99558	0.00068	0.0007	0.00834	0.01068	24	200	Softplus	Adam
BTE	0.99865	0.97812	0.00466	0.0051						
BSFC	-0.75161	0.77261	0.03926	0.0275						

NOX	0.99484	0.99774	0.00195	0.00057						
HC	0.9962	0.99446	0.0009	0.00072						
CO2	0.98557	0.99621	0.00103	0.0006	0.00163	0.00353	24	400	Softplus	Adam
BTE	0.99597	0.99954	0.00039	0.00011						
BSFC	0.3697	0.94814	0.0134	0.00618						
NOX	0.99408	0.99828	0.0024	0.00043						
HC	0.99654	0.99562	0.00073	0.00057						
CO2	0.98516	0.99673	0.00114	0.00052	0.00212	0.00472	24	600	Softplus	Adam
BTE	0.99708	0.99939	0.00023	0.00014						
BSFC	0.15887	0.92392	0.01908	0.00895						
NOX	0.99024	0.99694	0.00209	0.00076						
HC	0.99773	0.99682	0.00051	0.00041						
CO2	0.98495	0.99712	0.00109	0.00046	0.00057	0.0013	24	800	Softplus	Adam
BTE	0.99965	0.99966	0.00023	0.00008						
BSFC	0.89203	0.99081	0.00258	0.00113						
NOX	0.99327	0.99746	0.00201	0.00063						
HC	0.99634	0.99765	0.00068	0.0003						
CO2	0.97937	0.9964	0.00164	0.00057	0.00055	0.00208	24	1000	Softplus	Adam
BTE	0.99832	0.9995	0.00026	0.00012						
BSFC	0.7508	0.99071	0.00581	0.00114						
NOX	0.99376	0.99091	0.00628	0.00228						
HC	0.99646	0.99037	0.00135	0.00125						
CO2	0.98672	0.99496	0.00093	0.00081	0.0058	0.00943	32	200	Softplus	Adam
BTE	0.99966	0.98641	0.00308	0.00321						
BSFC	-0.61045	0.82666	0.03549	0.02147						
NOX	0.99485	0.9979	0.00241	0.00052						
HC	0.99622	0.99357	0.00099	0.00083						
CO2	0.98464	0.99553	0.00109	0.00071	0.00175	0.0034	32	400	Softplus	Adam
BTE	0.99489	0.9994	0.00054	0.00014						
BSFC	0.44287	0.94491	0.01196	0.00655						

NOX	0.99507	0.99816	0.0018	0.00046						
HC	0.99647	0.99566	0.00078	0.00056						
CO2	0.98629	0.99724	0.00095	0.00044	0.00132	0.003	32	600	Softplus	Adam
BTE	0.9953	0.99916	0.00036	0.0002						
BSFC	0.49304	0.95862	0.01112	0.00496						
NOX	0.9959	0.99789	0.00164	0.00053						
HC	0.99795	0.99722	0.00063	0.00036						
CO2	0.98596	0.99712	0.00104	0.00046	0.00088	0.00267	32	800	Softplus	Adam
BTE	0.99871	0.99979	0.00018	0.00005						
BSFC	0.54932	0.97534	0.00985	0.00299						
NOX	0.99164	0.99721	0.00212	0.0007						
HC	0.9989	0.99722	0.00035	0.00036						
CO2	0.9861	0.99703	0.00101	0.00047	0.00051	0.00143	32	1000	Softplus	Adam
BTE	0.99955	0.99964	0.00019	0.00009						
BSFC	0.85166	0.99243	0.00347	0.00093						
NOX	0.98486	0.99358	0.00289	0.00162						
HC	0.98704	0.99346	0.00149	0.00085						
CO2	0.98294	0.99468	0.00175	0.00085	0.00142	0.00247	8	200	Softmax	Adam
BTE	0.99988	0.99877	0.00017	0.00029						
BSFC	0.72464	0.97104	0.00602	0.0035						
NOX	0.99853	0.99955	0.00062	0.00011						
HC	0.99727	0.99691	0.00076	0.0004						
CO2	0.99276	0.99763	0.00061	0.00038	0.00027	0.00047	8	400	Softmax	Adam
BTE	0.99933	0.99921	0.00023	0.00019						
BSFC	0.99415	0.99771	0.00016	0.00028						
NOX	0.99891	0.99966	0.00044	0.00009						
HC	0.99678	0.99761	0.00057	0.00031						
CO2	0.98857	0.99866	0.00082	0.00021	0.00017	0.00043	8	600	Softmax	Adam
BTE	0.9994	0.99957	0.0001	0.0001						
BSFC	0.99486	0.99871	0.00019	0.00016						

NOX	0.99788	0.99941	0.00056	0.00015						
HC	0.99804	0.99677	0.00052	0.00042						
CO2	0.98992	0.99669	0.00101	0.00052	0.00028	0.00051	8	800	Softmax	Adam
BTE	0.99833	0.99936	0.00015	0.00015						
BSFC	0.99656	0.99877	0.0003	0.00015						
NOX	0.99965	0.99988	0.00007	0.00003						
HC	0.99386	0.9985	0.00088	0.00019						
CO2	0.99165	0.99905	0.00072	0.00015	0.00011	0.00038	8	1000	Softmax	Adam
BTE	0.99747	0.99968	0.00015	0.00008						
BSFC	0.99923	0.9992	0.00009	0.0001						
NOX	0.99649	0.99842	0.00072	0.0005						
HC	0.99563	0.99724	0.0007	0.00037						
CO2	0.98998	0.99811	0.00064	0.00033	0.00036	0.0008	16	200	Softmax	Adam
BTE	0.99991	0.99916	0.00032	0.00021						
BSFC	0.93786	0.99695	0.0016	0.00037						
NOX	0.99794	0.99945	0.00056	0.00014						
HC	0.99388	0.99789	0.00079	0.00027						
CO2	0.9803	0.99831	0.00124	0.00027	0.00019	0.00067	16	400	Softmax	Adam
BTE	0.99948	0.99974	0.00007	0.00006						
BSFC	0.98379	0.99813	0.0007	0.00023						
NOX	0.99904	0.99975	0.00036	0.00006						
HC	0.9946	0.99773	0.00071	0.00029						
CO2	0.98675	0.99845	0.00087	0.00025	0.00016	0.00051	16	600	Softmax	Adam
BTE	0.99868	0.99975	0.00018	0.00006						
BSFC	0.98573	0.99898	0.00042	0.00012						
NOX	0.99952	0.99987	0.00014	0.00004						
HC	0.99629	0.99885	0.00081	0.00015						
CO2	0.98578	0.99904	0.00103	0.00015	0.0001	0.00048	16	800	Softmax	Adam
BTE	0.99792	0.99975	0.00014	0.00006						
BSFC	0.99193	0.99917	0.00026	0.0001						

NOX	0.99967	0.99989	0.00009	0.00005						
HC	0.99351	0.99911	0.00138	0.00012						
CO2	0.9914	0.99961	0.00096	0.00007	0.00008	0.00063	16	1000	Softmax	Adam
BTE	0.9981	0.99985	0.00016	0.00004						
BSFC	0.98204	0.99917	0.00057	0.0001						
NOX	0.99094	0.99721	0.00183	0.0007						
HC	0.99656	0.99742	0.00068	0.00033						
CO2	0.98625	0.99695	0.00091	0.00048	0.0006	0.00176	24	200	Softmax	Adam
BTE	0.99926	0.99949	0.00028	0.00012						
BSFC	0.77521	0.98879	0.00508	0.00136						
NOX	0.99851	0.99978	0.00028	0.00006						
HC	0.99388	0.99919	0.00098	0.00011						
CO2	0.98754	0.999	0.00084	0.00016	0.00011	0.00049	24	400	Softmax	Adam
BTE	0.99937	0.99963	0.00007	0.00009						
BSFC	0.99329	0.99904	0.00027	0.00012						
NOX	0.99979	0.99992	0.00005	0.00004						
HC	0.99404	0.99924	0.00124	0.0001						
CO2	0.98993	0.99921	0.00075	0.00013	0.00009	0.00054	24	600	Softmax	Adam
BTE	0.99729	0.99958	0.00026	0.0001						
BSFC	0.99001	0.99921	0.00042	0.0001						
NOX	0.99972	0.9999	0.00007	0.00002						
HC	0.99601	0.99922	0.00128	0.0001						
CO2	0.9896	0.99951	0.00081	0.00008	0.00007	0.00055	24	800	Softmax	Adam
BTE	0.99731	0.99978	0.00019	0.00005						
BSFC	0.99154	0.99925	0.00041	0.00009						
NOX	0.99971	0.99993	0.00005	0.00002						
HC	0.99563	0.99942	0.00124	0.00008						
CO2	0.99323	0.99973	0.00073	0.00004	0.00006	0.00052	24	1000	Softmax	Adam
BTE	0.99746	0.99978	0.00021	0.00005						
BSFC	0.9922	0.99927	0.00037	0.00009						

NOX	0.99444	0.99917	0.00151	0.00021					
HC	0.99655	0.99893	0.0007	0.00014					
CO2	0.98558	0.99864	0.00091	0.00022	0.00017	0.00104	32	200	Softmax	Adam
BTE	0.99888	0.99952	0.00022	0.00011					
BSFC	0.95402	0.9985	0.00187	0.00018					
NOX	0.99899	0.99973	0.00019	0.00007					
HC	0.99439	0.99853	0.00085	0.00019					
CO2	0.98904	0.99898	0.00072	0.00016	0.00012	0.00049	32	400	Softmax	Adam
BTE	0.9982	0.99959	0.00014	0.0001					
BSFC	0.99031	0.99913	0.00054	0.00011					
NOX	0.99837	0.99959	0.00235	0.00302					
HC	0.99482	0.99899	0.00169	0.00029					
CO2	0.98862	0.99926	0.00166	0.00078	0.00096	0.00133	32	600	Softmax	Adam
BTE	0.99719	0.99958	0.00042	0.0003					
BSFC	0.99013	0.99844	0.00052	0.00041					
NOX	0.99983	0.99994	0.00006	0.00001					
HC	0.99561	0.99945	0.00137	0.00007					
CO2	0.99334	0.99965	0.00075	0.00006	0.00005	0.00051	32	800	Softmax	Adam
BTE	0.99651	0.99982	0.00024	0.00004					
BSFC	0.99815	0.99938	0.00014	0.00008					
NOX	0.99987	0.99996	0.00004	0.00001					
HC	0.99551	0.99951	0.00149	0.00006					
CO2	0.99649	0.99986	0.00073	0.00002	0.00004	0.00054	32	1000	Softmax	Adam
BTE	0.99848	0.9999	0.00013	0.00002					
BSFC	0.99273	0.99948	0.00034	0.00006					
NOX	0.99226	0.99059	0.0026	0.00235					
HC	0.99749	0.99733	0.00047	0.00034					
CO2	0.99413	0.99737	0.00062	0.00042	0.00156	0.00236	8	200	Sigmoid	Adam
BTE	0.9971	0.99948	0.00021	0.00012					
BSFC	0.79235	0.9624	0.00789	0.00455					

NOX	0.99548	0.99874	0.00093	0.00032						
HC	0.99964	0.99787	0.00043	0.00027						
CO2	0.9924	0.99748	0.00057	0.0004	0.00043	0.00131	8	400	Sigmoid	Adam
BTE	0.99893	0.99961	0.00036	0.00009						
BSFC	0.93222	0.99121	0.00424	0.00107						
NOX	0.9952	0.99778	0.00091	0.00055						
HC	0.9987	0.99821	0.00056	0.00023						
CO2	0.99342	0.99792	0.00048	0.00033	0.00076	0.00125	8	600	Sigmoid	Adam
BTE	0.9992	0.99948	0.00012	0.00012						
BSFC	0.8217	0.97883	0.00416	0.00257						
NOX	0.99987	0.9998	0.00009	0.00005						
HC	0.99844	0.99862	0.00085	0.00018						
CO2	0.9908	0.99868	0.0007	0.00021	0.00013	0.00045	8	800	Sigmoid	Adam
BTE	0.99989	0.99957	0.00008	0.0001						
BSFC	0.98545	0.99905	0.0005	0.00012						
NOX	0.99682	0.99922	0.00078	0.00019						
HC	0.99922	0.99842	0.00039	0.0002						
CO2	0.99071	0.99813	0.00071	0.0003	0.00029	0.00103	8	1000	Sigmoid	Adam
BTE	0.99799	0.99942	0.00051	0.00014						
BSFC	0.94169	0.99514	0.00276	0.00059						
NOX	0.99474	0.9956	0.00217	0.00116						
HC	0.9963	0.99435	0.00066	0.00073						
CO2	0.97884	0.99494	0.00156	0.0008	0.00426	0.00689	16	200	Sigmoid	Adam
BTE	0.99902	0.98608	0.00327	0.00325						
BSFC	-0.2918	0.87303	0.02677	0.01536						
NOX	0.99093	0.99221	0.00405	0.00194						
HC	0.99825	0.9976	0.00063	0.00031						
CO2	0.99513	0.99789	0.00077	0.00034	0.00157	0.00398	16	400	Sigmoid	Adam
BTE	0.98973	0.99911	0.00087	0.00021						
BSFC	0.54955	0.95788	0.01359	0.00507						

NOX	0.98868	0.99587	0.00216	0.00103						
HC	0.99841	0.9984	0.00052	0.00021						
CO2	0.9903	0.9982	0.00069	0.00029	0.00052	0.00097	16	600	Sigmoid	Adam
BTE	0.99958	0.99958	0.00005	0.0001						
BSFC	0.94719	0.99213	0.00141	0.00096						
NOX	0.99788	0.99964	0.00046	0.00009						
HC	0.99703	0.99864	0.00056	0.00018						
CO2	0.98709	0.99831	0.00081	0.00027	0.00017	0.0007	16	800	Sigmoid	Adam
BTE	0.99943	0.99981	0.00006	0.00005						
BSFC	0.96908	0.9977	0.00163	0.00028						
NOX	***0.99953***	***0.99992***	***0.00011***	***0.00002***						
HC	***0.99704***	***0.99888***	***0.00078***	***0.00015***						
CO2	***0.99068***	***0.99959***	***0.00085***	***0.00007***	***0.00006***	***0.00037***	***16***	***1000***	***Sigmoid***	***Adam***
BTE	***0.99877***	***0.99989***	***0.0001***	***0.00003***						
BSFC	***0.99971***	***0.99969***	***0.00001***	***0.00004***						
NOX	0.99259	0.99745	0.00146	0.00064						
HC	0.99724	0.99614	0.00059	0.0005						
CO2	0.9926	0.99704	0.00048	0.00047	0.00201	0.0033	24	200	Sigmoid	Adam
BTE	0.99812	0.99947	0.00013	0.00013						
BSFC	0.28771	0.93216	0.01386	0.00833						
NOX	0.98774	0.99412	0.00283	0.00147						
HC	0.99911	0.998	0.00031	0.00026						
CO2	0.99355	0.99741	0.00049	0.00041	0.00083	0.00219	24	400	Sigmoid	Adam
BTE	0.99887	0.99972	0.00031	0.00007						
BSFC	0.8881	0.98406	0.00704	0.00195						
NOX	0.99421	0.99875	0.00137	0.00031						
HC	0.99754	0.99835	0.0005	0.00021						
CO2	0.98603	0.99773	0.0009	0.00036	0.00023	0.0008	24	600	Sigmoid	Adam
BTE	0.99954	0.99982	0.00008	0.00004						
BSFC	0.97278	0.99816	0.00117	0.00023						

NOX	0.99663	0.99907	0.00073	0.00023						
HC	0.99744	0.99867	0.00054	0.00017						
CO2	0.98557	0.99821	0.00089	0.00028	0.0002	0.00074	24	800	Sigmoid	Adam
BTE	0.99984	0.99981	0.00011	0.00004						
BSFC	0.96717	0.998	0.00142	0.00025						
NOX	0.99712	0.99962	0.00063	0.0001						
HC	0.99723	0.99885	0.00067	0.00015						
CO2	0.9861	0.99879	0.00088	0.00019	0.00013	0.00076	24	1000	Sigmoid	Adam
BTE	0.99853	0.99982	0.00012	0.00004						
BSFC	0.95179	0.9985	0.00153	0.00018						
NOX	0.99038	0.98689	0.00484	0.00337						
HC	0.99663	0.99387	0.00033	0.0008						
CO2	0.98719	0.99452	0.00113	0.00087	0.00455	0.00728	32	200	Sigmoid	Adam
BTE	0.99868	0.99422	0.00183	0.00136						
BSFC	-0.35478	0.86459	0.02829	0.01633						
NOX	0.98824	0.99533	0.00252	0.00117						
HC	0.999	0.99825	0.00044	0.00023						
CO2	0.99281	0.99734	0.00073	0.00042	0.00084	0.00184	32	400	Sigmoid	Adam
BTE	0.99698	0.99901	0.00116	0.00023						
BSFC	0.84834	0.98236	0.00435	0.00217						
NOX	0.9951	0.99891	0.00117	0.00027						
HC	0.99706	0.99811	0.00075	0.00024						
CO2	0.98759	0.99793	0.00082	0.00033	0.00026	0.00094	32	600	Sigmoid	Adam
BTE	0.99869	0.99971	0.0001	0.00007						
BSFC	0.93364	0.99679	0.00185	0.0004						
NOX	0.9932	0.99869	0.00137	0.00033						
HC	0.99853	0.99882	0.00059	0.00015						
CO2	0.98889	0.9983	0.00078	0.00027	0.00031	0.00143	32	800	Sigmoid	Adam
BTE	0.9988	0.99971	0.0001	0.00007						
BSFC	0.89952	0.99402	0.00432	0.00073						

NOX	0.99843	0.99975	0.0003	0.00006						
HC	0.99685	0.99887	0.00061	0.00015						
CO2	0.98899	0.99859	0.00072	0.00022	0.00012	0.00042	32	1000	Sigmoid	Adam
BTE	0.99989	0.99974	0.00001	0.00006						
BSFC	0.99011	0.99915	0.00046	0.0001						

Table 4.4Optimum configuration of the ANN model

Preprocessing	MinMaxScaler
Evaluation metrics	r and MSE
No: of epochs	1000
Optimizer	Adam
Transfer functions	Sigmoid
Hidden layer neurons	16
Normalized range	0 to 1
Output layer neurons	5
Input layer neurons	3

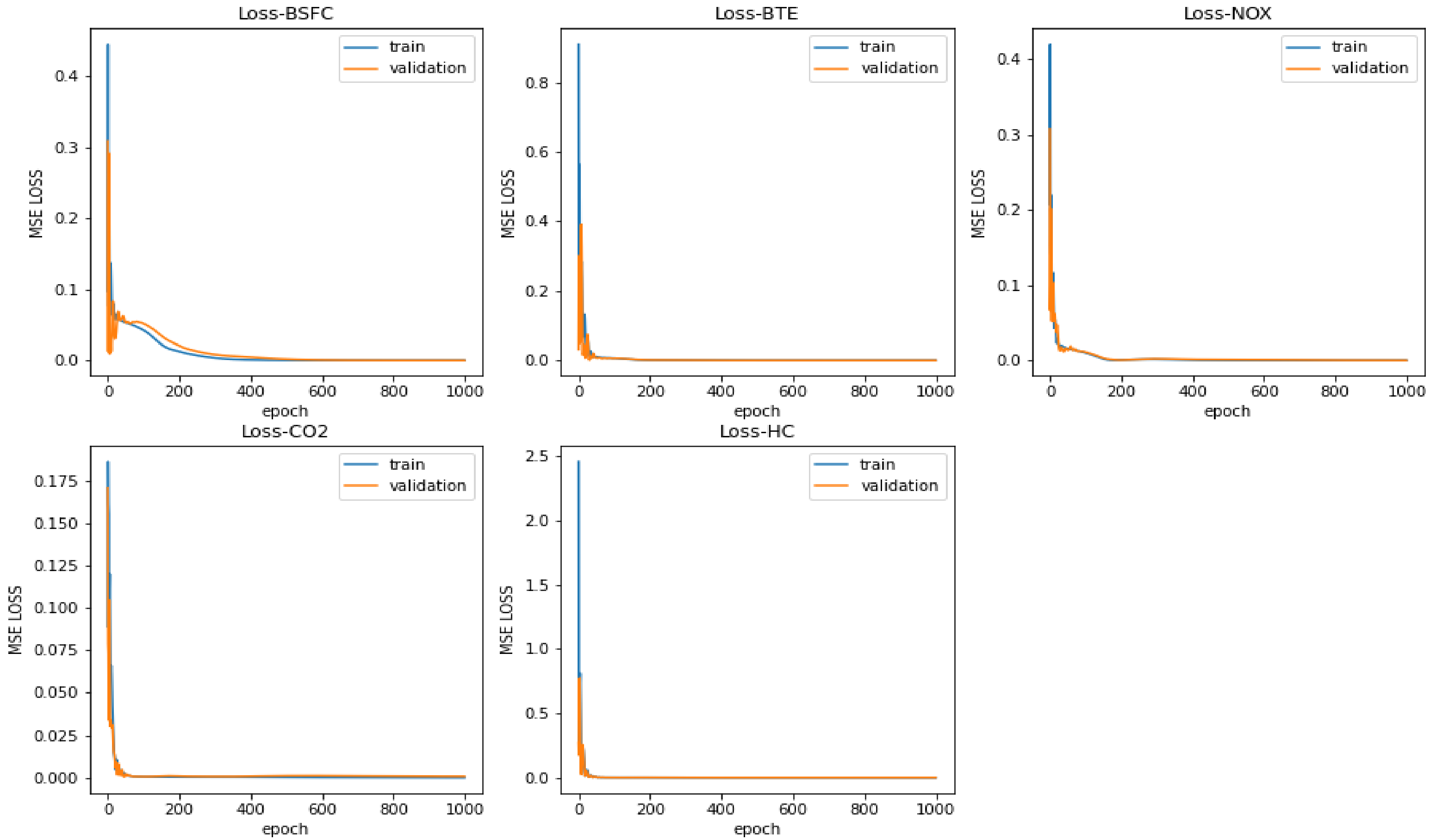

Figure 4.11 For optimum network configuration, change of MSE (validation-training).

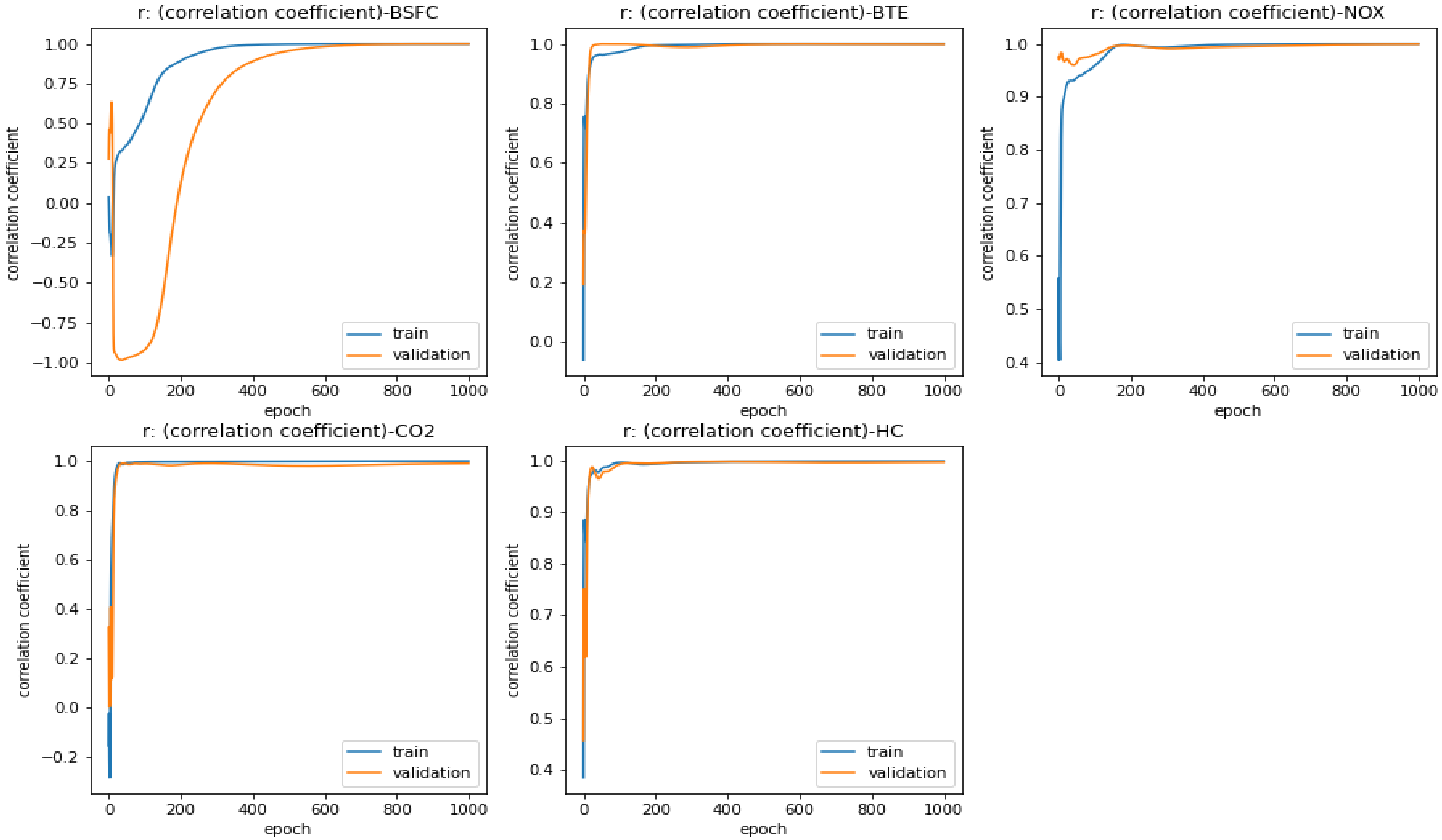

Figure 4.12 For optimum network configuration, change of r value (validation-training).

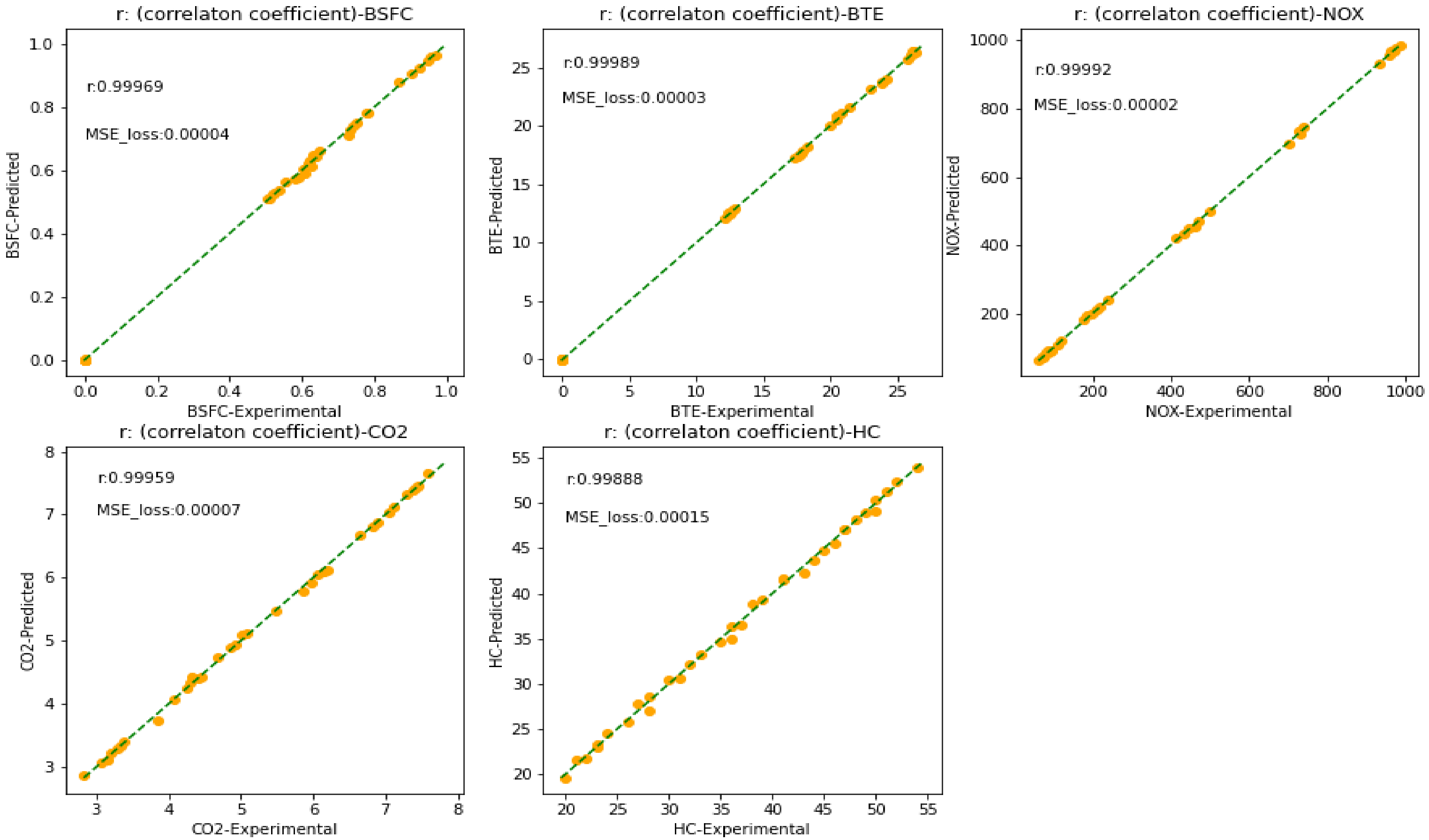

Figure 4.13 For optimum network configuration, ANN predictions for the target parameters.

CHAPTER 5

RESULTS AND DISCUSSION

This chapter outlines the interpretations of experimental investigations of 4-stroke, single cylinder CI engine fueled with SB0, SB20, SB35, SB50, SB65, SB80, SB100, SB20 Al_2O_3, SB35 Al_2O_3, SB50 Al_2O_3, SB65 Al_2O_3, SB80 Al_2O_3, SB100 Al_2O_3, SB20 MgO, SB35 MgO, SB50 MgO, SB65 MgO, SB80 MgO, and SB100 MgO at varied load circumstances. Performance and emittants attributes like brake thermal efficiency, brake specific fuel consumption, NO_X, CO_2, and HC are explored.

5.1 Effect of varied fuel blends on Brake Thermal Efficiency (BTE)

It is a parameter for assessing an engine's fuel efficiency. The ratio of brake power to the heat input is referred to as BTE. At any given engine load, BTE and BSFC are inversely correlated. It is mainly influenced by fuel's physcio-chemical attributes like calorific value, density, and viscosity. It is evident from Figure 5.1 that BTE enhanced with increased engine load and subsequently decreased with an increase in volumetric proportions of biodiesel (spirulina) in diesel. Similar findings have been observed [140]. As compared to diesel, at maximum load, the % drop in BTE was observed to be 1.42, 2.19, 3.40, 4.84, 6.02, and 7.19% respectively for SB20, SB35, SB50, SB65, SB80, and SB100. This can be attributed to the higher viscosity and LCV of microalgae-spirulina blends resulting in increased BSFC that leads to lower BTE [141]. Figure 5.2 displays the variation of BTE without and with nano additives concerning load. In comparison to test fuels without nano additives, the doping of Al_2O_3 and MgO additives resulted in improved BTE. At full load, the % uptick in BTE is 0.42, 0.53, 0.56, 0.78, 0.84, 0.91, 0.77, 0.82, 1.06, 1.08, 1.19, and 1.33% for SB20 Al_2O_3, SB35 Al_2O_3, SB50 Al_2O_3, SB65 Al_2O_3, SB80 Al_2O_3, SB100 Al_2O_3, SB20 MgO, SB35 MgO, SB50 MgO, SB65 MgO, SB80 MgO, and SB100 MgO respectively, when correlated to SB20, SB35, SB50, SB65, SB80, and SB100. However, it is less than SB0 (diesel). The resultant improvement in BTE is owing to the enhanced surface area to volume of Al_2O_3 and MgO additives which results in HCV. The BTE is thereby gradually improved. The same correlations are reported by [142]. The magnitude of BTE of test fuels is in the order of diesel (SB0) > SB MgO > SB Al_2O_3> spirulina biodiesel blends.

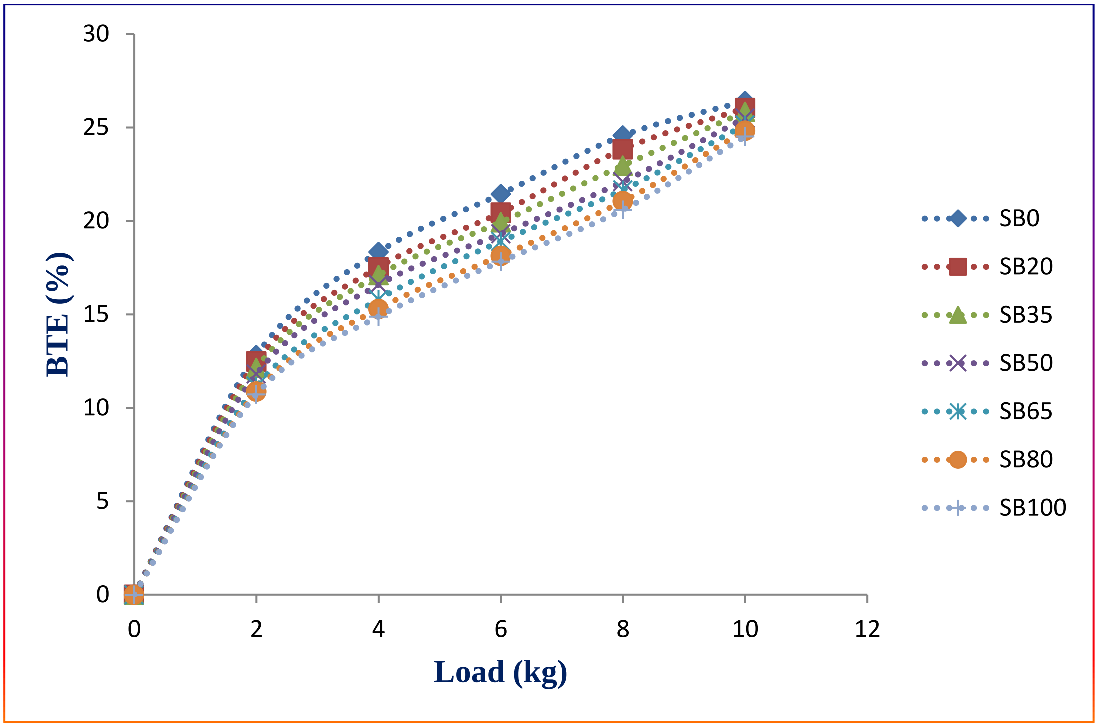

Figure 5.1 BTE (withoutAl_2O_3 and MgO additives) variation with respect to load.

5.2 Effect of varied fuel blends on Brake Specific Fuel Consumption (BSFC)

It is the ratio between the mass of the fuel consumed and BP. The term "BSFC" refers to the quantity of power required to generate 1KW of energy. The key variables that influence the BSFC of the Compression Ignition engine are volumetric fuel injection, calorific value, density, and viscosity. However, it is significantly governed by the calorific value and density of the fuel. As fuel with LHV, more fuel is needed to achieve the same energy output. The lower density of the fuel results in a reduced mass of fuel consumption for the same volume. Comparing spirulina biodiesel blends to diesel, an enhancement in BSFC was seen (in Figure 5.3). Increased BSFC reflects a decreased BTE. At peak load, BSFC was reported to be 0.5168, 0.5225, 0.554, 0.58, 0.612, 0.638, and 0.657 (kg/kWh) for SB0, SB20, SB35, SB50, SB65, SB80, and SB100 respectively. As illustrated in Figure 5.3, with the improvement in engine load, the BSFC drops. As the volumetric concentrations of spirulina in SB0 increase, so does BSFC. Prior experiment studies had revealed similar BSFC trends [143]. With the doping of Al_2O_3 and MgO nanoparticles in spirulina biodiesel, the BSFC decreases (in Figure 5.4). Compared to spirulina blends, Al_2O_3 and MgO additives amalgams have 1.44 % and 2.57 % (on median) less BSFC at full load. Compared to SB20, SB35, SB50, SB65, SB80, and SB100, the % downturn in BTE was found to be 0.86, 0.971, 1.20, 1.461, 1.62, 2.45, 1.89, 2.037, 2.09, 2.61, 3.068, and 3.75% for SB20 Al_2O_3, SB35 Al_2O_3, SB50 Al_2O_3, SB65 Al_2O_3, SB80 Al_2O_3, SB100 Al_2O_3, SB20 MgO, SB35 MgO, SB50 MgO, SB65 MgO, SB80 MgO, and SB100 MgO respectively. The drop in BSFC is due to the improved fuel attributes (calorific value) caused by the addition of Al_2O_3 and MgO nanoparticles. Experimental studies on Compression Ignition engines utilizing nano additives amalgams perceived similar findings [144]. The magnitude of BSFC of test fuels is in the order of spirulina biodiesel blends > SB Al_2O_3> SB MgO > diesel (SB0).

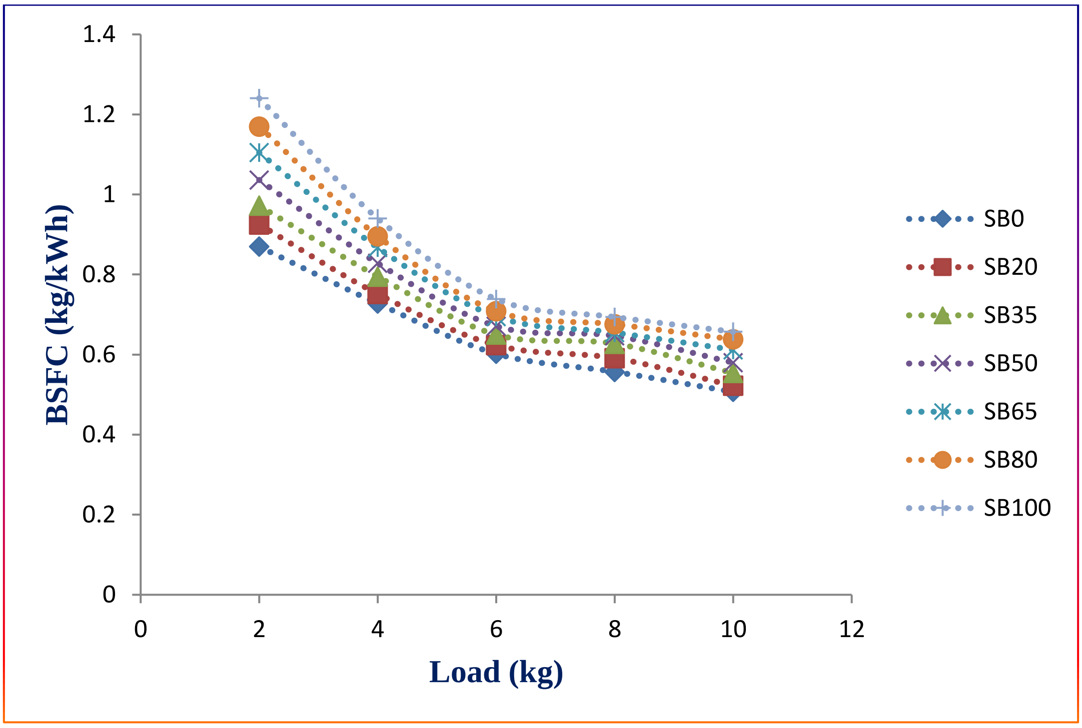

Figure 5.3 BSFC (without Al_2O_3 and MgO additives) variation with respect to load.

5.3 Effect of varied fuel blends on Oxides of Nitrogen (NO_X)

NO_X continues to be a profound pivotal byproduct of the engine exhaust that must be reduced. The combustion in CI engines takes place at above 1800K; hence they generate higher concentrations of NO_X than engines fuelled with gasoline. Usually, NO_X is constituted of nitrogen dioxide and nitrogen monoxide. In general, combustion temperature and volumetric concentrations of oxygen in the fuel are the pivotal parameters governing the occurrence of NO_X [145]. Primarily NO (nitric oxide) is released as a consequence of NOx emissions from combustion. For NOx formation three mechanisms are involved primarily Thermal NO_X, Fuel NO_X, and Prompt NO_X. According to Zeldovich mechanism NOx reaction is attributed as:

$$N_2 + O \rightarrow NO + N \quad (11)$$

$$N + O_2 \rightarrow NO + O \quad (12)$$

$$N + OH \rightarrow NO + H \quad (13)$$

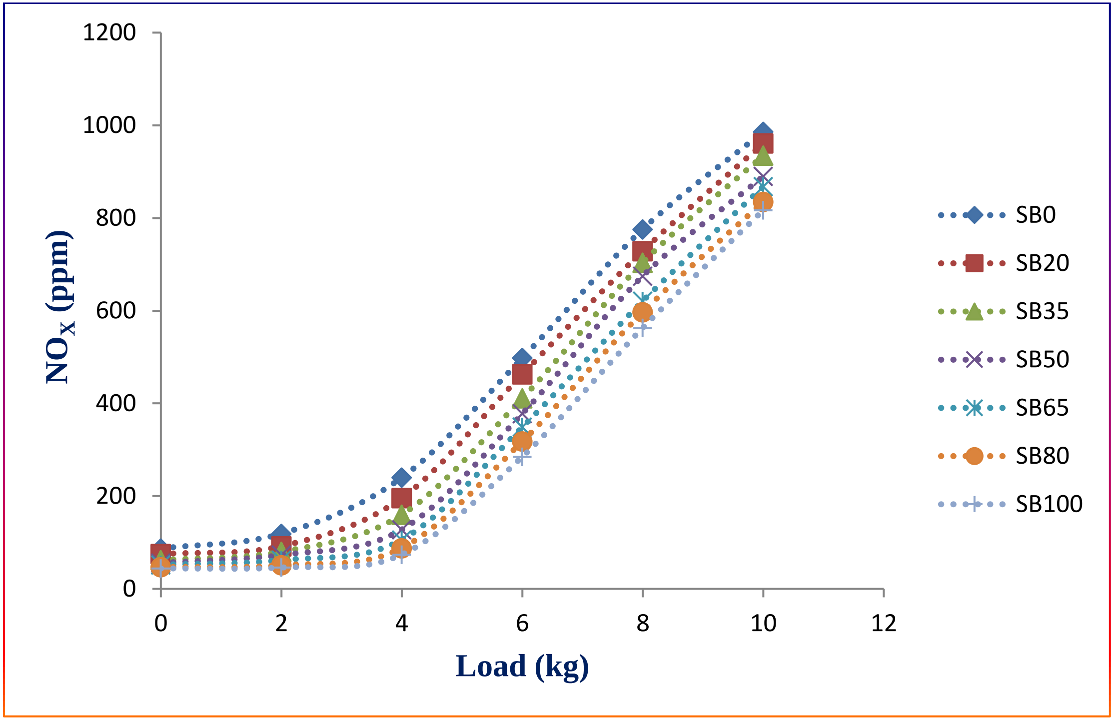

Figure 5.5 NO_X (without Al_2O_3 and MgO additives) variation with respect to load.

It was noticed from Figure 5.5 that, when correlated to diesel, for all loads, spirulina biodiesel amalgams had lower concentrations of oxides of nitrogen. With the increased engine load, NO_X emittants keep improving. Simultaneously, utilizing higher spirulina bio-diesel proportions in base fuel, a downturn in NO_X was observed. At 100% load, the % reduction in NO_X for SB20, SB35, SB50, SB65, SB80, and SB100 was found to be 2.53, 5.17, 9.73, 11.96, 15.31, and 17.13 respectively, than diesel (SB0). The downturn in NO_X could be ascribed to a lower combustion temperature caused by LCV of microalgae-spirulina mixtures. The identical findings were obtained when utilizing biodiesel mixtures [146]. The addition of AL2O3 and MgO additives in microalgae spirulina biodiesel mixtures resulted in improved NO_X emittants (in Figure 5.6). This was anticipated because the doping of AL2O3 and MgO additives increased the heating value through the catalytic effect resulting in enhanced combustion temperature. Yet, corresponding to SB0, concentrations of NO_X remained lower. 1.41, 1.46, 2.33, 4.91, 8.57, 11.32, 0.91, 1.40, 1.58, 2.83, 6.18, and 9.41 % drop in NO_X was observed for SB20

Al_2O_3, SB35 Al_2O_3, SB50 Al_2O_3, SB65 Al_2O_3, SB80 Al_2O_3, SB100 Al_2O_3, SB20 MgO, SB35 MgO, SB50 MgO, SB65 MgO, SB80 MgO, and SB100 MgO. The concentrations of NO_X of test fuels is in the order of diesel (SB0) > SB MgO > SB Al_2O_3> spirulina biodiesel amalgams.

5.4 Effect of varied fuel blends on Hydro carbons (HC)

Figures 5.7 and 5.8 illustrate the variation of hydrocarbons of test fuels without and with Al_2O_3 and MgO additives. According to findings, incomplete combustion is the major cause of hydro carbons generation [147]. Slow air mixing with the fuel and its pyrolysis byproducts can quench the combustion reaction, leading to insufficient combustion. The generation of a reactive HC is caused by the higher concentrations of olefins and aromatics in fuels. The chemical composition of the fuel has a substantial influence on HC formation. Too rich and too lean fuel-air mixture results in the formation of unburned hydrocarbons [148]. At all loads, relative to SB0, HC concentrations of microalgae-spirulina blends were lower (in Figure 5.7). The existence of higher O_2 content in the microalgae spirulina biodiesel results in improved combustion can be attributed to this behavior.

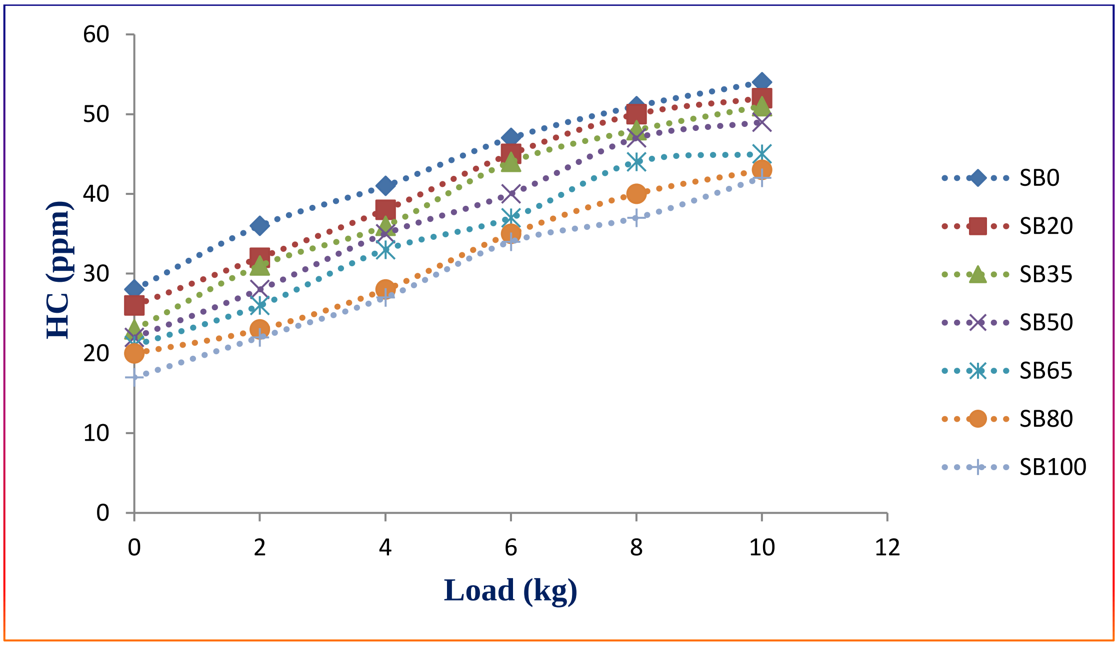

Figure 5.7 HC (without Al_2O_3 and MgO additives) variation with respect to load.

HC dwindled as the volumetric fraction of the spirulina biodiesel in SB0 increased. Compared to SB0, the percentage decrease in HC is 3.70, 5.51, 9.25, 16.6, 20.37, and 21.6 with SB20, SB35, SB50, SB65, SB80, and SB100, respectively at 10 kg load. On the other hand, nano particles Al_2O_3 and MgO blended microalgae biodiesel led to a further downturn in hydrocarbon emission. On average, at peak load, HC was reduced by 13.66% and 13.37 % respectively, for MgO and Al_2O_3 doped microalgae spirulina biodiesel amalgams. The minimum and maximum HC concentrations are observed for SB MgO and SB0 (diesel). Similar outcomes were obtained, by utilizing nano additives blended fuels [149]. The HC emittants of the test fuels is in the order of diesel (SB0) > spirulina biodiesel amalgams > SB Al_2O_3> SB MgO.

5.5 Effect of varied fuel blends on Carbon dioxide (CO_2)

One of the most prominent greenhouse gases is CO_2, which is discharged into the atmosphere alongside other flue gas. CO_2emissions contribute to global warming. As plants require CO_2 to thrive, it has a reduced influence on air quality than CO. CO_2 emissions are emitted when carbon compounds are fully and effectively oxidized. The fuel's oxygen proportion is directly proportional to CO_2 [150]. The enhanced oxidation of carbon caused by fuel's higher oxygen composition will lead to increased carbon dioxide [151]. From Figure 5.9, it is observed that at all loads, microalgae spirulina blended fuel emits higher CO_2 than SB0. Furthermore, when the engine load gradually increases from no load to peak load, carbon dioxide concentrations are enhanced as well.

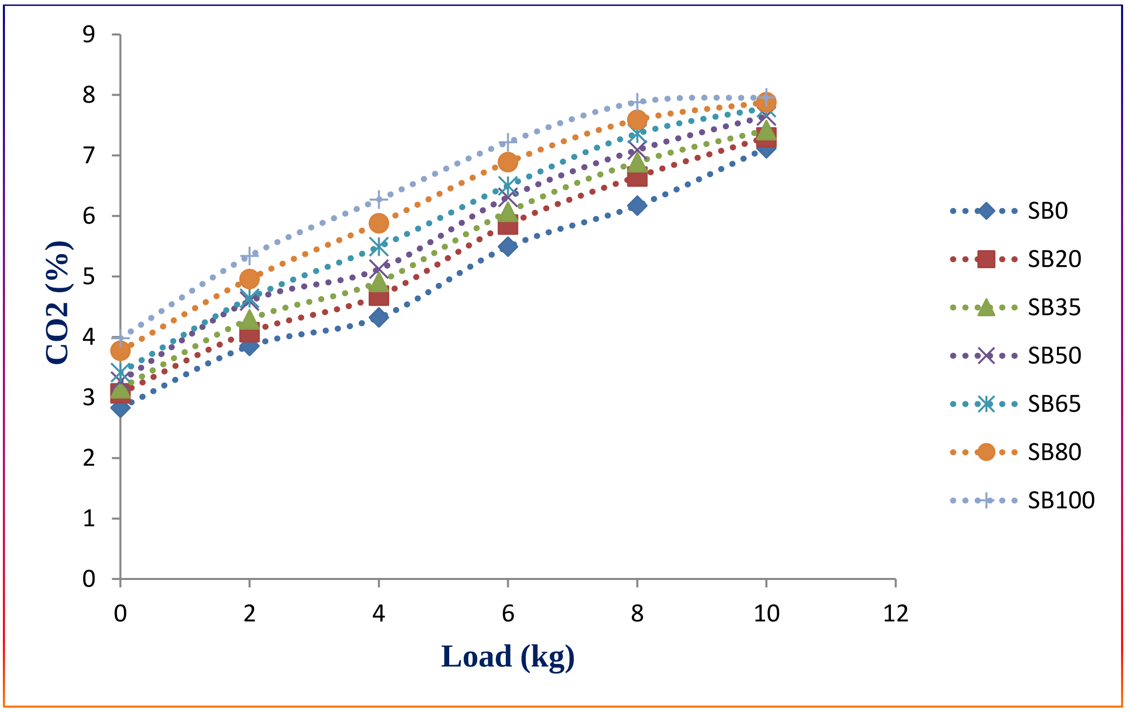

Figure 5.9 CO_2 (without Al_2O_3 and MgO additives) variation with respect to load.

Also, from Figure 5.9, an upsurge in carbon dioxide is seen with increased proportions of spirulina biodiesel mixtures. At 10 kg load, compared to SB0, the increase in emission for SB20, SB35, SB50, SB65, SB80, and SB100 is 2.5, 4.21, 7.44, 9.41, 10.67, and 11.72%, respectively. The variation of CO_2 with load utilizing Al_2O_3 and MgO doped biodiesel blends is illustrated in Figure 5.10. The concentration of carbon dioxide is substantially enhanced in the presence of Al_2O_3 and MgO additives. At all loads, the minimum CO_2 emissions were obtained with SB0 (diesel). In comparison to diesel and microalgae biodiesel amalgams, the mean rise in CO_2 emission with Al_2O_3 additive blends is observed to 9.35 and 1.69%, and for MgO additive blends is found to be 10.11 and 2.34%, respectively. Similar results have been obtained by [152]. The magnitude of CO_2 emissions of test fuels is in the order of SB MgO > SB Al_2O_3> spirulina biodiesel amalgams > diesel (SB0).

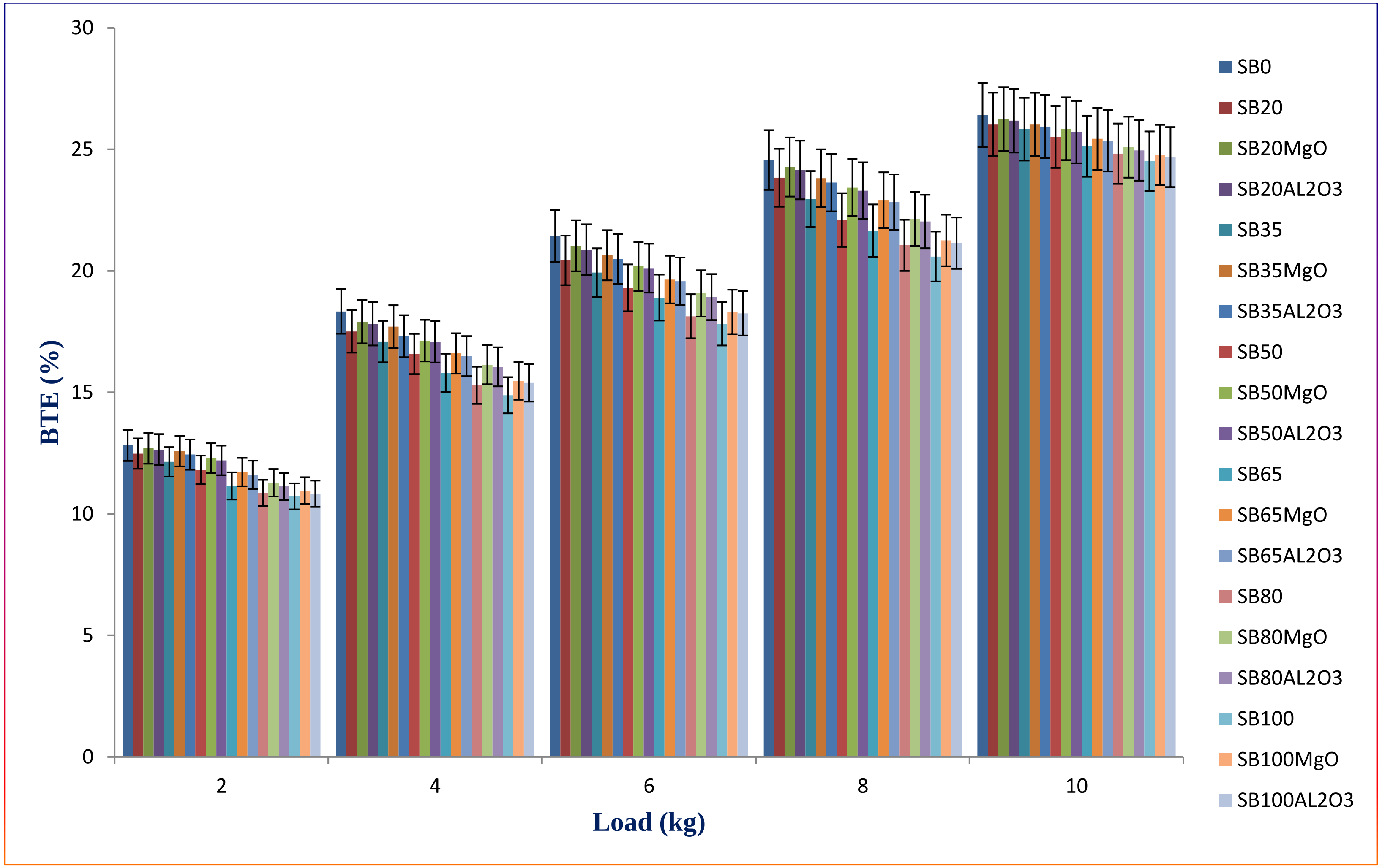

Figure 5.2 BTE variations with respect to load.

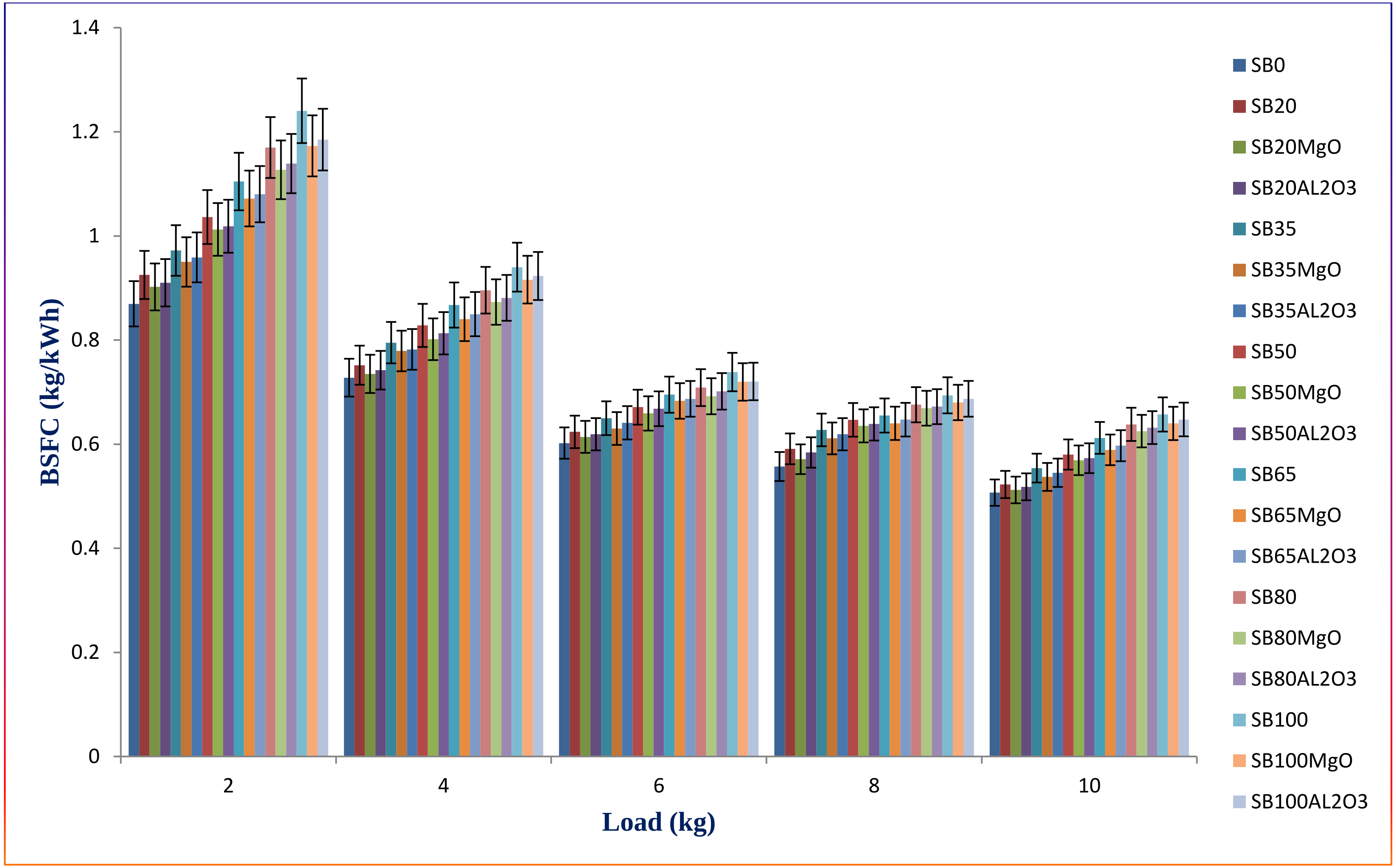

Figure 5.4 BSFC variations with respect to load.

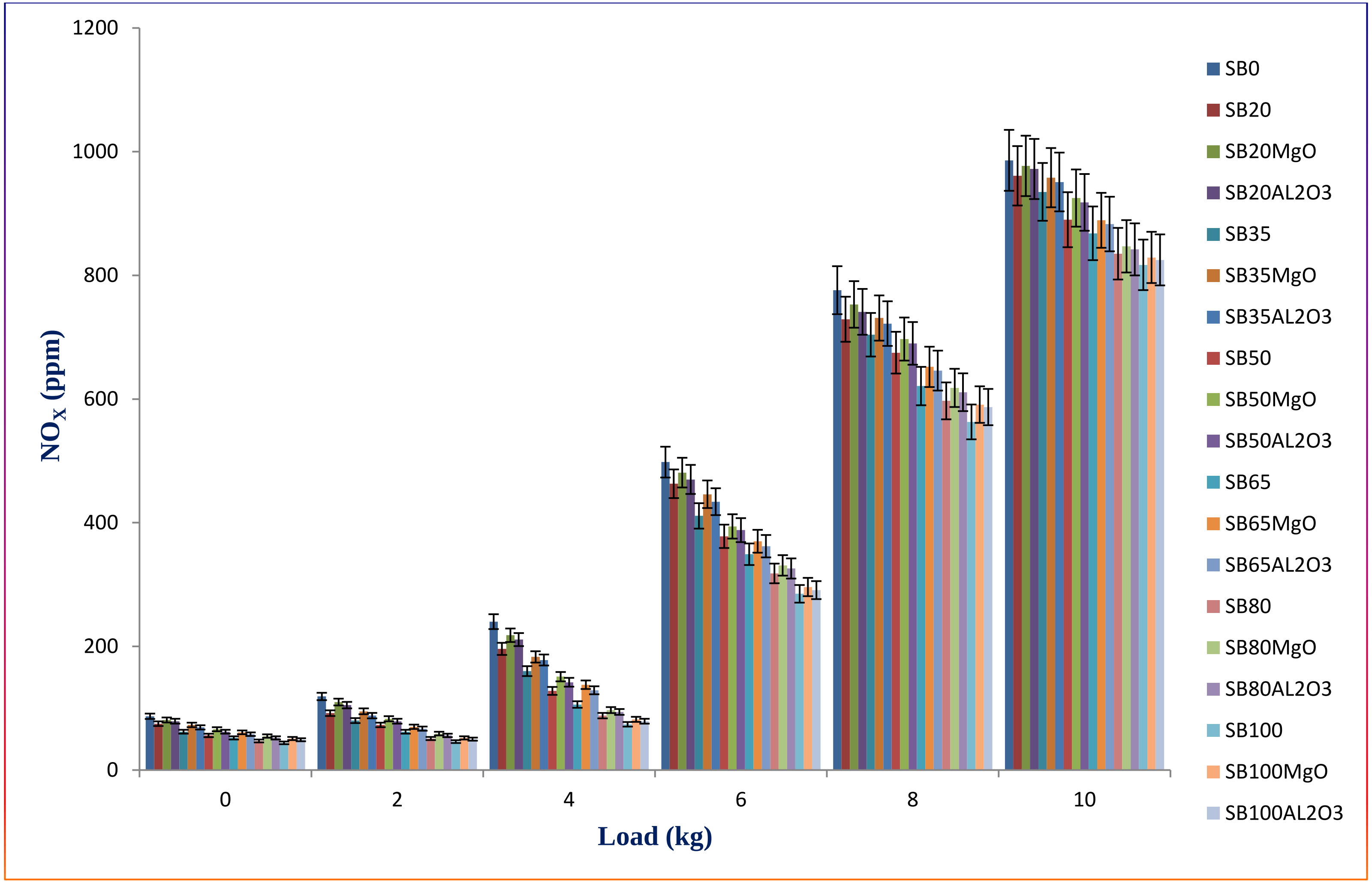

Figure 5.6 NO_X variations with respect to load.

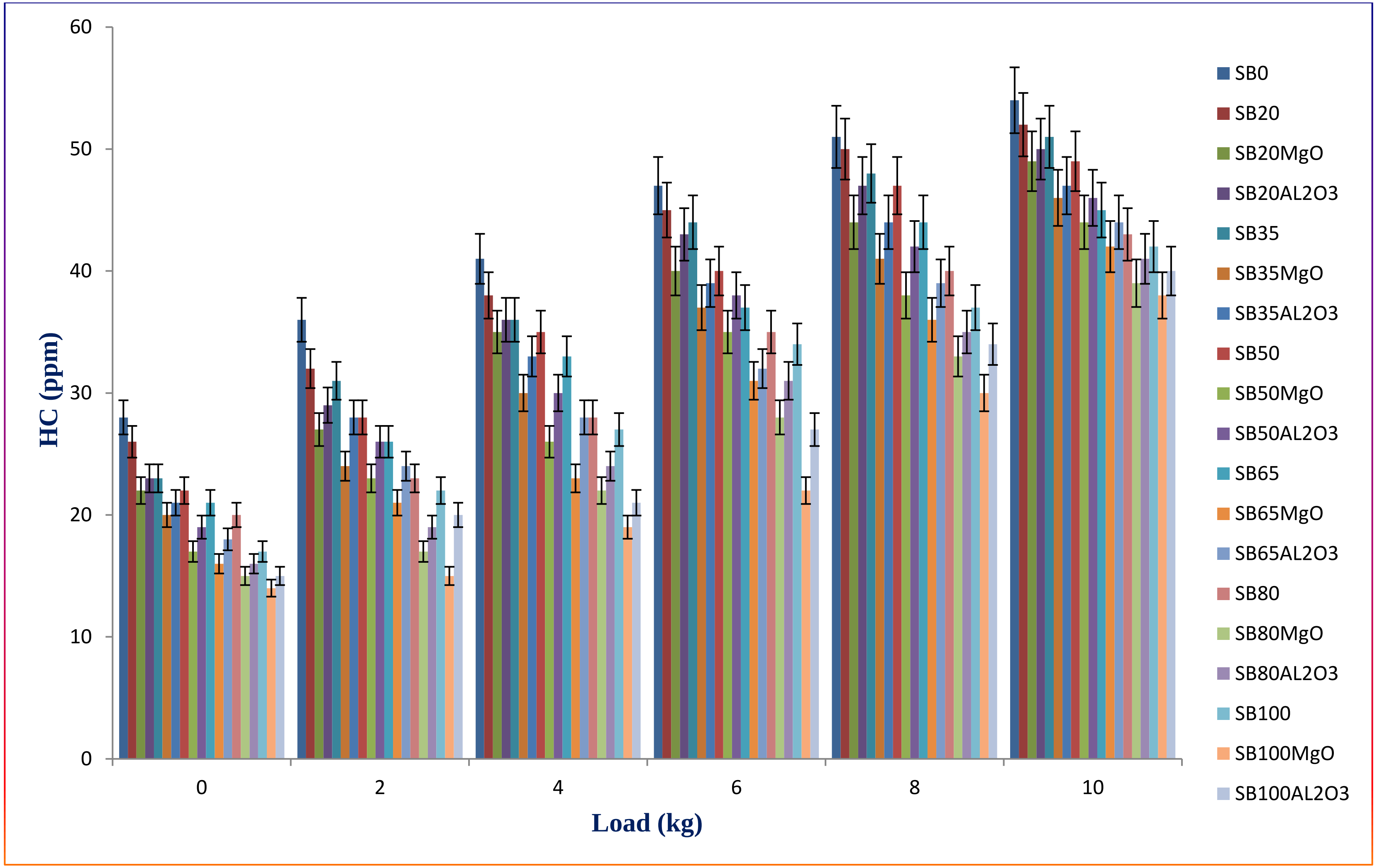

Figure 5.8 HC variations with respect to load.

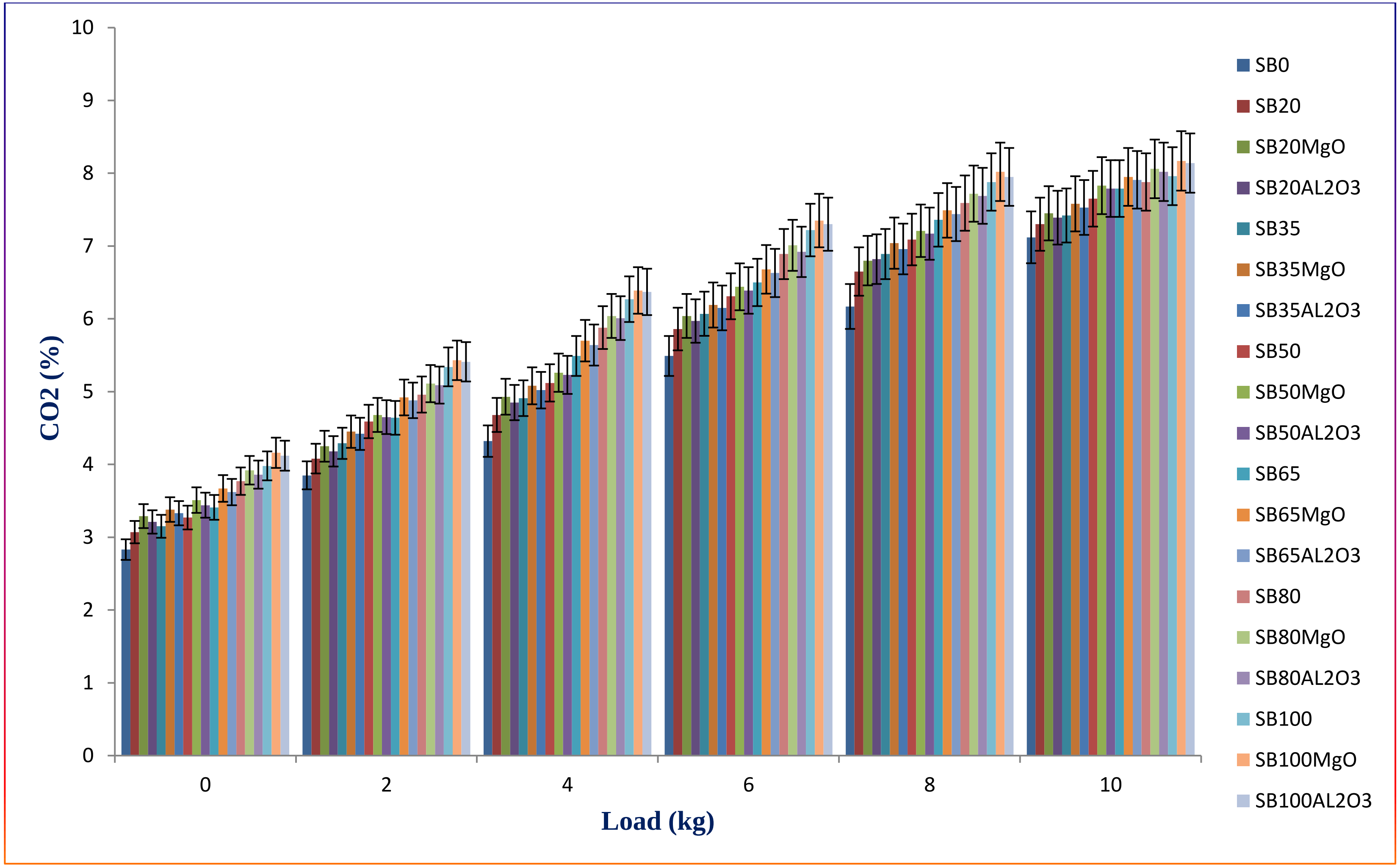

Figure 5.10 CO_2 variations with respect to load.

CHAPTER 6

CONCLUSIONS AND SCOPE FOR FUTURE RESEARCH

The outcomes drawn from the present experimental analysis and ANN optimization are as follows.

- SB100 exhibited a lower heating value (41 MJ/kg)which in turn resulted in the least BTE among all other test fuels.
- Compared to test fuels, SB100 MgO showed higher flash point (130 °C).
- For all test fuels, NO_X improved, with the increased load.
- Spirulina biodiesel mixtures exhibited lower concentrations of NO_X, as compared with nano doped blends and SB0.
- For all load conditions, SB100 exhibited lower emissions of NO_X (817 ppm).
- Compared to spirulina mixtures, spirulina mixtures with nano doped additives showed enhanced CO_2 emissions.
- CO_2 improved by 1.69 and 2.34%, respectively, for Al_2O_3 and MgO additives amalgams than mixtures without additives.
- HC reduced with the enhancement in the proportion of spirulina biodiesel in the base fuel (SB0).
- The lowest HC emissions are observed with MgO doped spirulina mixtures (reduced by 13.66 %).
- For all load conditions, engine that utilizes spirulina amalgams without additives has a higher BSFC.
- Engine with doped Al_2O_3 and MgO additives has improved BTE than mixtures without nano additives.
- In contrast to spirulina blends, at maximum load, without nano doped additives, BTE of Al_2O_3 and MgO mixture enhanced by 7.70 and 8.16% (on median), respectively.
- Pure diesel (SB0) resulted in lower BSFC, compared to test fuels.
- The nano additives doped biodiesel mixtures resulted in decreased BSFC than blends without nano additives.
- In terms of efficiency SB20 MgO found to be the optimum blend, compared to diesel.

- It was apparent from the study that the ANN projected outcome effectively correlated the test dataset with strong r values.
- The 3-16-5 network topology yields the least MSE.
- The results indicated that Adam optimizer with Sigmoid transfer function is the optimum configuration to project the engine attributes.
- The r values of all target variables are almost near to 1.
- The MSE were observed in the range between 0.00002-0.00015.

Overall, it is concluded that doping Al_2O_3 and MgO in spirulina biodiesel competently enhanced the performance of the engine while reducing HC concentrations. The strong correlation between model target outcomes and experimental observations indicated that the ANN approach has generated optimal results. Per other prominent AI methodologies, the current analysis endorses ANN as a viable modeling optimization technique for projecting engine characteristics.

Future scope

- By varying the engine CR, IT, and IP the emissions and performance attributes can be investigated using a multi-cylinder CI engine.
- ANN optimization can be carried out for test outcomes of multi-cylinder CI engines under varied CR, IT, and IP.
- An exhaustive study is necessary to assess the long-term impact ofAl_2O_3 and MgO doped fuelled emittants on human health.

`

REFERENCES

[1] Sari A, Akkaya M. Contribution of Renewable Energy Potential to Sustainable Employment. Procedia - Soc Behav Sci 2016;229:316–25.

[2] Owusu PA, Asumadu-Sarkodie S. A review of renewable energy sources, sustainability issues and climate change mitigation. Cogent Eng 2016;3:1–14.

[3] Güney T. Renewable energy, non-renewable energy and sustainable development. Int J Sustain Dev World Ecol 2019;26:389–97.

[4] Khan I, Han L, Khan H, Kim Oanh LT. Analyzing Renewable and Nonrenewable Energy Sources for Environmental Quality: Dynamic Investigation in Developing Countries. Math Probl Eng 2021;2021. https://doi.org/10.1155/2021/3399049.

[5] https://www.bp.com/content/dam/bp/businesssites/en/global/corporate/pdfs/energy-economics/statistical-review/bp-stats-review-2021-oil.pdf (dated: 03 July 2022).

[6] Ismaila SO, Bolaji BO, Yusuf TA, Sanusi HO. On Vehicular Emissions of Petrol and Diesel Engines. Int J Eng 2013;177–80.

[7] Reşitoılu IA, Altinişik K, Keskin A. The pollutant emissions from diesel-engine vehicles and exhaust aftertreatment systems. Clean Technol Environ Policy 2015;17:15–27.

[8] Mirhashemi FS, Sadrnia H. NOX emissions of compression ignition engines fueled with various biodiesel blends: A review. J Energy Inst 2020;93:129–51.

[9] https://www.siam.in/statistics.aspx?mpgid=8&pgidtrail=13(dated: 03 July 2022).

[10] http://164.100.47.193/Refinput/New_Reference_Notes/English/Vehicular%20pollution%20in%20India.pdf (dated: 03 July 2022).

[11] Synák F, Čulík K, Rievaj V, Gaňa J. Liquefied petroleum gas as an alternative fuel. Transp Res Procedia 2019;40:527–34.

[12] Surawski NC, Miljevic B, Bodisco TA, Situ R, Brown RJ, Ristovski ZD. Performance and gaseous and particle emissions from a liquefied petroleum gas (LPG) fumigated

compression ignition engine. Fuel 2014;133:17–25.

[13] Ianniello R, Blasio G Di, Marialto R, Beatrice C, Cardone M. Assessment of direct injected liquefied petroleum gas-diesel blends for ultra-low soot combustion engine application. Appl Sci 2020;10:4949. https://doi.org/10.3390/app10144949.

[14] Masi M. Experimental analysis on a spark ignition petrol engine fuelled with LPG (liquefied petroleum gas). Energy 2012;41:252–60.

[15] Nithyanandan K, Zhang J, Li Y, Meng X, Donahue R, Lee C-F, et al. Diesel-Like Efficiency Using Compressed Natural Gas/Diesel Dual-Fuel Combustion. J Energy Resour Technol 2016;138. https://doi.org/10.1115/1.4032621.

[16] Mattson JMS, Langness C, Depcik C. An Analysis of Dual-Fuel Combustion of Diesel with Compressed Natural Gas in a Single-Cylinder Engine. SAE Tech Pap 2018;2018-April:1–12.

[17] Khan MI, Yasmin T, Shakoor A. Technical overview of compressed natural gas (CNG) as a transportation fuel. Renew Sustain Energy Rev 2015;51:785–97.

[18] Hora TS, Shukla PC, Agarwal AK. Particulate emissions from hydrogen enriched compressed natural gas engine. Fuel 2016;166:574–80.

[19] Ağbulut Ü, Sarıdemir S, Karagöz M. Experimental investigation of fusel oil (isoamyl alcohol) and diesel blends in a CI engine. Fuel 2020;267:117042.

[20] Safieddin Ardebili SM, Solmaz H, İpci D, Calam A, Mostafaei M. A review on higher alcohol of fusel oil as a renewable fuel for internal combustion engines: Applications, challenges, and global potential. Fuel 2020;279:118516.

[21] Yesilyurt MK. A detailed investigation on the performance, combustion, and exhaust emission characteristics of a diesel engine running on the blend of diesel fuel, biodiesel and 1-heptanol (C7 alcohol) as a next-generation higher alcohol. Fuel 2020;275:117893.

[22] Uslu S, Celik MB. Combustion and emission characteristics of isoamyl alcohol-gasoline blends in spark ignition engine. Fuel 2020;262:116496.

[23] Korakianitis T, Namasivayam AM, Crookes RJ. Natural-gas fueled spark-ignition (SI) and compression-ignition (CI) engine performance and emissions. Prog Energy Combust Sci 2011;37:89–112.

[24] Chen Z, Zhang F, Xu B, Zhang Q, Liu J. Influence of methane content on a LNG heavy-duty engine with high compression ratio. Energy 2017;128:329–36.

[25] Song J, Zhang C, Lin G, Zhang Q. Performance and emissions of an electronic control common-rail diesel engine fuelled with liquefied natural gas-diesel dual-fuel under an optimization control scheme. Proc Inst Mech Eng Part D J Automob Eng 2019;233:1380–90.

[26] Dwivedi G, Sharma MP. Potential and limitation of straight vegetable oils as engine fuel - An Indian perspective. Renew Sustain Energy Rev 2014;33:316–22.

[27] Singh D, Sharma D, Soni SL, Sharma S, Kumar Sharma P, Jhalani A. A review on feedstocks, production processes, and yield for different generations of biodiesel. Fuel 2020;262:116553.

[28] Dwivedi G, Sharma MP. Prospects of biodiesel from Pongamia in India. Renew Sustain Energy Rev 2014;32:114–22.

[29] Shirazi SA, Abdollahipoor B, Windom B, Reardon KF, Foust TD. Effects of blending C3-C4 alcohols on motor gasoline properties and performance of spark ignition engines: A review. Fuel Process Technol 2020;197:106194.

[30] Varuvel EG, Mrad N, Tazerout M, Aloui F. Experimental analysis of biofuel as an alternative fuel for diesel engines. Appl Energy 2012;94:224–31.

[31] Sanghamitra S, Deshmukh SS. Prominence of bio-fuels as an alternate fuel in CI engines. Int J Eng Adv Technol 2019;8:67–71.

[32] Patel PD, Lakdawala A, Chourasia S, Patel RN. Bio fuels for compression ignition engine: A review on engine performance, emission and life cycle analysis. Renew Sustain Energy Rev 2016;65:24–43.

[33] Firoz S. A review : Advantages and Disadvantages of Biodiesel. Int Res J Eng Technol 2017;04:530–5.

[34] Niculescu R, Clenci A, Iorga-Siman V. Review on the use of diesel-biodiesel-alcohol blends in compression ignition engines. Energies 2019;12:1–41.

[35] http://www.worldbioenergy.org/uploads/201210%20WBA%20GBS%202020.pdf (dated: 03 July 2022).

[36] https://www.cbs.nl/en-gb/figures/detail/84714ENG#shortTableDescription (dated: 03 July 2022).

[37] Abdullah B, Syed Muhammad SAF ad, Shokravi Z, Ismail S, Kassim KA, Mahmood AN, et al. Fourth generation biofuel: A review on risks and mitigation strategies. Renew Sustain Energy Rev 2019;107:37–50.

[38] Alalwan HA, Alminshid AH, Aljaafari HAS. Promising evolution of biofuel generations. Subject review. Renew Energy Focus 2019;28:127–39.

[39] Aro EM. From first generation biofuels to advanced solar biofuels. Ambio 2016;45:24–31.

[40] Kumbhar V, Pandey A, Varghese A, Wanjari S. An overview of production, properties and prospects of tamarind seed oil biodiesel as an engine fuel. Int J Ambient Energy 2022;43:3356–64.

[41] Venu H, Appavu P. Combustion and emission characteristics of tamarind seed biodiesel-diesel blends in a compression ignition engine. Int J Ambient Energy 2021;42:1441–6.

[42] Harun Kumar M, Dhana Raju V, Kishore PS, Venu H. Influence of injection timing on the performance, combustion and emission characteristics of diesel engine powered with tamarind seed biodiesel blend. Int J Ambient Energy 2020;41:1007–15.

[43] Patil V V., Patil RS. Investigations on Effects of Varying Ignition Delay Period for the Sunflower Oil Methyl Ester. J Inst Eng Ser C 2022;103:435–44.

[44] Santos BS, Capareda SC, Capunitan JA. Sunflower Methyl Ester as an Engine Fuel: Performance Evaluation and Emissions Analysis. ISRN Renew Energy 2013;2013:1–12.

[45] Kirankumar S, Govind N, Nagendrababu R. Performance and Emission Characteristics of Diesel Engine with Methyl Ester Sunflower Oil and Its Blends. International Journal of Advanced Research in Science, Engineering and Technology2019;6:577-85.

[46] Raman LA, Deepanraj B, Rajakumar S, Sivasubramanian V. Experimental investigation on performance, combustion and emission analysis of a direct injection diesel engine fuelled with rapeseed oil biodiesel. Fuel 2019;246:69–74.

[47] Reza Miri SM, Mousavi Seyedi SR, Ghobadian B. Effects of biodiesel fuel synthesized from non-edible rapeseed oil on performance and emission variables of diesel engines. J Clean Prod 2017;142:3798–808.

[48] Aldhaidhawi M, Chiriac R, Badescu V. Ignition delay, combustion and emission characteristics of Diesel engine fueled with rapeseed biodiesel – A literature review. Renew Sustain Energy Rev 2017;73:178–86.

[49] Gad MS, El-Araby R, Abed KA, El-Ibiari NN, El Morsi AK, El-Diwani GI. Performance and emissions characteristics of C.I. engine fueled with palm oil/palm oil methyl ester blended with diesel fuel. Egypt J Pet 2018;27:215–9.

[50] Devarajan Y, Munuswamy DB, Mahalingam A, Nagappan B. Performance, Combustion, and Emission Analysis of Neat Palm Oil Biodiesel and Higher Alcohol Blends in a Diesel Engine. Energy and Fuels 2017;31:13796–801.

[51] Gorey N, Ghosh S, Srivastava P, Kumar V. Characterization of Palm Oil as Biodiesel. IOP Conf Ser Mater Sci Eng 2017;225:012220.

[52] Mehra KS, Pant G. Production Of Biofuel From Sesame Oil And Its Characterization As An Alternative Fuel For Diesel Engine. IOP Conf Ser Mater Sci Eng 2021;1116:012076.

[53] Hoang AT, Noor MM, Pham XD. Comparative Analysis on Performance and Emission Characteristic of Diesel Engine Fueled with Heated Coconut Oil and Diesel Fuel. International Journal of Automotive and Mechanical Engineering 2018;15:5110-25.

[54] Edík JC, Pexa M, Holúbek M, AleÅi Z, Pražan R, Kuchar P. Effect of Diesel Fuel-Coconut Oil-Butanol Blends on Operational Parameters of Diesel Engine. Energies

2020;13:1–16.

[55] Lugo-Méndez H, Sánchez-Domínguez M, Sales-Cruz M, Olivares-Hernández R, Lugo-Leyte R, Torres-Aldaco A. Synthesis of biodiesel from coconut oil and characterization of its blends. Fuel 2021;295:120595.

[56] Sundaram GV, Thirumalini S. Experimental Study of Emission and Performance of Single Cylinder Diesel Engine Running On Groundnut Oil Based Biodiesel.International Journal of Scientific & Engineering Research 2014;5:110–4.

[57] Deivajothi P, Manieniyan V, Sivaprakasam S. An impact of ethyl esters of groundnut acid oil (vegetable oil refinery waste) used as emerging fuel in DI diesel engine. Alexandria Eng J 2018;57:2215–23.

[58] Oluwole OO, Adeleke IB. The performance characteristics of groundnut (Arachis hypogea, L.) biodiesel in a diesel engine. African J Environ Sci Technol 2013;7:504–17.

[59] Balamurugan T, Arun A, Sathishkumar GB. Biodiesel derived from corn oil – A fuel substitute for diesel. Renew Sustain Energy Rev 2018;94:772–8.

[60] Sathyamurthy R, Balaji D, Gorjian S, Muthiya SJ, Bharathwaaj R, Vasanthaseelan S, et al. Performance, combustion and emission characteristics of a DI-CI diesel engine fueled with corn oil methyl ester biodiesel blends. Sustain Energy Technol Assessments 2021;43:100981.

[61] Nagaraja S, Soorya Prakash K, Sudhakaran R, Sathish Kumar M. Investigation on the emission quality, performance and combustion characteristics of the compression ignition engine fueled with environmental friendly corn oil methyl ester – Diesel blends. Ecotoxicol Environ Saf 2016;134:455–61.

[62] Attia AMA, Hassaneen AE. Influence of diesel fuel blended with biodiesel produced from waste cooking oil on diesel engine performance. Fuel 2016;167:316–28.

[63] Abed KA, El Morsi AK, Sayed MM, Shaib AAE, Gad MS. Effect of waste cooking-oil biodiesel on performance and exhaust emissions of a diesel engine. Egypt J Pet 2018;27:985–9.

[64] Mercy Nisha Pauline J, Sivaramakrishnan R, Pugazhendhi A, Anbarasan T, Achary A. Transesterification kinetics of waste cooking oil and its diesel engine performance. Fuel 2021;285:119108.

[65] Kannan M, Sathish Babu R, Sathish S. Experimental investigations on the performance and emission characteristics of CI engine fuelled with biodiesel from neem oil. Int J Ambient Energy 2022;43:2351–9.

[66] Mathiyazhagan M, Meenakshi Sundaram K, Bupesh G. Production and emission evaluation of neem biodiesel blends in a single cylinder diesel engine. Mater Today Proc 2022;62:2124–32.

[67] Chhabra M, Saini BS, Dwivedi G. Impact assessment of biofuel from waste neem oil. Energy Sources, Part A Recover Util Environ Eff 2021;43:3381–92.

[68] Arunkumar M, Mohanavel V, Afzal A, Sathish T, Ravichandran M, Khan SA, et al. A study on performance and emission characteristics of diesel engine using Ricinus Communis (Castor oil) ethyl esters. Energies 2021;14:1–17.

[69] Das M, Sarkar M, Datta A, Santra AK. An experimental study on the combustion, performance and emission characteristics of a diesel engine fuelled with diesel-castor oil biodiesel blends. Renew Energy 2018;119:174–84.

[70] Attia AMA, Nour M, El-Seesy AI, Nada SA. The effect of castor oil methyl ester blending ratio on the environmental and the combustion characteristics of diesel engine under standard testing conditions. Sustain Energy Technol Assessments 2020;42:100843.

[71] Anjana PA, Niju S, Begum KMMS, Anantharaman N, Anand R, Babu D. Studies on biodiesel production from Pongamia oil using heterogeneous catalyst and its effect on diesel engine performance and emission characteristics. Biofuels 2016;7:377–87.

[72] Perumal V, Ilangkumaran M. Experimental analysis of engine performance, combustion and emission using pongamia biodiesel as fuel in CI engine. Energy 2017;129:228–36.

[73] Arul Nicholas T, Venkatakrishna A, Joy N, Mariadhas A. Performance and emission analysis on diesel engine fuelled with neat pongamia biodiesel. Int J Ambient Energy

2022;43:21–7.

[74] Gad MS, El-Shafay AS, Abu Hashish HM. Assessment of diesel engine performance, emissions and combustion characteristics burning biodiesel blends from jatropha seeds. Process Saf Environ Prot 2021;147:518–26.

[75] Mahmood T, Khan ZA, Hassan S, Chaudhry IA. Performance characteristics of diesel engine using blends of Jatropha biodiesel. J Mech Eng Sci 2021;15:8219–27.

[76] Khalaf M, Abdel-FadEel W, Abdelhady S, Esmail mohamed. Performance and Emissions of a Diesel Engine Fueled with a Biofuel Extracted from Jatropha Seeds. Int J Appl Energy Syst 2022;4:40–51.

[77] Al-lwayzy SH, Yusaf T. Diesel engine performance and exhaust gas emissions using Microalgae Chlorella protothecoides biodiesel. Renew Energy 2017;101:690–701.

[78] Jagadevkumar AP, Pravin VK. Evaluation of performance and emission characeristics of heterotrophic chlorella protothecoides microalgae biodiesel and its blends with diesel in a direct injection diesel engine. J Phys Conf Ser 2020;1473.

[79] Subramani L, Venu H. Evaluation of methyl ester derived from novel Chlorella emersonii as an alternative feedstock for DI diesel engine & its combustion, performance and tailpipe emissions. Heat Mass Transf 2019;55:1513–34.

[80] Ge S, Brindhadevi K, Xia C, Salah Khalifa A, Elfasakhany A, Unpaprom Y, et al. Performance, combustion and emission characteristics of the CI engine fueled with Botryococcus braunii microalgae with addition of TiO2 nanoparticle. Fuel 2022;317:121898.

[81] Karthikeyan S, Dharma Prabhakaran T. Emission analysis of Botryococcus braunii algal biofuel using Ni-Doped ZnO nano additives for IC engines. Energy Sources, Part A Recover Util Environ Eff 2018;40:1060–7.

[82] Aisosa Oni B, Eshorame Sanni S, Daramola M, Victoria Olawepo A. Effects of oxy-acetylation on performance, combustion and emission characteristics of Botryococcus braunii microalgae biodiesel-fuelled CI engines. Fuel 2021;296:120675.

[83] Kalaimurugan K, Karthikeyan S, Periyasamy M, Mahendran G, Dharmaprabhakaran T. Performance, emission and combustion characteristics of RuO2 nanoparticles addition with neochloris oleoabundans algae biodiesel on CI engine. Energy Sources, Part A Recover Util Environ Eff 2019;00:1–15. https://doi.org/10.1080/15567036.2019.1694102.

[84] Kalaimurugan K, Karthikeyan S, Periyasamy M, Mahendran G. Experimental investigations on the performance characteristics of CI engine fuelled with cerium oxide nanoparticle added biodiesel-diesel blends. Mater Today Proc 2020;33:2882–5.

[85] Mathimani T, Senthil Kumar T, Chandrasekar M, Uma L, Prabaharan D. Assessment of fuel properties, engine performance and emission characteristics of outdoor grown marine Chlorella vulgaris BDUG 91771 biodiesel. Renew Energy 2017;105:637–46.

[86] Mao G, Shi K, Zhang C, Li J, Chen S, Wang P. Biodiesel Fuel from Chlorella vulgaris and Effects of Its Low-Level Blends on the Performance, Emissions, and Combustion Characteristics of a Nonroad Diesel Engine . J Energy Eng 2020;146:1–12.

[87] Arunprasad J, Thirugnanasambantham R, Elango T, Pachiannan T, Thangaraj S, Basha S, et al. Performance and emissions of Chlorella vulgaris with ruthenium oxide in CI engines. Fuel 2022;314:122764.

[88] Nirmala N, Dawn SS, Harindra C. Analysis of performance and emission characteristics of Waste cooking oil and Chlorella variabilis MK039712.1 biodiesel blends in a single cylinder, four strokes diesel engine. Renew Energy 2020;147:284–92.

[89] Venkatesan H, Sivamani S, Sampath S, Gopi V, Dinesh Kumar M. A comprehensive review on the effect of nano metallic additives on fuel properties, engine performance and emission characteristics. Int J Renew Energy Res 2017;7:825–43.

[90] Seela CR, Ravi Sankar B, Sai Kiran D. Influence of biodiesel and its blends on CI engine performance and emissions: a review. Biofuels 2017;8:163–79.

[91] Damanik N, Ong HC, Tong CW, Mahlia TMI, Silitonga AS. A review on the engine performance and exhaust emission characteristics of diesel engines fueled with biodiesel blends. Environ Sci Pollut Res 2018;25:15307–25.

[92] Hasan MM, Rahman MM. Performance and emission characteristics of biodiesel–diesel blend and environmental and economic impacts of biodiesel production: A review. Renew Sustain Energy Rev 2017;74:938–48.

[93] Shaafi T, Sairam K, Gopinath A, Kumaresan G, Velraj R. Effect of dispersion of various nanoadditives on the performance and emission characteristics of a CI engine fuelled with diesel, biodiesel and blends—A review. Renew Sustain Energy Rev 2015;49:563–73.

[94] Prabu A. Nanoparticles as additive in biodiesel on the working characteristics of a DI diesel engine. Ain Shams Eng J 2018;9:2343–9.

[95] Kaushik Y, Verma V, Saxena KK, Prakash C, Gupta LR, Dixit S. Effect of Al2O3 Nanoparticles on Performance and Emission Characteristics of Diesel Engine Fuelled with Diesel–Neem Biodiesel Blends. Sustain 2022;14:7913.

[96] Ağbulut U, Elibol E, Demirci T, Sarıdemir S, Etem Gürel A, Rajak U, et al. Synthesis of graphene oxide nanoparticles and the influences of their usage as fuel additives on CI engine behaviors. Energy 2022;244:122603.

[97] Kumar N, Raheman H. Thermal and environmental performance of CI engine using CeO2 nanoparticles as additive in water–diesel–biodiesel fuel blend. Int J Environ Sci Technol 2022;19:3287–304.

[98] Sundar SP, Vijayabalan P, Kaliappan VK, Sathyamurthy R, Kabeel AE, Kamalakkannan K. Emission reduction and performance enhancement of diesel engine fuelled using palm oil biodiesel and nanoparticle as additive. Environ Dev Sustain 2022. https://doi.org/10.1007/s10668-022-02467-4.

[99] Kumar SS, Rajan K, Mohanavel V, Ravichandran M, Rajendran P, Rashedi A, et al. Combustion, performance, and emission behaviors of biodiesel fueled diesel engine with the impact of alumina nanoparticle as an additive. Sustain 2021;13:12103.

[100] Dhahad HA, Abdul Ghafar S, Dhahad HA, Hamadi AS, Ali SA. Effect of Aluminum Oxide Nanoparticles Fuel Additives on the Performance and Emissions of Diesel Engine. Eng Technol J 2017;35:956–60.

[101] Debbarma S, Misra RD. Effects of Iron Nanoparticles Blended Biodiesel on the Performance and Emission Characteristics of a Diesel Engine. J Energy Resour Technol Trans ASME 2017;139:1–8.

[102] Kumar MV, Babu AV, Kumar PR. Influence of metal-based cerium oxide nanoparticle additive on performance, combustion, and emissions with biodiesel in diesel engine. Environ Sci Pollut Res 2019;26:7651–64.

[103] Chen AF, Akmal Adzmi M, Adam A, Othman MF, Kamaruzzaman MK, Mrwan AG. Combustion characteristics, engine performances and emissions of a diesel engine using nanoparticle-diesel fuel blends with aluminium oxide, carbon nanotubes and silicon oxide. Energy Convers Manag 2018;171:461–77.

[104] Kumar S, Dinesha P, Bran I. Influence of nanoparticles on the performance and emission characteristics of a biodiesel fuelled engine: An experimental analysis. Energy 2017;140:98–105.

[105] Hussain F, Soudagar MEM, Afzal A, Mujtaba MA, Rizwanul Fattah IM, Naik B, et al. Enhancement in combustion, performance, and emission characteristics of a diesel engine fueled with Ce-ZnO nanoparticle additive added to soybean biodiesel blends. Energies 2020;13:1–20.

[106] Dinesha P, Kumar S, Rosen MA. Effects of particle size of cerium oxide nanoparticles on the combustion behavior and exhaust emissions of a diesel engine powered by biodiesel/diesel blend. Biofuel Res J 2021;8:1374–83.

[107] Kumar Patel H, Kumar S. Experimental analysis on performance of diesel engine using mixture of diesel and bio-diesel as a working fuel with aluminum oxide nanoparticle additive. Therm Sci Eng Prog 2017;4:252–8.

[108] Sivakumar M, Shanmuga Sundaram N, Ramesh kumar R, Syed Thasthagir MH. Effect of aluminium oxide nanoparticles blended pongamia methyl ester on performance, combustion and emission characteristics of diesel engine. Renew Energy 2018;116:518–26.

[109] D'Silva R, Binu KG, Bhat T. Performance and Emission Characteristics of a C.I. Engine Fuelled with Diesel and TiO2 Nanoparticles as Fuel Additive. Mater Today Proc 2015;2:3728–35.

[110] Wei J, Yin Z, Wang C, Lv G, Zhuang Y, Li X, et al. Impact of aluminium oxide nanoparticles as an additive in diesel-methanol blends on a modern DI diesel engine. Appl Therm Eng 2021;185:116372.

[111] Wu Q, Xie X, Wang Y, Roskilly T. Effect of carbon coated aluminum nanoparticles as additive to biodiesel-diesel blends on performance and emission characteristics of diesel engine. Appl Energy 2018;221:597–604.

[112] Deb S, Dixit U. Intelligent Machining: Computational Methods and Optimization.Machining: Fundamentals and recent advances 2008.https://doi.org/10.1007/978-1-84800-213-5.

[113] Walker JM, Ditor SEE, Martin S, Murray C. Artificial Neural Networks METHODS IN MOLECULAR BIOLOGY TM. n.d.

[114] https://intellipaat.com/blog/what-is-artificial-intelligence/ (dated: 08 Jul 2022).

[115] http://www.cs.cmu.edu/afs/cs.cmu.edu/user/mitchell/ftp/mlbook.html(dated: 08 Jul 2022)

[116] https://www.javatpoint.com/supervised-machine-learning(dated: 11 Jul 2022)

[117] https://www.javatpoint.com/unsupervised-machine-learning(dated: 11 Jul 2022)

[118] Yusri IM, Abdul Majeed APP, Mamat R, Ghazali MF, Awad OI, Azmi WH. A review on the application of response surface method and artificial neural network in engine performance and exhaust emissions characteristics in alternative fuel. Renew Sustain Energy Rev 2018;90:665–86.

[119] Kumar S, Pai PS, Rao BRS, Vijay GS. Prediction of performance and emission characteristics in a biodiesel engine using WCO ester: a comparative study of neural networks. Soft Comput 2016;20:2665–76.

[120] Liu Y. The Review of Intelligent Mechanical Engineering Based on Artificial Neural Network. Proc 2015 Int Conf Intell Syst Res Mechatronics Eng 2015;121:1969–73.

[121] Narendranathan SK, Thiyagu M, Shankar. A, Sureshkumar TN. Implementation of ANN for Predication of Performance and Emission Characteristics in CI Engine. Proc 2022 Int Conf Electron Syst Intell Comput ICESIC 2022 2022:264–9.

[122] Barnawal SK, Kumar N. Experimental investigation and artificial neural network modeling of performance and emission of a CI engine using orange peel oil- diesel blends. Energy Sources, Part A Recover Util Environ Eff 2022;44:232–46.

[123] El-Shafay AS, Alqsair UF, Abdel Razek SM, Gad MS. Artificial neural network prediction of performance and emissions of a diesel engine fueled with palm biodiesel. Sci Rep 2022;12:1–15.

[124] Dhahad HA, Hasan AM, Chaichan MT, Kazem HA. Prognostic of diesel engine emissions and performance based on an intelligent technique for nanoparticle additives. Energy 2022;238:121855.

[125] Hosamani BR, Abbas Ali S, Katti V. Assessment of performance and exhaust emission quality of different compression ratio engine using two biodiesel mixture: Artificial neural network approach. Alexandria Eng J 2021;60:837–44.

[126] Subramanian K, Sathiyagnanam AP, Damodharan D, Sivashanmugam N. Artificial Neural Network based prediction of a direct injected diesel engine performance and emission characteristics powered with biodiesel. Mater Today Proc 2020;43:1049–56.

[127] Raghuvaran S, Ashok B, Veluchamy B, Ganesh N. Evaluation of performance and exhaust emission of C.I diesel engine fuel with palm oil biodiesel using an artificial neural network. Mater Today Proc 2020;37:1107–11.

[128] Esonye C, Onukwuli OD, Ofoefule AU, Ogah EO. Multi-input multi-output (MIMO) ANN and Nelder-Mead’s simplex based modeling of engine performance and combustion emission characteristics of biodiesel-diesel blend in CI diesel engine. Appl Therm Eng 2019;151:100–14.

[129] Kshirsagar CM, Anand R. Artificial neural network applied forecast on a parametric study of Calophyllum inophyllum methyl ester-diesel engine out responses. Appl Energy 2017;189:555–67.

[130] Acharya N, Acharya S, Panda S, Nanda P. An artificial neural network model for a diesel engine fuelled with mahua biodiesel. Adv Intell Syst Comput 2017;556:193–201.

[131] Channapattana S V., Pawar AA, Kamble PG. Optimisation of operating parameters of DI-CI engine fueled with second generation Bio-fuel and development of ANN based prediction model. Appl Energy 2017;187:84–95.

[132] Kullolli S, Sakthivel G, Ilangkumaran M. A neural network model for the prediction of compression ignition engine performance at different injection timings. Int J Ambient Energy 2016;37:227–36.

[133] Tekin M, Saridemir S. Prediction of engine performance and exhaust emissions with different proportions of ethanol–gasoline blends using artificial neural networks. Int J Ambient Energy 2019;40:470–6.

[134] Soukht Saraee H, Taghavifar H, Jafarmadar S. Experimental and numerical consideration of the effect of CeO2 nanoparticles on diesel engine performance and exhaust emission with the aid of artificial neural network. Appl Therm Eng 2017;113:663–72.

[135] Prasada Rao K, Victor Babu T, Anuradha G, Appa Rao B V. IDI diesel engine performance and exhaust emission analysis using biodiesel with an artificial neural network (ANN). Egypt J Pet 2017;26:593–600.

[136] Uslu S. Optimization of diesel engine operating parameters fueled with palm oil-diesel blend: Comparative evaluation between response surface methodology (RSM) and artificial neural network (ANN). Fuel 2020;276:117990.

[137] Uslu S, Celik MB. Prediction of engine emissions and performance with artificial neural networks in a single cylinder diesel engine using diethyl ether. Eng Sci Technol an Int J 2018;21:1194–201.

[138] Nurdiyana Wan Mansor W, Abdullah S, Ashraf Razali N, Albani A, Ramli A, Olsen D.

Prediction of emissions of a dual fuel engine with Artificial Neural Network (ANN). IOP Conf Ser Earth Environ Sci 2019;373. https://doi.org/10.1088/1755-1315/373/1/012007.

[139] Saraee HS, Jafarmadar S, Alizadeh-Haghighi E, Ashrafi SJ. Experimental investigation of pollution and fuel consumption on a CI engine operated on alumina nanoparticles-Diesel fuel with the aid of artificial neural network. Environmental Progress & Sustainable Energy 2015;35:540–46.

[140] Shrivastava P, Verma TN, David Samuel O, Pugazhendhi A. An experimental investigation on engine characteristics, cost and energy analysis of CI engine fuelled with Roselle, Karanja biodiesel and its blends. Fuel 2020;275:117891.

[141] Thiruvenkatachari S, Saravanan CG, Edwin Geo V, Vikneswaran M, Udayakumar R, Aloui F. Experimental investigations on the production and testing of azolla methyl esters from Azolla microphylla in a compression ignition engine. Fuel 2021;287:119448.

[142] Prabakaran S, Mohanraj T. Optimization of biodiesel production from Azolla pinnata: investigation of CI engine characteristics using nano dosed biodiesel. J Mech Sci Technol 2021;35:4765–73.

[143] Padmanabhan S, Rajasekar S, Ganesan S, Saravanan S, Chandrasekaran M. Performance and emission analysis on ci engine using soapnut oil as biofuel. ARPN J Eng Appl Sci 2017;12:2491–5.

[144] Karthikeyan S, Prathima A, Periyasamy M, Mahendran G. Performance analysis of Al2O3 and C18H34O2 with Kappaphycus Alvarezil-Brown algae biodiesel in CI engine. Mater Today Proc 2020;33:4180–4.

[145] Viswanathan VK, Thomai P. Performance and emission characteristics analysis of Elaeocarpus Ganitrus biodiesel blend using CI engine. Fuel 2021;288:119611.

[146] Narayanasamy B, Jeyakumar N. Performance and emission analysis of methyl ester of Azolla algae with TiO2 Nano additive for diesel engine. Energy Sources, Part A Recover Util Environ Eff 2019;41:1434–45.

[147] Baweja S, Trehan A, Kumar R. Combustion, performance, and emission analysis of a CI engine fueled with mustard oil biodiesel blended in diesel fuel. Fuel 2021;292:120346.

[148] Jayaprabakar J, Karthikeyan A, Saikiran K, Beemkumar N, Joy N. Comparative study of performance and emissions of a CI engine using biodiesel of microalgae, macroalgae and rice bran. IOP Conf Ser Mater Sci Eng 2017;197:0–7.

[149] Tamilvanan A, Balamurugan K, Vijayakumar M. Effects of nano-copper additive on performance, combustion and emission characteristics of Calophyllum inophyllum biodiesel in CI engine. J Therm Anal Calorim 2019;136:317–30.

[150] Nantha Gopal K, Ashok B, Senthil Kumar K, Thundil Karuppa Raj R, Denis Ashok S, Varatharajan V, et al. Performance analysis and emissions profile of cottonseed oil biodiesel–ethanol blends in a CI engine. Biofuels 2018;9:711–8.

[151] Nalgundwar A, Paul B, Sharma SK. Comparison of performance and emissions characteristics of di CI engine fueled with dual biodiesel blends of palm and jatropha. Fuel 2016;173:172–9.

[152] Thomas TJ, Thangapandian N, Sakthivel D, Mohideen SMSF, Basha S, Brindhadevi K, et al. Experimental analysis of C.I. engine using pyrolyzed plastic oil blended with alumina nano additive. Fuel 2022;312:122929.

[153] Rehman M, Kesharvani S, Dwivedi G. Numerical investigation of performance, combustion, and emission characteristics of various microalgae biodiesel on CI engine. Fuels 2023; 4:132–55.

[154] Ramachandran E, Krishnaiah R, Venkatesan EP, Murugan M, Medapati SR, Sekar P. Experimental Investigation for Determining an ideal algal biodiesel−diesel blend to improve the performance and mitigate emissions using a response surface methodology. ACS Omega 2023;8:9187−97.

[155] Moulali P, Tarigonda H, Prasad BD. Optimization of performance characteristics of homogeneous charge Compression Ignition engine with biodiesel using Artificial Neural Network (ANN) and Response Surface Methodology (RSM). J. Inst. Eng. India Ser. C

2022, 103(4):875–88.

[156] Manimaran R, Mohanraj T, Venkatesan M. ANN modeling for forecasting of VCR engine performance and emission parameters fuelled with green diesel extracted from waste biomass resources. Environ Sci Pollut Res 2022;29: 51183–210.

[157] Lalhriatpuia S, Pal A. Computational optimization of engine performance and emission responses for dual fuel CI engine powered with biogas and Co_3O_4 nanoparticles doped biodiesel. Fuel 2023;344: 127892.

[158] Khatri KK, Singh M, Khatri N. An artificial neural network model for the prediction of performance and emission parameters of a CI engine-operated micro-tri-generation system fueled with diesel, Karanja oil, and Karanja biodiesel. Fuel 2023;334: 126549.

LIST of PUBLICATIONS

JOURNALS

1. **Kumar SC**, Thakur AK, Aseer JR, Natarajan SK. An Experimental Investigation on the Effects of Magnesia and Alumina Nano Additives on the Exhaust Emissions and Performance of CI Engine Using Spirulina Microalgae Biodiesel. Environmental Science and Pollution Research 2023; 30:34612–22. https://doi.org/10.1007/s11356-022-24733-8 **(SCI : IF: 5.190)**
2. **Kumar SC**, Thakur AK, Aseer JR, Natarajan SK, Singh R, Priyadarshi N, et al. An Experimental Analysis and ANN Based Parameter Optimization of the Influence of Microalgae Spirulina Blends on CI Engine Attributes. Energies 2022;15:1–20. https://doi.org/10.3390/en15176158. **(SCI : IF: 3.252)**
3. **Kumar SC**, Thakur AK, Aseer JR, Dwivedi G. Comprehensive review on effects of exhaust gas recirculation on nitrogen oxide emission in various biodiesel and nano additives blends fuelled compression ignition engine. Int J Ambient Energy 2022;43:1, 6233-49. https://doi.org/10.1080/01430750.2021.2009367.

CONFERENCE

1. **Kumar SC**, Thakur AK, Aseer JR. Algae Biofuel as a Substitute for Compression Ignition Engine: A Review. Lect Notes Mech Eng 2022:43–51. https://doi.org/10.1007/978-981-16-5371-1_5.
2. **Kumar SC**, Thakur AK. Prediction of Exhaust Emissions and Performance Characteristics of CI Engine Using ANN. Lect Notes Mech Eng **(PUBLICATION STAGE).**

APPENDICES

ANN CODE

```
import numpy as np
import pandas as pd
import matplotlib.pyplot as plt
import tensorflow.keras as keras
import tensorflow as tf
from tensorflow.keras import activations
from tensorflow.keras.metrics import RootMeanSquaredError as rms
e
from tensorflow.keras.losses import MeanSquaredError as mse
import seaborn as sns
from collections import OrderedDict
from sklearn.model_selection import train_test_split, GridSearch
CV
from sklearn.preprocessing import MinMaxScaler, StandardScaler,P
owerTransformer
import os


from google.colab import drive
drive.mount('/content/drive')


data = pd.read_csv('complete experimental values table for ann.c
sv')
data.head()


data.info()


data['BSFC (kg/kWh)']= data['BSFC (kg/kWh)'].fillna(0)
data_ip = data[["Diesel","SB20","SB20Mag25","SB20Aul25",
                "SB35","SB35Mag25","SB35Aul25","SB50","SB50Mag25
",
                "SB50Aul25","SB65","SB65Mag25","SB65Aul25","SB80
",
                "SB80Mag25","SB80Aul25","SB100","SB100Mag25","SB
100Aul25","Load (kg) ","BP (kW)"]]
data_op = data[["BSFC (kg/kWh)","BTE (%)","NOX (ppm)","CO2 (%)",
" HC (ppm)"]]
```

```
data_ip.shape, data_op.shape


data_ip.describe()

data_op.describe()


data[["Load (kg) ","BP (kW)"]].hist(figsize=(10,5))


mx_ip = MinMaxScaler()
data_ip_mx = mx_ip.fit_transform(data_ip[["Load (kg) ","BP (kW)"
]])
data_ip_mx = pd.DataFrame(data_ip_mx,columns=["Load (kg) ","BP (
kW)"])
data_ip_mx.hist(figsize=(8,5))


data_ip_new = data[["Diesel","SB20","SB20Mag25","SB20Aul25","SB3
5","SB35Mag25","SB35Aul25","SB50","SB50Mag25","SB50Aul25","SB65"
,"SB65Mag25","SB65Aul25","SB80","SB80Mag25","SB80Aul25","SB100",
"SB100Mag25","SB100Aul25"]].join(data_ip_mx)
data_ip_new.head()


data_ip_mx.describe()


data[["BSFC (kg/kWh)","BTE (%)","NOX (ppm)","CO2 (%)"," HC (ppm)
"]].hist(figsize=(10,10))

mx = MinMaxScaler()
data_op_mx = mx.fit_transform(data_op)
data_op_mx = pd.DataFrame(data_op_mx,columns=["BSFC (kg/kWh)","B
TE (%)","NOX (ppm)","CO2 (%)"," HC (ppm)"])
data_op_mx.hist(figsize=(10,10))


data_op_mx.describe()

sns.pairplot(data,hue="Fuel",x_vars=["Load (kg) ","BP (kW)"], \y
_vars=["BSFC (kg/kWh)","BTE (%)","NOX (ppm)","CO2 (%)"," HC (ppm
)"],\kind='scatter')
```